CRANIODENTAL ANATOMY OF A NEW LATE CRETACEOUS MULTITUBERCULATE MAMMAL FROM UDAN SAYR, MONGOLIA

GUILLERMO W. ROUGIER, AMIR S. SHETH, BARTON K. SPURLIN, MINJIN BOLORTSETSEG, and MICHAEL J. NOVACEK

Rougier, G.W., Sheth, A.S., Spurlin, B.K., Bolortsetseg, M., and Novacek M.J. 2016. Craniodental anatomy of a new Late Cretaceous multituberculate mammal from Udan Sayr, Mongolia. *Palaeontologia Polonica* **67**, 197–248.

The multituberculate *Mangasbaatar udanii* gen. et sp. n., represented by two specimens from Udan Sayr locality in the Gobi desert (Mongolia), is a derived member of a speciose group of Late Cretaceous Mongolian multituberculates (LCMM), clustering together with large-size forms such as *Catopsbaatar*, *Tombaatar*, and *Djadochtatherium*, forming a monophyletic group. *Tombaatar sabuli* is the sister taxon and shares with the new form the dental formula, overall dental morphology, and approximate size. The new multituberculate has a very large middle ear cavity, housing a petrosal and promontorium that are deeply sunk into the braincase. The expansion of the middle ear cavity seems to be absent among basal LCMM, only developing among members of Djadochtatherioidea, and to an extreme degree in the Udan Sayr multituberculate and *Tombaatar*. Among living mammals, enlarged middle ear cavities confer enhanced low frequency audition and are often found in fossorial species, such as golden moles, and several groups of rodents adapted to open, arid environments. Burrowing is a possible behavior for the new mammal and its closest relatives with similarly expanded middle ear regions and an arid environment has been proposed for the sediments where most LCMM are found. The new taxon further demonstrates the morphological, and possibly ecological, diversity among multituberculates.

Key words: Multituberculata, Djadochtatherioidea, skull structure, phylogeny.

Guillermo W. Rougier [grougier@louisville.edu] and Amir S. Sheth [amirssheth@gmail.com], Department of Antomical Sciences and Neurobiology, University of Louisville, KY 40202, USA.
Barton K. Spurlin [bartspurlin@yahoo.com], Medical Center, Bowling Green, KY 42101, USA.
Minjin Bolortsetseg [bminjin@amnh.org], Institute for the Study of Mongolian Dinosaurs, Ulaanbaatar, Mongolia and Division of Paleontology, American Museum of Natural History, New York, NY 10024, USA.
Michael J. Novacek [novacek@amnh.org], Division of Paleontology, American Museum of Natural History, New York, NY 10024, USA.

Received 28 June 2015, accepted 7 December 2015.

http://dx.doi.org/10.4202/pp.2016.67_197

INTRODUCTION

Since 1990, the American Museum of Natural History (AMNH) and the Mongolian Academy of Sciences have been prospecting the Mesozoic outcrops of Mongolia in search of fossil vertebrates. This new project is the heir of a similar series of expeditions organized by the AMNH during the 1920s that recovered some of the first early mammals from Central Asia (Gregory and Simpson 1926; Simpson 1928a, b; Matthew *et al.* 1928, 1929). The recent American-Mongolian expeditions (1990 to the present) have followed that tradition and results have been plentiful, including the discovery of one of the richest Mesozoic localities in the world, Ukhaa Tolgod (Norell *et al.* 1994; Novacek *et al.* 1994; Dashzeveg *et al.* 1995, 2005; Dingus *et al.* 2008). The Cretaceous localities of Mongolia, especially those of the Djadochta and similarly-aged Barun Goyot formations (Shuvalov 2000; Jerzykiewicz 2000; Dashzeveg *et al.* 2005; Dingus *et al.* 2008), are exceptionally rich in well-preserved small vertebrates in comparison to those in other parts of the world. During 1940–1980 most of the paleontological exploration of Central Asia was undertaken by joint Russian-Mongolian and Polish-Mongolian expeditions that resulted in the discovery of new Cretaceous localities in the Nemegt Valley, raising the bar regarding specimen quality and allowing for much more detailed anatomical work than previously possible (Clemens *et al.* 1979; Lillegraven *et al.* 1979). Professor Kielan-Jaworowska, in whose memory the present volume is compiled, was the leader of the Polish expeditions, a prolific and accomplished scientist who for years shaped the debate on early mammalian evolution (see summary and review in Kielan-Jaworowska *et al.* 2004; Kielan-Jaworowska 2013). With very few exceptions, the most complete Late Cretaceous mammalian skeletons known to date have been recovered from those Mongolian localities (Kielan-Jaworowska 1969a, b, 1970, 1974, 1975a, b, c, 1977, 1978, 1979, 1984a, b, 2013; Kielan-Jaworowska and Sochava 1969; Kielan-Jaworowska and Dashzeveg 1978; Kielan-Jaworowska and Trofimov 1980; Kielan-Jaworowska and Gambaryan 1994; Gambaryan and Kielan-Jaworowska 1995; Kielan-Jaworowska and Hurum 1997, 2001; Kielan-Jaworowska *et al.* 2005). Multituberculates are the most common mammalian specimens collected in the Cretaceous localities of Mongolia. The Late Cretaceous Mongolian Multituberculates (LCMM) are the best-known specimens of multituberculates and currently eleven genera are recognized (Wible and Rougier 2000; Kielan-Jaworowska and Hurum 2001, 2005; Kielan-Jaworowska *et al.* 2004). To those we add a new one here.

Multituberculates possess the longest fossil record of all mammals, extending from the early middle Jurassic to the late Eocene (Prothero and Swisher 1992; Freeman 1976, 1979; Kielan-Jaworowska *et al.* 2004). Several recent studies (Zheng *et al.* 2013; Zhou *et al.* 2013; Bi *et al.* 2014) have opened discussion regarding the timing of certain events within the basal branches of the mammalian tree, namely the origin of the very first mammals via the relationships between Haramiyidae and Allotheria (including multituberculates). It is at present unresolved if multituberculates are closely related to haramiyids, eleutherodontids and other forms with cusps in line, and while multituberculates are consistently regarded as mammals in recent studies (Bi *et al.* 2014; Luo *et al.* 2015; Meng *et al.* 2015), opinions differ regarding haramiyids and eleutherodontids.

Multituberculates are also one of the best-represented groups of Mesozoic mammals: over five hundred partial or complete skulls and skeletons have been collected from Ukhaa Tolgod since 1993. However, the taxonomic diversity in Ukhaa Tolgod and other localities of the Djadochta Formation is relatively low, the fauna being dominated by medium-sized forms such as *Kryptobaatar dashzevegi* Kielan-Jaworowska, 1970 (Wible and Rougier 2000). The specimens described here are from a different locality, Udan Sayr (Fig. 1), which is considered to be somewhat younger than traditional localities like the Flaming Cliffs, probably corresponding to the Barun Goyot Formation (Jerzykiewicz and Russell 1991; Kielan-Jaworowska *et al.* 2004) and of late Campanian age. A few tantalizing mammalian specimens have been collected at Udan Sayr, including basal metatherians (Trofimov and Szalay 1994; Szalay and Trofimov 1996), eutherians, and multituberculates (Bolortsetseg 2008).

The collection of complete or nearly complete specimens of LCMM led to a revival in the study of multituberculate phylogeny (Simmons 1993; Miao 1993; Rougier *et al.* 1997; Kielan-Jaworowska and Hurum 1997, 2001; Kielan-Jaworowska *et al.* 2002, 2005), which excepting a few publications (Ladevèze *et al.* 2010; Smith and Codrea 2015) has subsided in recent years. One of the most notable results of the work on the late 1990s and early 2000s has been the recognition of an endemic LCMM clade, Djadochtatheria, later reclassified as superfamily Djadochtatherioidea Kielan-Jaworowska *et* Hurum, 1997 (Rougier *et al.* 1997; Kielan-Jaworowska and Hurum 1997; Kielan-Jaworowska and Hurum 2001). Multituberculate cranial anatomy has been monographically treated in two instances: Miao (1988) described the taeniolabidoid

Fig. 1. Map of Mongolia with location of the Udan Sayr locality, Gobi Desert, Mongolia.

Lambdopsalis bulla Chow *et* Qi, 1978 and Wible and Rougier (2000) described *Kryptobaatar dashzevegi*. Later, Kielan-Jaworowska *et al.* (2005) provided a revised description of *Catopsbaatar* Kielan-Jaworowska, 1994 with a high level of detail, and even more recently a CT study of the ear region of a cf. *Tombaatar* skull from a Djadochta equivalent in China was presented by Ladevèze and co-authors (Ladevèze *et al.* 2010). *Kryptobaatar* is a member of Djadochtatherioidea consistently recovered in a relatively basal position in the group and is a suitable generalized LCMM to serve as interpretative baseline for understanding the evolution of Djadochtatherioidea. On the other hand, *Tombaatar sabuli* Rougier *et al.*, 1997 is thought to be a much derived member of this clade, but the fragmentary skull so far described is quite poorly preserved and Ladevèze *et al.* (2010) described only the ear region in any detail. The well-preserved specimens described here are closely related to *Tombaatar* and provide a substantial amount of new information (of the jaw, ear region and basicranium in particular) about this highly-derived group. A detailed knowledge of a generalized form, such as *Kryptobaatar*, and derived forms, such as *Tombaatar* and allies, illuminates the range of morphological diversity for Djadochtatherioidea in particular and multituberculates in general.

Acknowledgments. — We would like to thank the Mongolian Academy of Sciences for its ongoing support and collaboration with the American Museum of Natural History, in particular Khand Yondon. Michael Eisenback and Lindsay Snow (both University of Louisville, USA) assisted with imaging and illustrations. Brian Davis (University of Louisville, KY, USA), Zhe-Xi Luo (University of Chicago, USA) and John Wible (Carnegie Museum of Natural History, Pittsburgh, PA, USA) provided helpful reviews of the manuscript. This study was supported by NSF grants DEB 0946430 and DEB 1068089 to GWR, with field work supported in part by the Frick Laboratory Endowment.

GEOLOGICAL SETTING AND MATERIAL

The holotype and refered specimen were found in the easternmost exposures of Udan Sayr (Fig. 1). Following current Mongolian legislation, precise coordinates are only available to qualified researchers. General coordinates for Udan Sayr are 43° N, 103° E, about 65 kilometers west of Bayan Dzag in Umnugovi Province, Mongolia. Udan Sayr was first discovered by the Soviet Mongolian Paleontological Expedition in the 1980s (Benton *et al.* 2000) and two joint expeditions have worked there, one between the Mongolian Academy of Sciences (MAS) and the American Museum of Natural History and another between the MAS and Hayashibara Museum of Natural Sciences. The former expedition collected the holotype of *Mangasbaatar* from Udan Sayr in 1997. Exposures of Udan Sayr are scattered across an area of more than 60 km^2. The lower

strata consist of fluvial sandstones and mudstones and with dinosaur footprints being the most common fossils, whereas the upper strata, where the holotype was found, consist of alternating red beds of cross-stratified and structureless sandstone (Watabe *et al.* 2010). The types of the ceratopsian dinosaur *Udanoceratops tschizhovi* (Kurzanov 1992; Dong and Currie 1993) and *Asiatherium reshetovi* Szalay *et* Trofimov, 1996, a basal metatherian (Rougier *et al.* 1998, 2015; Davis *et al.* 2008; Bi *et al.* 2014), are also from Udan Sayr.

The cross-stratified beds are likely eolian in origin, and the lithology and sedimentary structures of these beds and the structureless sandstones are very similar to exposures of the Djadochta Formation at Bayan Dzag and Ukhaa Tolgod (Gradziński *et al.* 1977; Jerzykiewicz and Russell 1991; Jerzykiewicz *et al.* 1993; Loope *et al.* 1998; Dingus *et al.* 2008), and for this reason previous workers have concluded that the beds at Udan Sayr are also Djadochta Formation (Saneyoshi *et al.* 2008; Watabe *et al.* 2010). The occurrence of two typical Djadochta taxa, *Protoceratops andrewsi* and *Pinacosaurus* sp. at Udan Sayr is consistent with this conclusion (Watabe *et al.* 2010; Handa *et al.* 2012). Preliminary magnetostratigraphic analyses of the Djadochta Formation from Bayan Dzag and Tugrigeen Shiree suggest that this formation was deposited during a period of rapidly changing polarity between 71 to 75 Mya (Dashzeveg *et al.* 2005).

The specimens were collected in friable red sandstones that vary from fine to medium in grain size. As in the Djadochta and Barun Goyot formations, the fossils are frequently complete including, in some instances, articulated specimens of which *Asiatherium* (Trofimov and Szalay 1996) is a good example. Isolated skulls are frequently included in harder carbonate concretions, which often result from the erosion of a partial skeleton. The postcranium associated with the specimen PSS-MAE 141 formed the core of a Ph.D. thesis and has been described elsewhere (Bolortstseg 2008), while PSS-MAE 142 shows portions of the skeleton enclosed in a concretion.

The skull morphology of multituberculates is distinct from that of other mammals and different authors have used various organizational schemes to describe them with a rather elaborate, sometimes incompatible nomenclature (Gidley 1909; Simpson 1937; Kielan-Jaworowska 1971; Kielan-Jaworowska *et al.* 1986, 2002, 2005; Gambaryan and Kielan-Jaworowska 1995; Wible and Rougier 2000; Kielan-Jaworowska and Hurum 2005). We follow the nomenclature of Wible and Rougier (2000) as developed in their glossary, incorporating recent additions by Kielan-Jaworowska *et al.* (2005). The term "Lateral Flange" has been used to denote two slightly different portions of the multituberculate braincase. Kielan-Jaworowska *et al.* (2005) followed earlier usage by Kielan-Jaworowska (1971), against that used by Rougier, Wible and Hopson (Rougier *et al.* 1992, 1996a; Wible and Hopson 1993; Wible and Rougier 2000; Rougier and Wible 2006). Kielan-Jaworowska *et al.* (2005) reported that Wible and Rougier (2000, pp. 40, 94) endorsed the interpretations of Kielan-Jaworowska (1971) of "Lateral Flange"; that is not so. The referred pages, in particular Wible and Rougier (2000, p. 40), are an almost textual use of Hopson's personal communication (Kielan-Jaworowska *et al.* 2005, pp. 488–489) defining his interpretation of "Lateral Flange". Here, "Lateral Flange" refers to the thickened lower edge of the anterior lamina that, in multituberculates, is inturned (medially directed) and contacts the promontorium.

The preliminary comparison and evaluation of the morphological features of the new specimens from Udan Sayr strongly suggest that they are members of Djadochtatherioidea, an endemic Late Cretaceous multituberculate clade of Asia (Rougier *et al.* 1997; Kielan-Jaworowska and Hurum 1997; Kielan-Jaworowska *et al.* 2003), representing fairly derived members of that clade (see analysis below). In fact, these new specimens are similar to *Catopsbaatar catopsaloides* from the classic Late Cretaceous locality of Kheermin Tsav (Kielan-Jaworowska 1994; Kielan-Jaworowska *et al.* 2002, 2005) and to the type of *Tombaatar sabuli* (Rougier *et al.* 1997), a species from the Mongolian Late Cretaceous locality of Ukhaa Tolgod (Dashzeveg *et al.* 1995; Novacek *et al.* 1997). *Tombaatar* was identified by Rougier *et al.* (1997) and Kielan-Jaworowska and Hurum (1997), as closely related to another large LCMM, *Catopsbaatar catopsaloides* (Kielan-Jaworowska 1974, 1994). *Tombaatar*, *Catopsbaatar*, and a third form, *Djadochtatherium* Simpson, 1925 are diagnosed by a relatively large suite of derived characters (Rougier *et al.* 1997; Kielan-Jaworowska and Hurum 1997; Kielan-Jaworowska *et al.* 2002, 2005) that are also present in this new species. Therefore, following Rougier *et al.* (1997) and Kielan-Jaworowska and Hurum (1997, 2001), this study accepts the existence of a group formed by the large-sized LCMM and will discuss the affinities of these specimens in this context.

The specimen PSS-MAE 141 consists of a skull (Figs 2–10), lower jaws (Figs 11–14), and postcranial elements (Bolortsetseg 2008). The skull has been dorsoventrally compressed, resulting in a moderate loss of height and a general oblique deformation of the skull to the left when viewed from the front. Missing are portions of the right zygomatic arch and basicranium. Only remnants of the skull roof elements are pre-

served. The sutures, however, can be followed in most instances. The left lower jaw is nearly complete with full dentition, while the dentary and three teeth are all that remain of the right lower jaw.

A second specimen, PSS-MAE 142, attributed to the hypodigm, is represented by an incomplete skull (Figs 15–18) and postcranial skeleton. The specimen includes a good portion of the rostrum, palate, braincase, fragments of both glenoids, and an isolated right premaxilla. The lower jaws are only partially preserved. The right lower jaw is a fragment showing p3–m2, while on the left only the m2 has been recovered. The postcranium includes most dorsal lumbar vertebrae, an articulated segment of the caudal series, fragmentary shoulder girdle and forelimbs, and nearly complete pelvis and hind limbs.

Institutional abbreviations. — AMNH, American Museum of Natural History, New York, NY, USA; PSS-MAE, Paleontological and Stratigraphic Section (PSS) of the Geological Institute, Mongolian Academy of Sciences, Ulaan Baatar, Mongolia; YPM-PU, Peabody Museum of Natural History, Princeton University Collection, Yale University, New Haven, CT, USA; ZPAL, Institute of Paleobiology of the Polish Academy of Sciences, Warsaw, Poland.

SYSTEMATIC PALEONTOLOGY

Class **Mammalia** Linnaeus, 1758

Subclass **Allotheria** Marsh, 1880

Order **Multituberculata** Cope, 1884

Superfamily **Djadochtatherioidea** Kielan-Jaworowska *et* Hurum, 2001

Family **Djadochtatheriidae** Kielan Jaworowska *et* Hurum, 1997

Genus ***Mangasbaatar*** gen. n.

Type and only species: *Mangasbaatar udanii*, new species.

Etymology: *Mangas*, transliteration from Mongolian: Mangas is a mythological monster of Mongolian folklore; *baatar*, transliteration from the Mongolian for hero, a suffix commonly used to designate Mongolian multituberculates; *udanii*, after the locality Udan Sayr where the specimens were found. Udan: probably a corruption of the Mongolian Ulaan, meaning red: red wash, or gulch, which describes the locality well.

Holotype: PSS-MAE 141, an almost complete skull and jaws (Figs 2–14).

Referred material: PSS-MAE 142, an incomplete skull and jaws associated with a fairly complete postcranium (Figs 15–18).

Locality: Udan Sayr, 85 km northwest of Bulgan-Somon, Umuni Gobi Aimak (southern region), Mongolia, from beds of similar lithology and age as the Barun Goyot Formation.

Diagnosis for monotypic genus and species: Large-sized multituberculate similar to *Tombaatar* and *Catopsbaatar*, but differing from other Late Cretaceous Mongolian Multituberculates in lacking the P2. *Mangasbaatar* shares with *Tombaatar* the proportions of the M1 and a similar cusp formula for the M1 (one extra cusp in each of the rows for *Mangasbaatar*), but differs in the slightly larger skull size, smaller size of the P1, and different M1 to M2 length ratio (1.78 *Mangasbaatar*, 1.46 *Tombaatar*). The M1 in *Mangasbaatar* is proportionately 20% longer than in *Tombaatar*. *Mangasbaatar* resembles *Catopsbaatar*, but differs from *Tombaatar* and *Djadochtatherium*, in having broad flat nasals. The frontals and parietals in *Mangasbaatar* are strongly convex, but less so in *Catopsbaatar* (the condition is unknown in *Djadochtatherium* and *Tombaatar*). The proportionally longer molars in *Mangasbaatar* determine that the root of the zygomatic arch is approximately at the level of the posterior root of the P4/M1 embrasure. *Mangasbaatar* resembles *Catopsbaatar* in this feature, but *Tombaatar*, and probably *Djadochtatherium*, share the primitive condition with the root of the zygomatic arch more anteriorly positioned at the level of the anterior root of the P4. All of the large-sized LCMM share a posterior position for the orbit, a derived feature absent in more generalized LCMM. The ear region of most LCMM lodges large tympanic sinuses. *Mangasbaatar*'s development of these features is extreme and similar to an as yet undescribed specimen of *Tombaatar* (PSS-MAE 60). *Catopsbaatar* has this sinus complex, although it is less developed. In Djadochtatherium the relevant portion of the skull is not known. *Mangasbaatar* shares with other LCMM except *Tombaatar* the premaxilla as the only element forming the alveolus for P3. *Mangasbaatar* shares with *Djadochtatherium* and *Catopsbaatar* the presence of a polygonal p4. It also shares with *Catopsbaatar*, but not with *Djadochtatherium*, an almost vertical anterior wall of the diastema in front of the p3. In *Mangasbaatar* the occlusal plane of the lower teeth forms a low angle to the plane of the bottom of the lower jaw similar to that in *Catopsbaatar*, but different than in *Djadochtatherium*. The p3 still has a more distinctive crown-root junction in *Mangasbaatar*, but it is more "peg-like" in *Catopsbaatar*. *Kryptobaatar*, *Nemegtbaatar* Kielan-Jaworowska, 1970, and *Chulsanbaatar* Kielan-Jaworowska, 1970 retain more primitive conditions for these characters of the lower dentition.

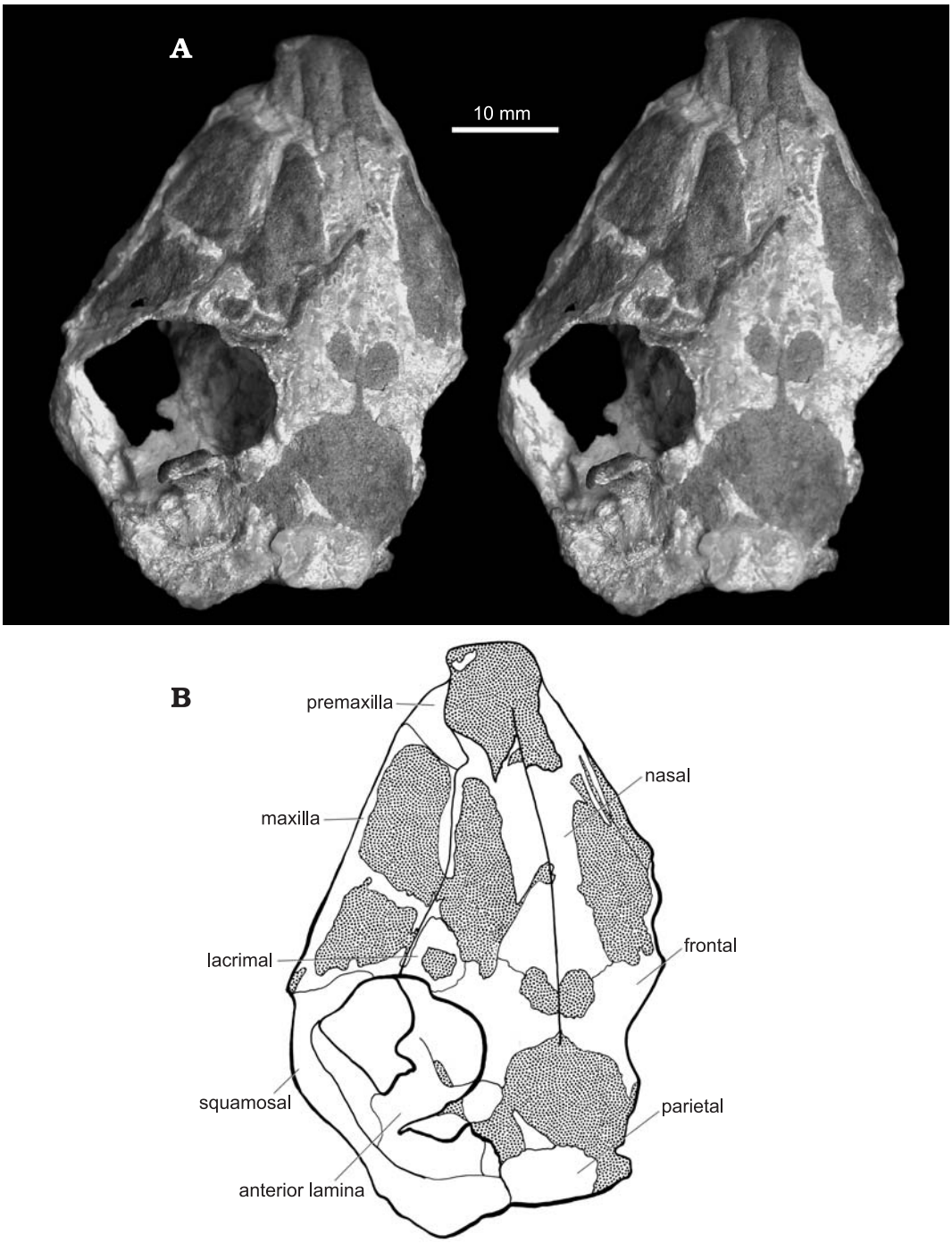

Fig. 2. Holotype of *Mangasbaatar udanii* gen. et sp. n., PSS-MAE 141, Udan Sayr, Late Cretaceous, Mongolia. Stereophotograph of the skull in dorsal view (**A**), and explanatory drawing (**B**). Dotted pattern represents matrix.

DESCRIPTION

General description. — *Mangasbaatar udanii*, with a body mass estimate of 0.879 kg (using formulas by Wilson *et al.* 2012), is one of the largest Late Cretaceous Mongolian multituberculates, and along with *Catopsbaatar* is among the largest mammalian herbivores of the Mesozoic. The two specimens described in this paper are preserved well enough to allow a reconstruction of the skull (Figs 19–22) and jaws (Fig. 23). Presented here is a bone-by-bone description of the skulls and lower jaws of the type specimen, PSS-MAE 141, and the referred specimen, PSS-MAE 142. The postcranial skeleton is described elsewhere (see Bolortsetseg 2008). The type specimen is a young adult with only little wear of the cheek teeth, while the referred specimen is an old adult whose cusps have been worn flat.

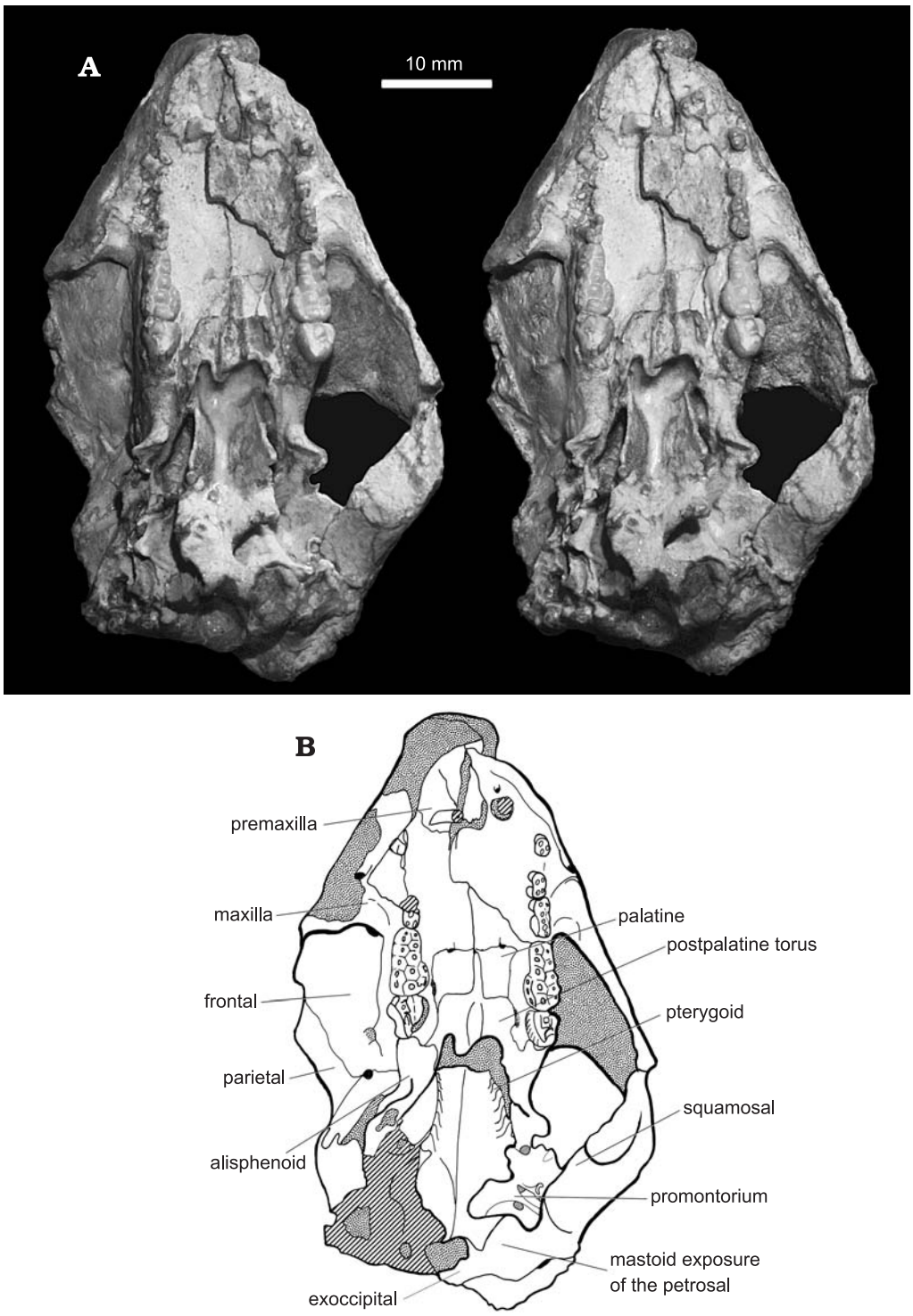

Fig. 3. Holotype of *Mangasbaatar udanii* gen. et sp. n., PSS-MAE 141, Udan Sayr, Late Cretaceous, Mongolia. Stereophotograph of the skull in ventral view (**A**) and explanatory drawing (**B**). Dotted pattern represents matrix; parallel lines represent damaged surfaces.

Premaxilla. — The premaxilla is a large bone with both horizontal (palatal) and vertical (facial) processes well developed, forming a substantial portion of the muzzle (Figs 2, 3, 7). The horizontal component forms the anterior portion of the palate and the floor of the nasal cavity. In ventral view of PSS-MAE 141, the point of contact between both premaxillae is obscured by the deformation of this specimen (Figs 3–5). The suture with the maxilla on the rostrum meanders posteromedially from the raised labial margin (*crista premaxillaris* of Kielan-Jaworowska *et al.* 2005). Most of the external surface of the right premaxilla in

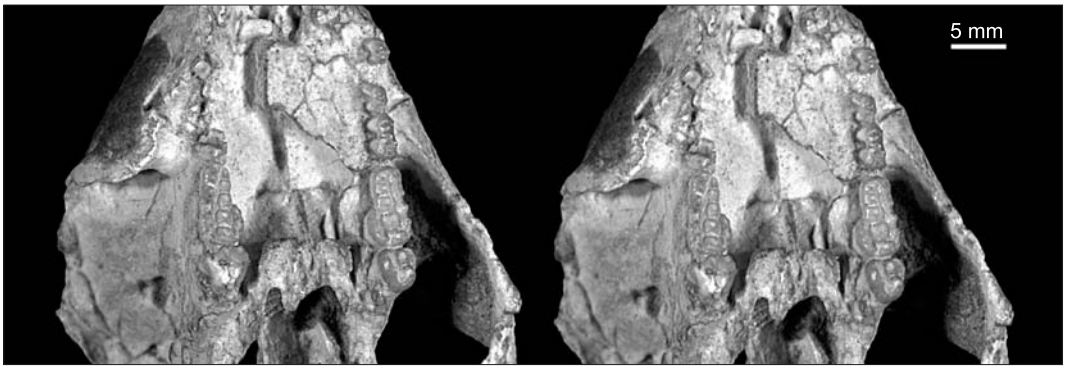

Fig. 4. Holotype of *Mangasbaatar udanii* gen. et sp. n., PSS-MAE 141, Udan Sayr, Late Cretaceous, Mongolia. Stereophotograph of the palatal region in ventral view.

PSS-MAE 141 is missing, exposing the broken I2 inside the alveolus. Enough is preserved of the premaxilla however to show that, as in *Tombaatar*, the maxilla extensively overlaps the premaxilla. This feature is also shown by the isolated premaxillae of PSS-MAE 142. The premaxilla lodges the ever-growing I2 that bulges into the nasal cavity.

In ventral view, the premaxilla-maxilla suture does not form the caudal rim of the alveolus for I3, as in *Tombaatar*, but rather runs posterior to this alveolus conforming to the condition present in most members of Djadochtatherioidea. Therefore, the circular alveolus for I3 is fully contained within the premaxilla (Fig. 3). Both alveoli, I2 and I3, are anteroposteriorly aligned along a parasagittal plane. Medial to the I3 alveoli are the large, anteroposteriorly oriented incisive foramina, which are jointly formed by premaxilla and maxilla. As in *Tombaatar*, the premaxilla is perforated by several nutrient foramina anterior to the incisive foramina and there are distinct thickenings of the premaxilla between the alveoli for I2 and I3 (Rougier *et al.* 1997). The crista premaxillaris (Kielan-Jaworowska *et al.* 2005) is well developed, but lacks most of the nutrient foramina seen in *Catopsbaatar*. Only a few are present in PSS-MAE 141 and 142.

The vertical component of the premaxilla, the facial process, forms the lateral wall of the nasal cavity and the lower margin of the external nares. The opening of the nares is oriented directly anteriorly and no indication of a septomaxilla or internarial bar is discernible (Fig. 2), as is found in, for example, the Late Cretaceous multituberculate *Lambdopsalis*. In lateral view, contact with the maxilla is along a rostrally-convex suture posterior to the alveolus of a large I2. A slender posterior process of the premaxilla extends between the maxilla and nasal, ending above P1 (Fig. 7). The narrow extension of the posterior process is similar to *Tombaatar* and *Catopsbaatar* but differs from the blunter process of other members of Djadochtatherioidea.

Maxilla. — The maxilla in multituberculates is a large bone that forms part of the palate, rostrum, and orbital areas. These three portions of the bone define individual processes: the palatal, facial, and orbital, respectively (Figs 3–5, 7, 18). The maxilla contacts the premaxilla anteriorly, the nasals and lacrimals dorsally, and the palatine posteriorly in the palate. Posteriorly in the orbital-temporal area, the maxilla contacts the frontal, the alisphenoid, and possibly the orbitosphenoid. The rostral process of the maxilla is large and is the main bone forming the rostrum. It is convex laterally, reflecting the large size of the maxillary sinuses as seen in multituberculate serial sections (Kielan-Jaworowska *et al.* 1986; Hurum 1994) and CT scans (Kik 2002; Macrini 2006). This conspicuous lateral bulging of the maxilla gives multituberculates their distinctly triangular-appearing rostrum. The extreme development of this feature is seen in members of Djadochtatherioidea, in which the rostrum and the side of the zygomatic arches become confluent (Rougier *et al.* 1997; Kielan-Jaworowska and Hurum 1997, 2001; Kielan-Jaworowska *et al.* 2004, 2005). The premaxillary-maxillary suture is well preserved only on the left side of PSS-MAE 142 (Fig. 18). The suture forms a long arcuate line that extends posteriorly both at the ventral and dorsal limits. The dominant feature on the rostral process is a large infraorbital foramen that is recessed in a depression and opens into the rostrum at the level corresponding to the diastema between P1 and P3 (Figs 7, 18, 22). The infraorbital foramen is depressed dorsoventrally and its exit forms a deep groove that extends anteriorly under the bulging sides of the maxilla. Thus far, with the sole exception of some specimens of *Catopsbaatar* (Kielan-Jaworowska *et al.* 2005), all LCMM have been described as having only one infraorbital foramen. This is a derived condition shared by all cimolodonts but absent in the Jurassic paulchoffatiids (Simpson, 1928a; Hahn 1985, 1987; Hahn and Hahn 1994). In *Mangasbaatar*, there is a second, small foramen anterior to the main infraorbital

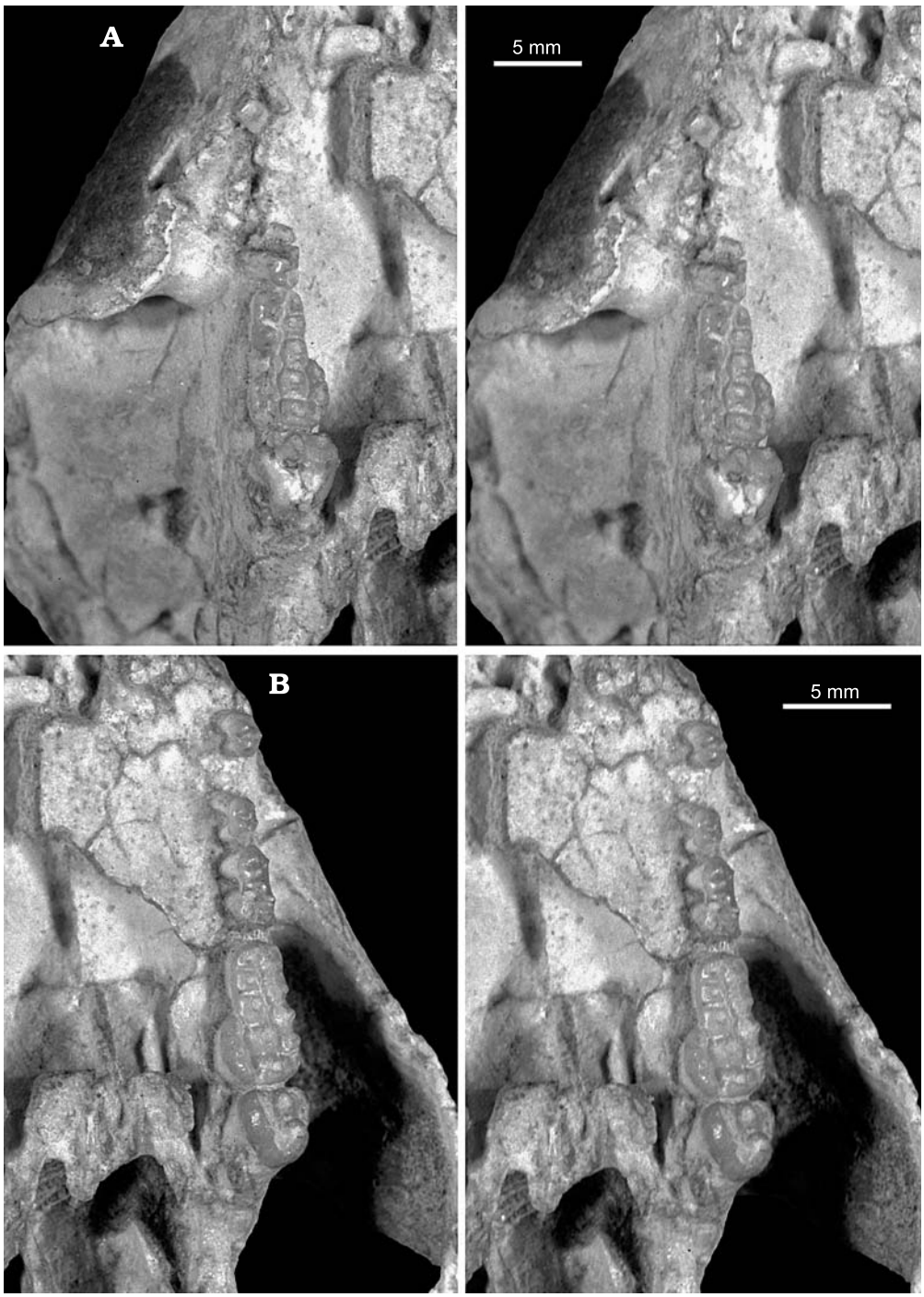

Fig. 5. Holotype of *Mangasbaatar udanii* gen. et sp. n., PSS-MAE 141, Udan Sayr, Late Cretaceous, Mongolia. Stereophotographs of the right and left sides of the palatal region in ventral view detail of the right half of the skull (**A**) and detail of the left side of the skull (**B**).

foramen just described (Fig. 22). This small aperture opens at the level of the P1, or slightly in front of it, and is present bilaterally in PSS-MAE 141 and 142. Given the distribution of the character among the remaining LCMM, it is likely that the presence of this secondary infraorbital foramen in *Mangasbaatar*, and those variably present in *Catopsbaatar*, are a convergence to the primitive morphology. The condition of this character in the closely related *Tombaatar* cannot be ascertained in the type specimen because of the poor preservation of the relevant area, but other available specimens show a single foramen.

The infraorbital canal is broken open on both sides of PSS-MAE 142 so that the communication between the maxillary foramen in the orbit and the infraorbital foramen in the rostrum can be traced. The left side

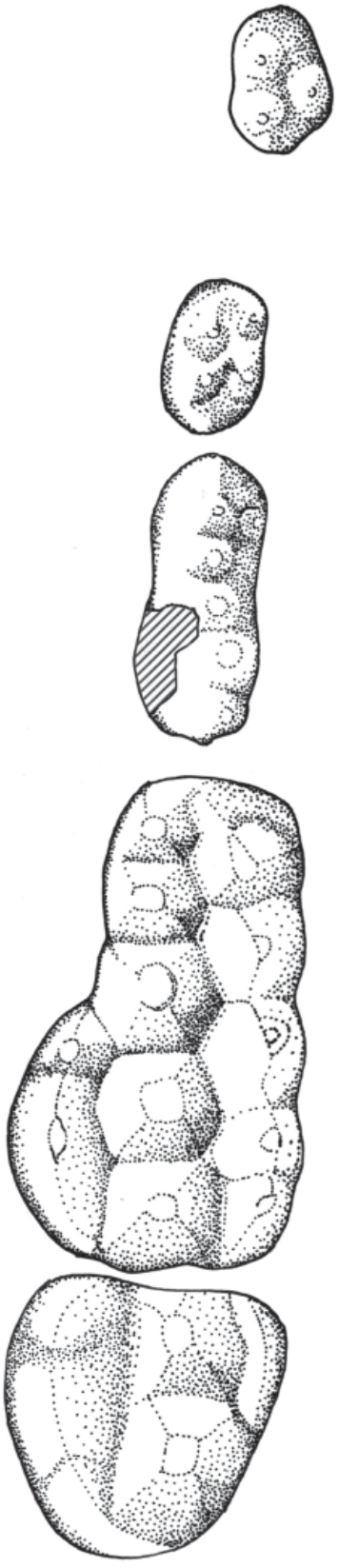

Fig. 6. Holotype of *Mangasbaatar udanii* gen. et sp. n., PSS-MAE 141. Ilustration of the left upper dentition in occlusal view. Parallel lines represent damaged surfaces.

of the specimen has been prepared, revealing several foramina of various sizes that open medially into the interior of the maxilla from the infraorbital canal. These foramina correspond to those described by Rougier *et al.* (1997) in *Tombaatar* and *Djadochtatherium*. These foramina likely correspond to alveolar nerves providing blood and nervous supply to the teeth and maxillary sinus. A similar pattern is known among recent mammals (Sisson and Grossman 1955; Evans and Christensen 1979; Moore and Agur 2002).

The facial process of the maxilla in PSS-MAE 142 is well preserved and shows numerous small nutrient foramina perforating the substance of the bone. A distinctive pattern of small ridges and rugosities mostly oriented anteroposteriorly are present on the lower half of the facial process indicating the area of attachment of superficial facial musculature. The *m. buccinatorius* is, most likely, responsible for the scars mentioned above; this muscle would extend posteriorly to reach the mesial edge of the anterior zygomatic ridge (Fig. 22) for the *pars anterior musculi masseteris superficialis* (see below).

The facial process continues posteriorly to form, together with the lacrimal, the anterior edge of the orbit. As in all other LCMM, *Mangasbaatar* lacks a distinct floor for the orbit, and the maxilla shows inside the orbit a well-developed orbital pocket (Figs 3–5, 16, 17) that extends anteriorly beyond the level of the orbital ridge (Kielan-Jaworowska *et al.* 1986; Gambaryan and Kielan-Jaworowska 1995; Wible and Rougier 2000). This orbital pocket, an important component of the orbital cavity, accounts for approximately one-third of the length of the preorbital region of *Mangasbaatar*. The root of the zygomatic arch marks the anterior extent of the orbital pocket. The zygomatic process of the maxilla is broad, originates at the level of the embrasure between P4 and M1, and extends backward to contact the zygomatic process of the squamosal at roughly the lowest point of the orbit. The dorsal edge of the zygomatic process is concave-convex determining a very peculiar orbital outline (Figs 7, 22), shared with *Tombaatar*. The area forming the orbital edge on the zygoma is slightly convex, becoming concave posteriorly, towards the maxillo-squamosal suture; this arrangement results in a very slender posterior portion of the zygoma. The great height of the zygomatic arch produces a relatively small, dorsally located orbit, positioned in the posterior half of the skull.

Between the root of the zygoma, the infraorbital foramen, and P1–P4, there is a flat area that forms a distinct platform on the lateral surface of the maxilla and dorsal to the teeth. A sharp ridge, the anterior zygomatic ridge, divides this platform. The anterior zygomatic ridge ends directly lateral to the anterior root of P4 and extends posteriorly into the zygoma (although the exact distal extension cannot be determined because of insufficient preservation). Enough is preserved in isolated maxilary fragments of PSS-MAE 142 to show that the ridge is well developed with a lightly rugose apex. What is preserved of the anterior zygomatic ridge conforms to the morphology present in other LCMM, but is longer and narrower than that present in *Catopsbaatar* (Kielan-Jaworowska and Hurum 2005).

In ventral view, the palatal process of the maxilla is preserved in both PSS-MAE 141 and 142 (Figs 3–5, 16, 17). Nevertheless, both specimens are broken and parts of the palate have been displaced and asymmetrically deformed. The result of this deformation is that right and left elements are not always aligned. The sutures are better shown by PSS-MAE 141, but PSS-MAE 142 conforms quite closely to the pattern of the type. The maxillary contribution to the incisive foramina is not well preserved in either

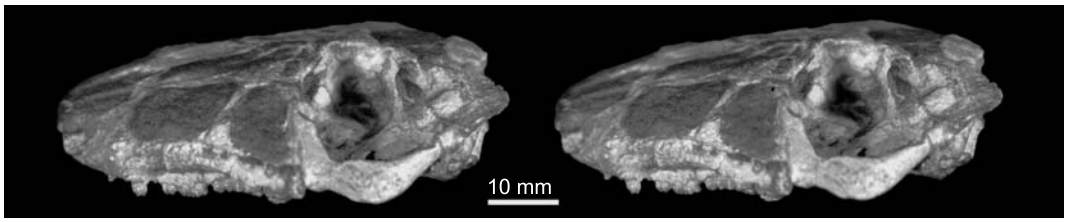

Fig. 7. Holotype of *Mangasbaatar udanii* gen. et sp. n., PSS-MAE 141. Stereophotograph of the left side of the skull in lateral view.

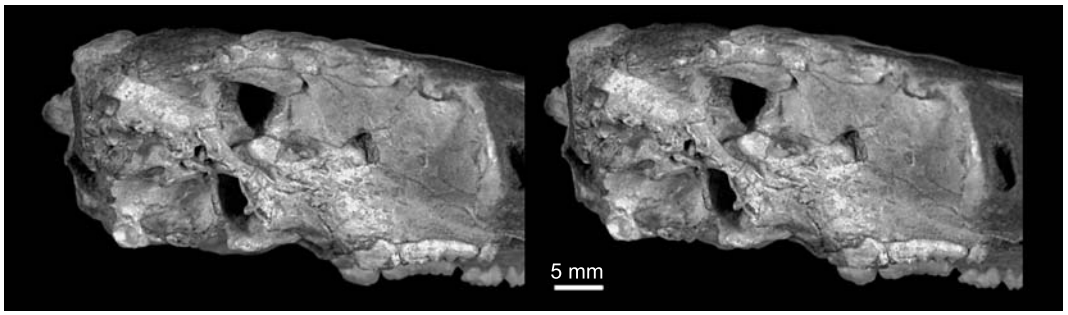

Fig. 8. Holotype of *Mangasbaatar udanii* gen. et sp. n., PSS-MAE 141. Stereophotograph of the right ear region in lateral view.

specimen, though it seems limited to the posteriormost edge of the apertures. The contact of the skull between the premaxilla and maxilla in this region has already been described but, in addition, along the suture on the right side of both PSS-MAE 141 and 142, there is a medium-sized foramen in the suture right behind I3. The anterior portions of the palatine processes of the maxillae are moderately concave, becoming more so posteriorly. This change in curvature of the maxilla is so pronounced that the palate can be considered almost flat at the level of P1 but very deep at the level of M1.

The maxilla contacts the subrectangular exposure of the palatine approximately at the level of the middle of M1 (Figs 5, 17). The contact between maxilla and palatine is made through an inverted L-shaped suture with an anterior transverse component and a posterior parasagittal component. A large foramen can be distinguished at the lateral extent of the transverse suture between the maxilla and the palatine bones. It is the major palatine foramen that grooves the maxilla only in the immediate vicinity of the opening. The foramen probably transmitted the major palatine artery and nerve that in modern mammals supply the roof of the mouth, to finally anastomose with the arteries and nerves reaching the incisive foramen from the nasal cavity, likely branches of the sphenopalatine artery and nasopalatine nerve.

The longitudinal portion of the maxillary-palatine suture runs close to the M2 and the posterior portion of M1. Along the longitudinal portion of this suture, there is a slit-like foramen, interpreted here as the minor palatine foramen, that opens in front of the M2. Kielan-Jaworowska *et al.* (2005) followed earlier interpretations (Kielan-Jaworowska *et al.* 1986) and identified the slit-like foramina, here identified as minor palatine foramina (following Wible and Rougier 2000), as a deep pocket called "palatonasal notch". Examination of CT scans of *Kryptobaatar* skull PSS-MAE 101 reaffirms the interpretation of Wible and Rougier (2000) and is thus followed here for *Mangasbaatar* (Fig. 22).

The maxilla has no contribution to the transverse aspect of the palate along the sagittal suture with the palatine. The maxilla is restricted to the bone immediately around the roots of the molars, the alveolar process. Immediately behind the M2, the maxilla contacts the alisphenoid through a sharply serrated suture (Figs 5, 9, 10, 20, 21).

The maxilla is extensively exposed in the orbitotemporal region (Figs 7, 18, 22); its orbital portion is broad and flat with the ascending process forming the medial wall of the orbit and contacting dorsally the lacrimal. The fronto-maxillary suture is extensive and runs obliquely from the anterodorsal aspect of the orbit to the sphenopalatine foramen, which occupies a posteroventral position in the orbit. After reaching the sphenopalatine foramen, the fronto-maxillary suture becomes approximately horizontal and runs posteriorly along the floor of the temporal area toward the sphenorbital fissure. In the deeper part of the temporal area, the frontal is replaced by the orbitosphenoid in its contact with the maxilla. The maxilla also contacts the alisphenoid in the floor of the temporal region. The suture between these two elements is well shown

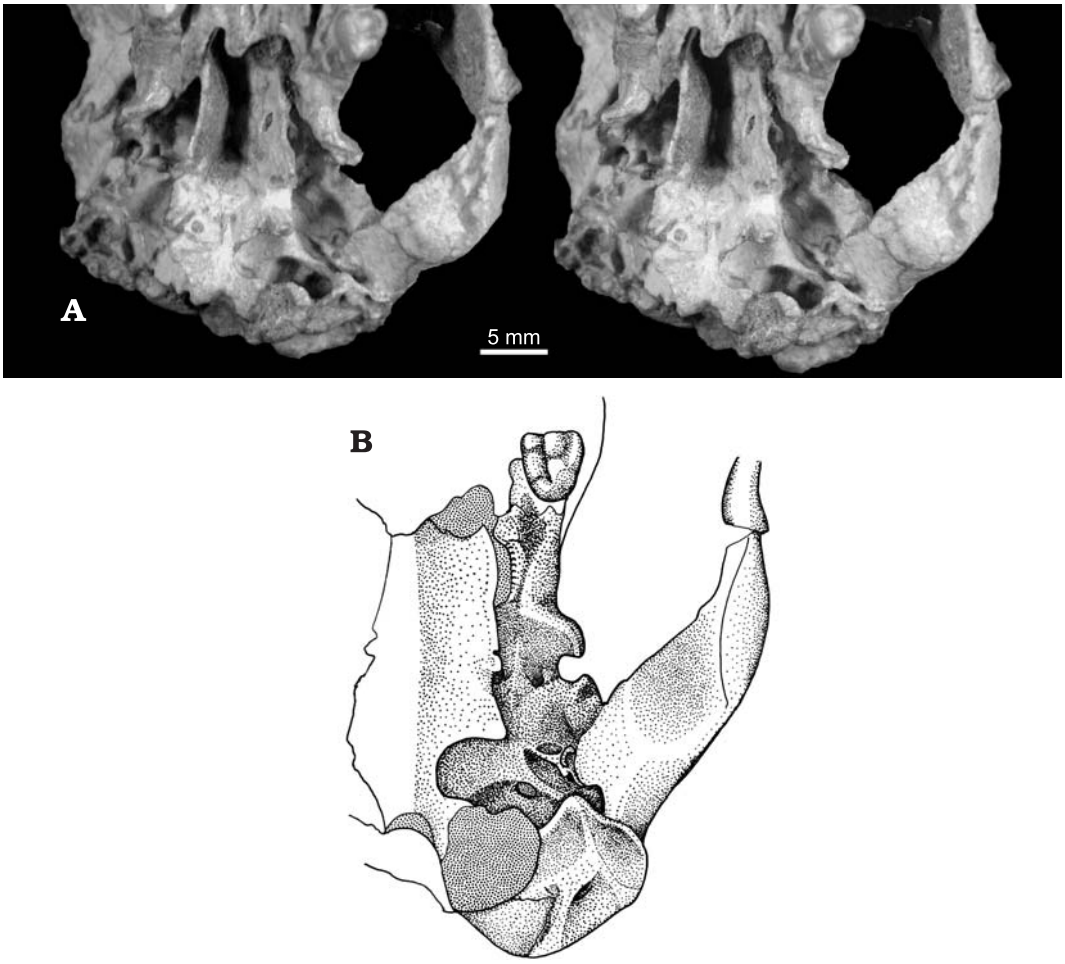

Fig. 9. Holotype of *Mangasbaatar udanii* gen. et sp. n., PSS-MAE 141. Stereophotograph of the basicranium in ventral view (**A**) with explanatory drawing (**B**).

by PSS-MAE 142 (Fig. 18). This serrated contact runs from immediately behind M2 to the lateral edge of the sphenorbital fissure. It follows, from the above-described contacts with the maxilla, that a prong of this bone is wedged between the alisphenoid, frontal, and probably the orbitosphenoid in the floor of the temporal area. This wedge of the maxilla forms a platform, originating in the vicinity of the sphenorbital fissure, which opens and broadens anteriorly to become continuous with the orbital contribution of the maxilla.

The sphenopalatine foramen is large, with a "dumb-bell" shape, and incompletely divided in half by a process that is well preserved only in the right side of PSS-MAE 142 (Fig. 18); the two areas likely represent a proper sphenopalatine foramen and a confluent caudal paltine foramen. The sphenopalatine foramen transmits the sphenopalatine artery and nerve, and the major palatine nerve and artery. Following the pattern in extant mammals (Evans and Christensen 1979), the former pair will occupy the anterodorsal subdivision of the sphenopalatine foramen on its way to the nasal cavity, while the latter pair would occupy the larger posteroventral subdivision of the sphenopalatine foramen on its way to the palate. Along the maxillo-frontal suture on the floor of the orbitotemporal region, there is a broad surface, the sphenopalatine groove, which leads to the sphenopalatine foramen.

As in *Kryptobaatar* (Wible and Rougier 2000) and *Tombaatar* (Rougier *et al*. 1997), there is a small foramen, posteroventral to the sphenopalatine foramen, which transmits the minor palatine nerve and companion vessels from the orbit into the minor palatine foramen of the hard palate. This foramen is preserved only on the right side of PSS-MAE 141 (Fig. 8). In the type specimen of *Tombaatar*, the orbital entrance of the minor palatine nerves and vessels and the minor palatine foramina are connected by a groove on the maxilla that is open to the choanae, and therefore leaves no doubts that the "palatonasal notch" transmitted a structure to, or from, the orbit to the palate; the status of this feature is *Mangasbaatar* cannot be ascertained.

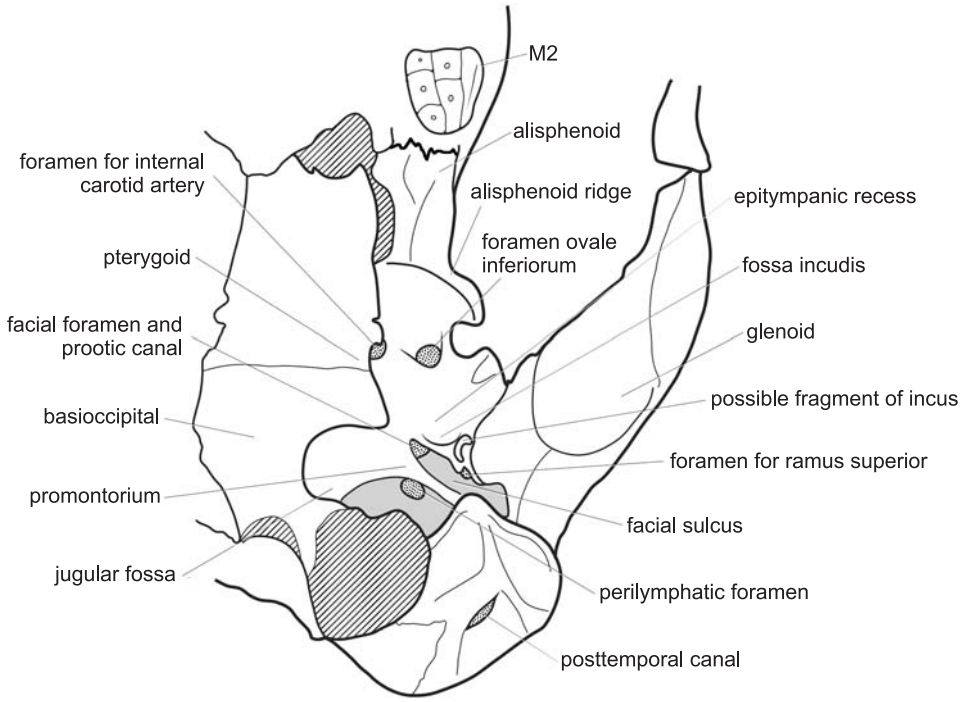

Fig. 10. Holotype of *Mangasbaatar udanii* gen. et sp. n., PSS-MAE 141. Line drawing of the basicranium in ventral view. Light shaded area, common space of the middle ear, eustachian tube, epitympanic recess and exit of V3 branches. Dark shaded area represents a postpromontorial tympanic sinus divided by the crista interfenestralis.

Palatine. — The palatine is well preserved in both PSS-MAE 141 and 142 (Figs 3–5, 16, 17). In *Mangasbaatar* the palatine is exposed only in the palate. There is no orbital exposure of this bone as in most other LCMM, with the possible exception of *Nemegtbaatar* (Hurum 1998a). Right and left palatines meet in the sagittal plane to form a sharp median crest that preserves an open suture throughout its length. The crest becomes taller posteriorly where it meets the robust postpalatine torus. The palatine is essentially flat between the median crest and its lateral contact with the maxilla.

Bordering the ventrolateral margin of the choanae is a massive postpalatine torus (Figs 5, 17). This is an unusually complex structure that resembles that of *Tombaatar*. The torus begins anteriorly at the level of the M1–M2 embrasure, where it rises abruptly from the palate. The torus is formed by two distinct wings, right and left, which project ventrally to the level of the occlusal plane. The wings are concave posteriorly and are limited medially by two sharp crests that result from the bifurcation of the median crest described above in the anterior portion of the palatine. Between these two crests that form the medial edge of the wings of the torus there is a deep recess occupying the midline. The function of this elaborate torus in *Mangasbaatar* is uncertain. The posterolateral corner of the torus extends posteriorly on the sides of the choanae through a "splint"-like process directly medial to the alisphenoid. This posterior extension of the palatine into the choanae is preserved only in PSS-MAE 141.

Nasal. — The nasals are large paired bones that form the roof of the nasal cavity. They are in contact with each other medially, with the premaxillae and maxillae laterally, and with the frontals posteriorly (Figs 2, 15, 19). Erosion of the dorsal surface of PSS-MAE 141 has destroyed most of the nasals, leaving the crest and sutures that projected into the nasal cavity. The overall features of the nasal are preserved mostly as natural molds. Enough remains, however, to show that the nasals become broader posteriorly and are overlapped by the frontals.

In PSS-MAE 141 (Fig. 2), the dorsal surface of the nasal cavity and the paranasal sinuses are exposed because of missing nasals and maxilla. Along the suture between nasal and maxilla, there is a ridge of bone that projects ventrally into the nasal cavity. This roughly parasagittal ridge is the remnant of the nasoturbinal ridge. Throughout its length, the nasal seems to be mostly cancellous bone with only a thin, dense layer of cortical bone. Based on natural endocasts (Rougier and Novacek 1997) and CT scanning of other Mongolian multituberculates like *Kryptobaatar* (PSS-MAE 101), it is likely that those intranasal cavities were con-

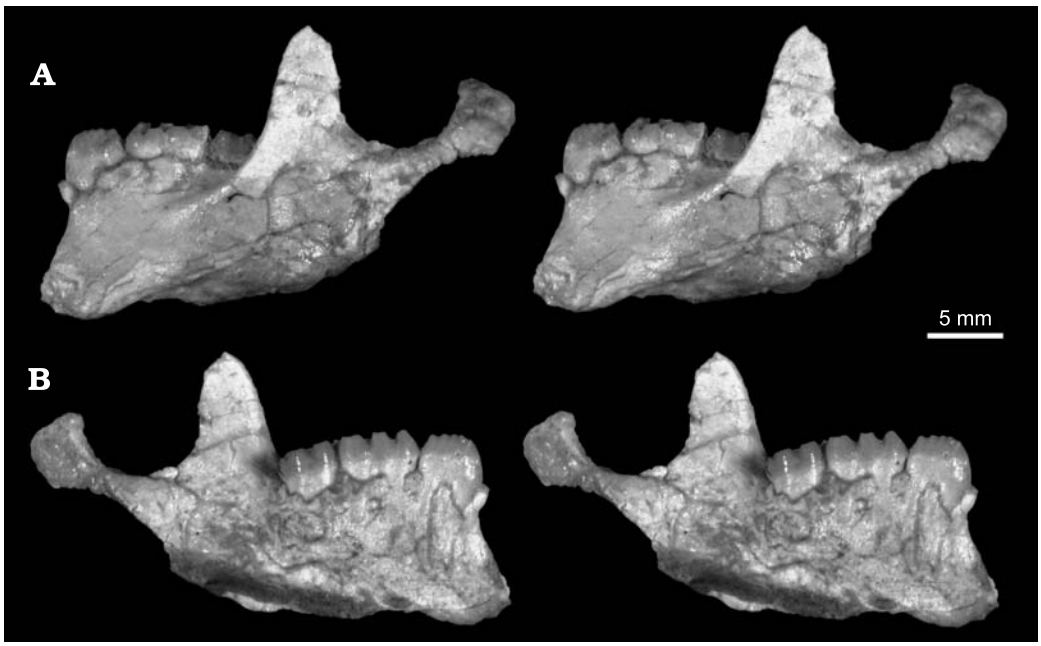

Fig. 11. Holotype of *Mangasbaatar udanii* gen. et sp. n., PSS-MAE 141. Stereophotographs of the left dentary in buccal (**A**) and medial (**B**) views.

nected to the nasal cavity, indicating an extreme degree of pneumatization of the multituberculate skull. The great development of pneumaticity is frequently reflected by the preservation of the specimens. When found as isolated specimens, the skulls are often missing the thin cortical bone forming the outer surface of nasals, frontals and parietals.

In the specimen PSS-MAE 142 (Figs 15, 18), the posterior one-third of the right nasal is well preserved, as is a small portion of the left nasal. Along the midline, right and left nasals are separated by a broad prong of the frontals that extends anteriorly at about the level of the lacrimal. This process of the frontal and the concomitant separation of the back part of the nasals is a primitive feature for mammals, present in various degrees almost universally among Mesozoic forms. *Catopsbaatar* has a more transverse nasal-frontal suture than most other LCMM (Kielan-Jaworowska *et al*. 2005). Not enough is preserved to determine the number of nasal foramina, but judging from the natural endocast it is likely that at least one relatively large foramen was present.

Lacrimal. — Portions of the lacrimal are preserved in both specimens, the most complete being the right side of PSS-MAE 142 (Figs 15, 18, 19, 22). The external exposure of the lacrimal is subrectangular and is wedged in the orbital margin between frontal and maxilla. The nasal contacts the lacrimal along its anteromedial edge. The lacrimal contribution to the orbital mosaic cannot be fully ascertained, but it is clear that it was restricted to the dorsal portions of the orbit without extensive ventral projection. The lacrimal was, however, involved in the formation of a very deep orbital pocket and sharp orbital ridge for the attachment of the anterior portion of the anterior portion of the superficial masseter muscle (Gambaryan and Kielan-Jaworowska 1995). Remnants of a bifid nasolacrimal canal are present on the right side of PSS-MAE 142 and most of its course can be traced through the denuded skull roof of the left side of PSS-MAE 141.

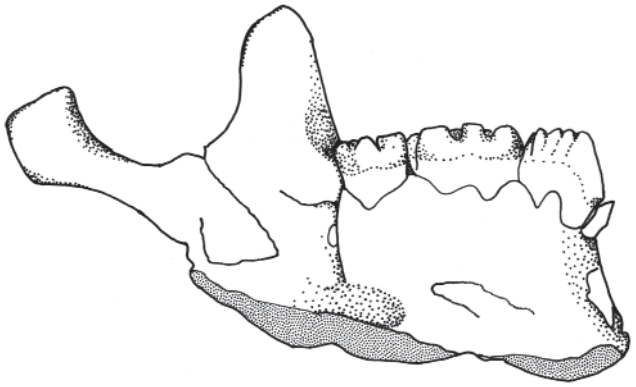

Fig. 12. Holotype of *Mangasbaatar udanii* gen. et sp. n., PSS-MAE 141. Illustration of the dentary in medial view.

Frontal. — Most of the contribution of the frontal to the skull roof is missing in PSS-MAE 141 (Fig. 2); however, the orbital portions of this bone are well preserved (Figs 7, 8). The right frontal in PSS-MAE 142 is mostly complete (Fig. 15). Sutures in the skull roof are well shown by PSS-

Fig. 13. Holotype of *Mangasbaatar udanii* gen. et sp. n., PSS-MAE 141. Stereophotograph of the dentary in occlusal view.

MAE 142 but those in the orbit are somewhat ambiguous in both specimens, especially in the area near the sphenorbital fissure. The frontal is the largest component of the skull roof and extends roughly from the level of the anterior root of M1 until the posterior one-third of the braincase. This moderately convex bone is slightly raised in the midline where it contacts the frontal from the other side via an open suture. Anteriorly, the frontal is wedged between the nasals and anterolaterally contacts the lacrimal. The parietal demarcates the posterior expansion of the frontal. The frontals contact the parietals through a broad V-shaped suture extending from just in front of the postorbital process backwards (Fig. 15). The frontal forms the dorsal-most portion of the rugose orbital edge. The lateralmost extension of the dorsal orbital rim is damaged in both specimens; however, the right side of PSS-MAE 142 may preserve some evidence of this feature.

In the orbit (Figs 8, 18, 22), the frontal forms most of the posteromedial wall, contacting the orbitosphenoid throughout much of its length and reaching the dorsal-most aspect of the anterior lamina through a narrow process. The frontal-orbitosphenoid suture forms a gentle arch from the floor of the orbitotemporal region to the dorsal portion of the anterior lamina. Approximately in the middle of this arch, there is a large foramen formed jointly by frontal and orbitosphenoid, the ethmoidal foramen; grooves from above and below the foramen lead to it. The one from below, the larger of the two, starts in the sphenopalatine groove and through a

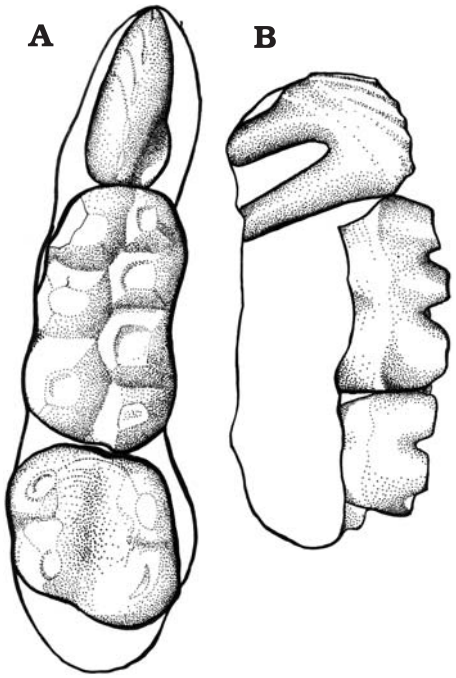

Fig. 14. Holotype of *Mangasbaatar udanii* gen. et sp. n., PSS-MAE 141. Illustrations of the lower dention in occlusal view (**A**) and fragment of the right dentary in lateral view (**B**).

gentle curve reaches the ethmoidal foramen from directly below. This groove follows the likely course of the frontal-orbitosphenoid suture in the area and it was likely occupied by the ethmoidal nerve and artery. The groove reaching the ethmoidal foramen from above has a sigmoid shape and is developed mostly above the frontal-orbitosphenoid suture, in the frontal. This groove is continuous with the anterior opening of the orbitotemporal canal, which is broken open on both sides of PSS-MAE 141. The rostral end of the orbitotemporal canal is formed mostly by the frontal and is completed by the parietal, which forms its roof. The likely occupant of this groove was a large orbitotemporal artery and its accompanying vein. A similar pattern is known in most LCMM including *Kryptobaatar* (Wible and Rougier 2000). The anterodorsal portion of the frontal contributes to the orbital ridge and orbital pocket, which is jointly formed by maxilla, lacrimal, and frontal.

Parietal. — The parietal has been mostly eroded away in PSS-MAE 141 (Fig. 2) but most of it is preserved in the right side of PSS-MAE 142 (Fig. 15). The parietal contributes to the posterior one-third of the braincase and helps separate the orbit from the temporal area by forming a postorbital process. The parietal contacts the frontal anteriorly, through the already described broad "V"-like suture anteroventrally with the anterior lamina, posteroventrally with the squamosal, and posteriorly with the supraoccipital. The parietal is slightly convex dorsally. This feature becomes more pronounced laterally than in the midline. Right and left parietals are separated by a suture that is difficult to trace because of partial fusion between these bones.

Temporal lines, for the attachment of the temporal muscle, are present but are not very sharp and they do not meet each other to form the sagittal crest. Instead, they contact the lambdoidal crest parasagittally. The temporal lines originate from the posterior edge of the postorbital process and extend posteromedially forming a broad arch. The relatively lateral position of the temporal lines implies a proportionally small area for the temporalis muscle, much smaller than that in other forms with a sagittal crest such as *Kryptobaatar* (Wible and Rougier 2000).

The parietals are the sole elements forming the median portions of the lambdoidal crests (*i.e.*, there is no supraoccipital participation). These crests are minimally developed sagittally but flare out and become quite large laterally. This development of the lambdoidal crests begins on the lateral portions of the parietal contribution to these crests and becomes more pronounced in the squamosal/petrosal portion of the crests.

As in all the other LCMM, the postorbital process is formed in its entirety by the parietal. It is preserved in its full length only on the left side of PSS-MAE 141 (Fig. 2). The process is inordinately long at 10.2 mm (measured from the root of the process). A very long process of similar dimensions is present in *Catopsbaatar* (Kielan-Jaworowska 1974, 1994), another large LCMM probably related to both *Tombaatar*, and *Mangasbaatar* (Rougier *et al.* 1997; Kielan-Jaworowska and Hurum 1997).

At the base of the postorbital process is the external opening of the orbitotemporal canal, which has already been described as being formed jointly by the frontal and parietal. The orbitotemporal canal is open internally into to the braincase as shown by the endocast of the skull PSS-MAE 141. The parietal forms the roof of the canal but the canal has no floor and is open internally into the cranial vault, until it reaches the petrosal in the back portion of the braincase (see below).

Squamosal. — The squamosal has sustained damage in both specimens, but the one on the left side of PSS-MAE 141 is the most complete (Figs 2, 7). The squamosal can be subdivided into two portions: the squama abutting the braincase, and the zygomatic process contacting the maxilla and bearing the glenoid fossa. The squamosal contacts the maxilla anteriorly, the petrosal medially, and the parietal dorsally.

As in all other multituberculates, the zygomatic arch is formed mostly by the squamosal and the maxillary bone, with a reduced jugal on the medial side of the zygoma (Hopson *et al.* 1989; Wible and Rougier 2000,

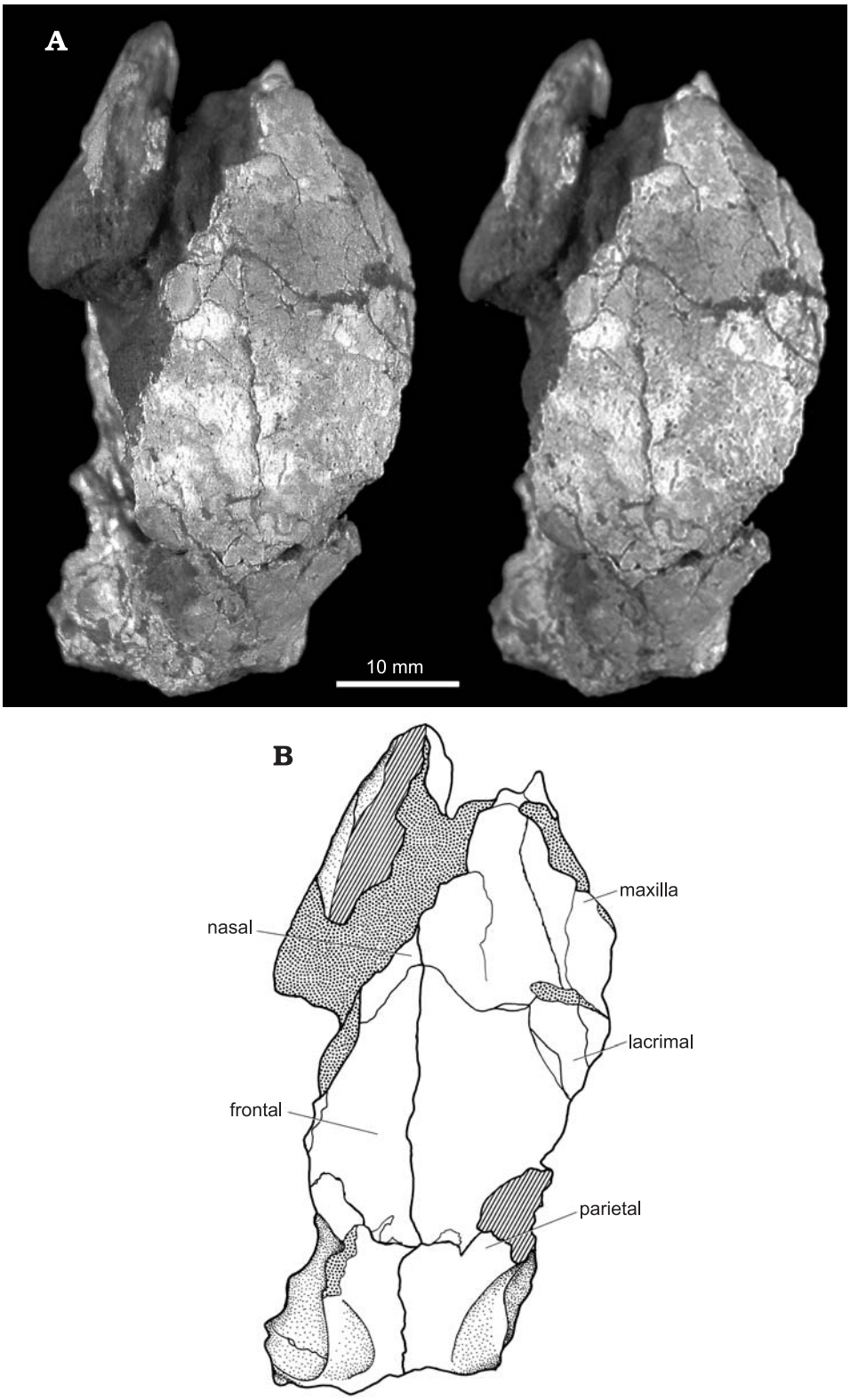

Fig. 15. *Mangasbaatar udanii* gen. et sp. n., PSS-MAE 142. Stereophotograph of the skull in dorsal view (**A**) and explanatory drawing (**B**). Dotted pattern represents matrix; parallel lines represent damaged surfaces.

fig. 32), or sole by these two bones, without the jugal. In *Mangasbaatar*, due to the posterior location of the orbit, the zygomatic arch is very short and throughout its length forms the ventral edge of the relatively small orbitotemporal fossa, characteristic of LCMM (Fig. 22). In other LCMM, a very small jugal has been described as occupying the medial surface of the arch (Hopson *et al.* 1989; Wible and Rougier 2000), but preser-

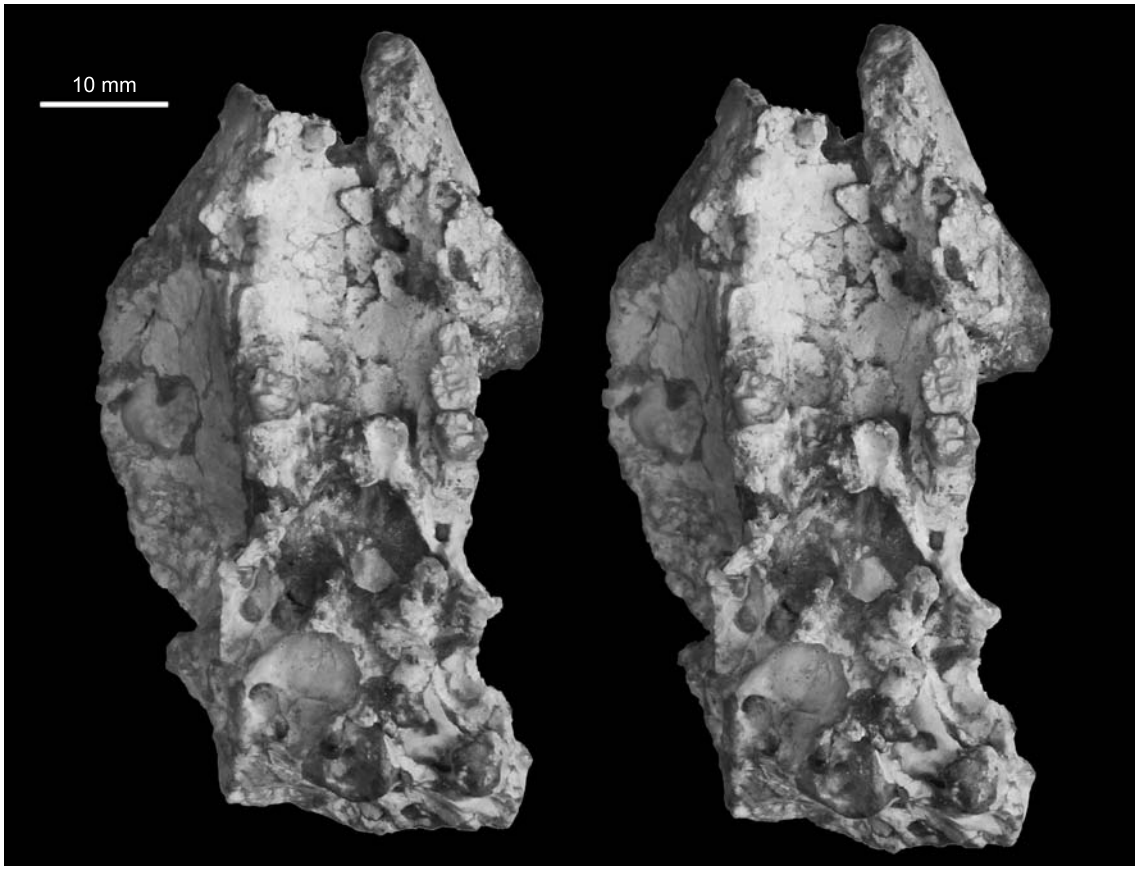

Fig. 16. *Mangasbaatar udanii* gen. et sp. n., PSS-MAE 142. Stereophotograph of the skull in ventral view.

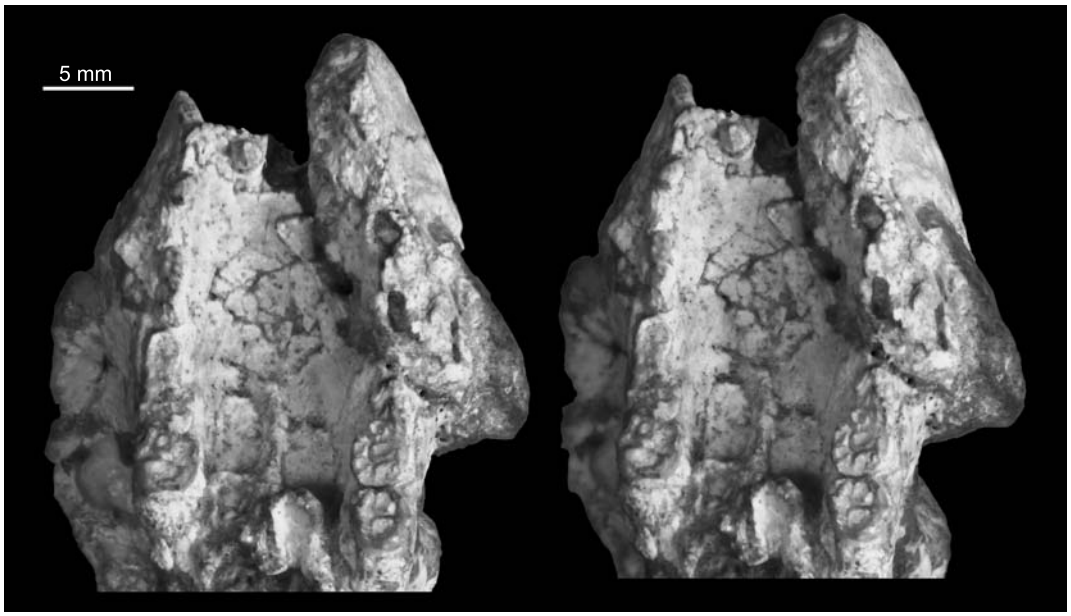

Fig. 17. *Mangasbaatar udanii* gen. et sp. n., PSS-MAE 142. Stereograph of the palatal region in ventral view.

vation in PSS-MAE 141 and 142 is not sufficient to confirm or deny the presence of this element. The contact of the squamosal with the maxilla occurs through a relatively long and oblique suture seen on the left side of PSS-MAE 141 that reaches anteriorly to the level of the anterior edge of the orbit. The shape of the anterior portion of the zygomatic process is very conspicuous and characteristic of *Mangasbaatar* and *Catopsbaatar* (*Tombaatar* unknown); unlike other LCMM the squamosal achieves its maximum dorsoventral development at the posterior end, achieving a greater height than the lowest part of the zygomatic process.

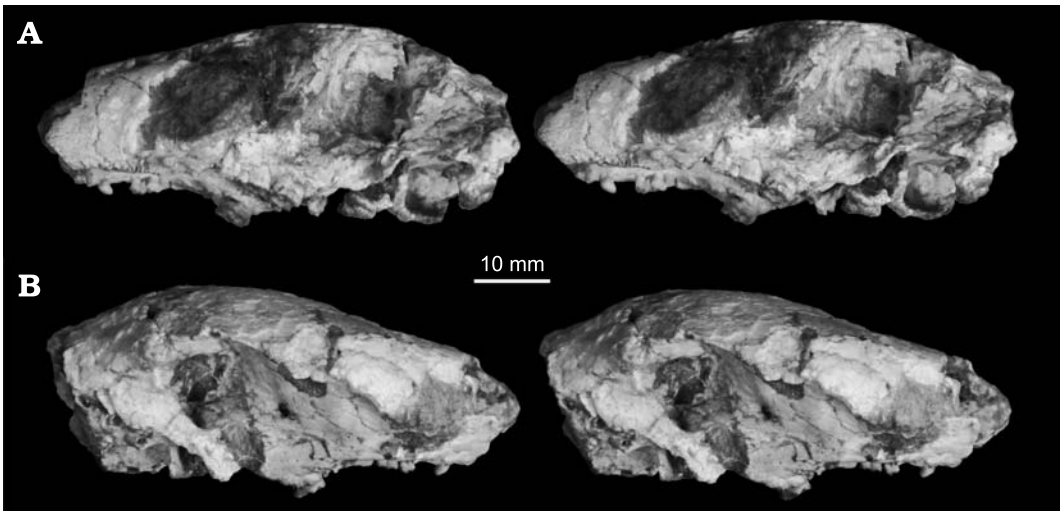

Fig. 18. *Mangasbaatar udanii* gen. et sp. n., PSS-MAE 142. Stereophotographs of the skull in lateral view from the right (**A**) and left (**B**) sides.

Most of the lateral surface of the very short zygomatic process of the squamosal is occupied by a concave surface limited dorsally by a blunt ridge. This is the intermediate zygomatic ridge, which might marginally extend into the maxillary's contribution to the zygomatic arch. Behind the intermediate zygomatic ridge, the squamosal becomes narrower and more robust, forming a neck connecting the glenoid with the braincase. The glenoid is best seen in ventral view (Figs 3, 9, 10, 20, 21) and is teardrop-shaped with its broader portion oriented posteriorly. There is no post-glenoid ridge, but a broad crest continuous with the lower edge of the zygomatic arch marks the lateral extent of the glenoid. The articular surface is mostly flat, with a shallow anterior concavity.

Behind the glenoid, the squamosal neck forms a flat area that ultimately becomes continuous with the epitympanic recess of the petrosal. The medial extension of the neck reaches the braincase, broadens slightly and becomes the squama of the squamosal. The squama overlies the petrosal and does not contribute directly to the braincase proper. The anterior extension of the squama is limited by its contact with the anterior lamina of the petrosal. The suture between these two elements is not very clear in any of these specimens, but it is best on the left side of PSS-MAE 141. The right squamosal of PSS-MAE 142 (Fig. 18) is completely lost, exposing its contact with the underlying petrosal. This specimen shows that the squamosal forms the lateral and dorsal walls of the ascending canal as described in *Kryptobaatar* and *Vincelestes* (Rougier *et al*. 1992; Wible and Rougier 2000). The squama of the squamosal also forms part of the ventrolateral portion of the lambdoidal crest overlying the mastoid exposure of the petrosal.

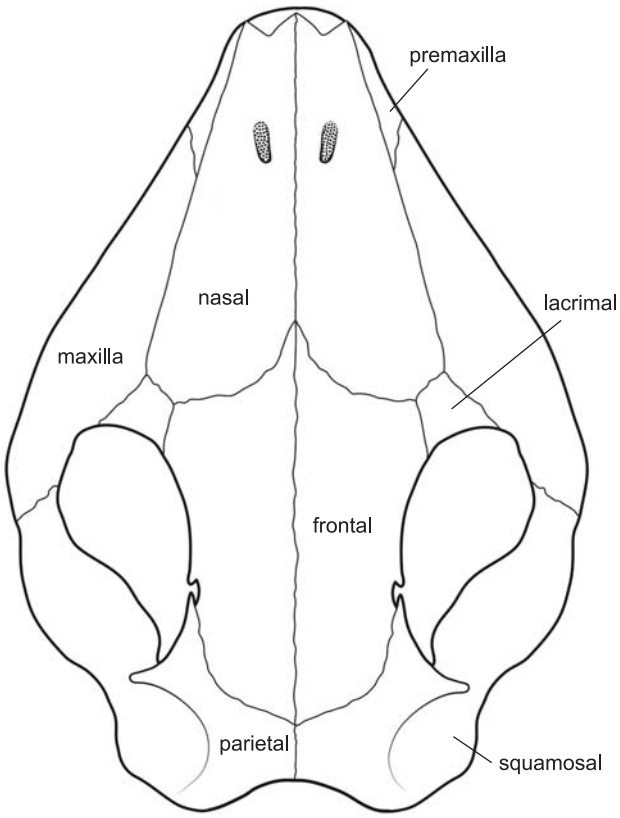

Fig. 19. Reconstruction of the skull of *Mangasbaatar* in dorsal view.

Pterygoid. — The area of the skull presumed to be formed by the pterygoids is preserved only in PSS-MAE 141 (Figs 3, 9, 10) but no sutures are visible in the specimen. This is not to say that sutures were not present, but fractures make recognition of them difficult. In order to describe these elements

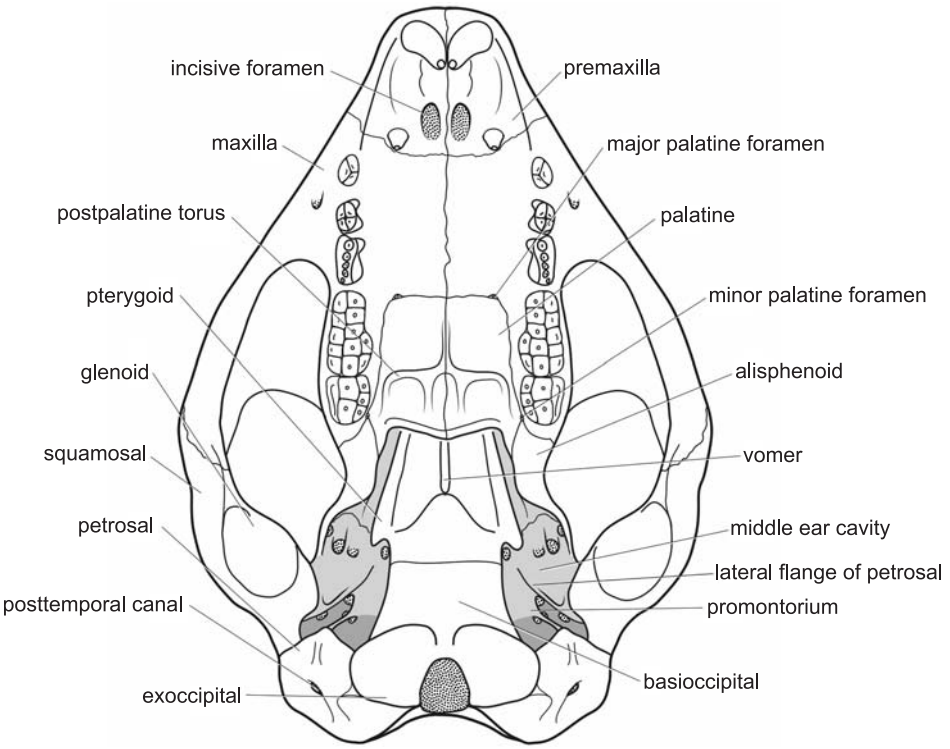

Fig. 20. Reconstruction of the skull of *Mangasbaatar* in ventral view.

in *Mangasbaatar*, particular reference is given to the morphology present in other LCMM. Specifically, the pterygoids are interpreted as forming the two tall, parasagittal flanges present in the choanae following a similar pattern as seen in *Kryptobaatar* (Wible and Rougier 2000). There is a suture at the level of the posterior extent of the pterygoids connecting right and left elements. Behind this suture and between the flanges of the pterygoids there is a triangular element on the roof of the choanae interpreted as the basisphenoid. If this interpretation is correct the pterygoids would meet along the midline, in front of the vomer, and they would be separated by the latter along the posterior one-third of their length.

The pterygoid flanges are tall and subdivide the choanae into three passages: a broad median palatine groove, between right and left laminae, and two lateral palatine troughs, between the pterygoid lamina and the lateral walls of the choanae formed by the alisphenoid. In other multituberculates, like *Chulsanbaatar*, *Nemegtbaatar* (Kielan-Jaworowska 1971; Gambaryan and Kielan-Jaworowska 1995) and *Kryptobaatar* (Wible and Rougier 2000) the medial passage is partially subdivided in two by the mid-line vomers and therefore a total of four channels are present. The full anterior extent of the pterygoid laminae cannot be traced into the choanae because the left one is incomplete and the right one is obscured by matrix. The lamina ends posteriorly in a short, rounded process separated from the main portion of the lamina by a shallow notch. This notch and process are likely to be homologous to the hamular process, serving as a "pulley" for the *m. tensor veli palatini*, a muscle originated from the primitive pterygoid musculature of non-mammalian cynodonts (Barghusen 1986).

In the lateral palatine troughs, which are between the pterygoid laminae and the walls of the choanae, the pterygoid forms most, or all, of the roof and medial walls of the enormously excavated lateral connection of the nasopharynx and the middle ear; this space serves as an equivalent of the eustachian tube of extant mammals. The exact contribution of the pterygoids to this region, however, cannot be fully determined.

Sphenoid. — The sphenoid is at least partially preserved in both specimens and lacks a full complement of sutures delimiting its individual components, namely the presphenoid, alisphenoid, orbitosphenoid, and basisphenoid (Figs 3, 16). The individual names will be used here in reference to the identified sutures and to standard anatomical areas formed by these components in other mammals for which the embryological origin of the individual elements is known or presumed.

The alisphenoid has contributions to the palate, choanae, mesocranial region, and middle ear cavity (Figs 20, 22). The three-dimensional arrangement of the alisphenoid is complex so that this element is exposed in

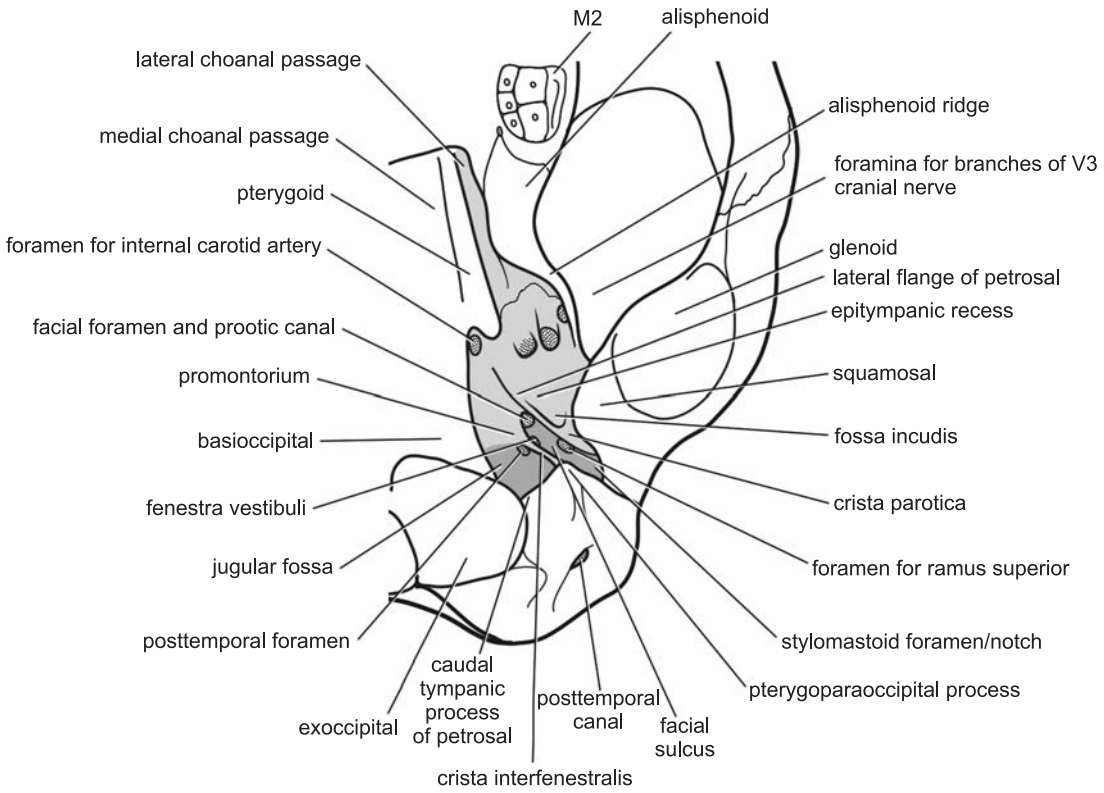

Fig. 21. Reconstruction of the basicranium of *Mangasbaatar* in ventral view.

ventral and lateral views, in addition to a sizeable portion around the sphenorbital recess that is not accessible in any of these views.

The alisphenoid is the portion of the sphenoid forming the lateral wall of the braincase in most mammals. In multituberculates, the alisphenoid is small (Kielan-Jaworowska 1971; Kermack and Kielan-Jaworowska 1971; Kielan-Jaworowska *et al*. 1986; Wible and Rougier 2000), probably reduced from a primitive condition in which it was large (Hopson and Rougier 1993; Rougier and Wible 2006). This reduced alisphenoid in multituberculates forms a small portion of the anteroventral area of the lateral wall of the cavum epiptericum (Kermack and Kielan-Jaworowska 1971). In *Mangasbaatar*, the alisphenoid, as recognized here, is also small and its braincase contribution is limited to the area surrounding the cavum epiptericum. The alisphenoid, however, has a long anterior process that reaches the back of the palate (Figs 5, 16, 17). The alisphenoid contacts the palatine, maxilla, pterygoid, and petrosal, and it becomes confluent with the basisphenoidal and orbitosphenoidal portions of the sphenoid. In ventral view, the most prominent feature of the alisphenoid is its anterior process that extends to the hard palate. A little slip of the alisphenoid forms part of the minor palatine foramen and wedges its way between the maxillary and palatine contributions to the rim of the foramen (Fig. 21). The anterior process of the alisphenoid has been described as having a Möbius strip shape (Wible and Rougier 2000), resembling the shape of a twisted ribbon. The alisphenoid of *Mangasbaatar* presents the same basic shape and, because of this "twisting" of the anterior process, the anterior, ventrally oriented surface becomes laterally oriented towards the back. This anterior portion of the alisphenoid is concave contacting anteriorly the maxilla. The medial limit of the alisphenoid in this area is formed by a ridge running along the edge of the choanae and its posterior limit is a tall and sharp crest that also bounds the middle ear cavity, this is the alisphenoid ridge (Fig. 21). This concave anterior surface is likely to provide the attachment for the medial pterygoid musculature. The alisphenoid is also likely to contribute to the formation of the lateral choanal passage or trough and contact the pterygoid in doing so. However, preservation in both specimens is deficient in this area and the morphology of the lateral wall of the choanae is, to some degree, uncertain.

Behind (distal to) the alisphenoid ridge in the alisphenoid is the middle ear contribution of the alisphenoid. The alisphenoid forms approximately one-fourth of the epitympanic recess. The alisphenoid portion of the epitympanic recess is restricted to the anterior pole of this cavity, forming the very prominent anterior and lateral walls of the recess. A thin, narrow process projects back medial to the petrosal contribution to the

epitympanic recess to almost reach the tip of the promontorium. Preservation on PSS-MAE 141 is not very satisfactory in this region; it is clearer to follow the morphology in PSS-MAE 142 (Figs 17, 20, 21). In the epitympanic recess, there are two large foramina for branches of V_3. The most anterior of these foramina is very near the serrated alisphenoid-petrosal suture, but the foramen is formed solely by the petrosal.

In lateral view, the alisphenoid is limited posteriorly by the tall ridge that marked the posterior edge of the Möbius strip in ventral view. The alisphenoid in this view (lateral) is the continuation of the alisphenoid surface immediately behind the palate in ventral view. The lateral aspect of the alisphenoid is best shown on the left side of PSS-MAE 142 (Fig. 18) and the right side of PSS-MAE 141 (Fig. 8). This surface is concave dorsally and anteriorly, extending toward the sphenorbital recess medial to the anterior lamina. This surface of the alisphenoid is broader anteriorly and tapers posteriorly. There is a small foramen anteriorly directed in the anterior lamina-alisphenoid suture or in its proximity depending on the specimen. Similar variation has been reported for *Kryptobaatar* (Wible and Rougier 2000). The foramen is lodged in a deep recess and, leading anteriorly from it, there is a deep groove. Given the orientation and position of the foramen, it is likely that this structure conveyed the buccal branch of the trigeminal nerve (V) and it is thus identified here (Figs 18, 22) as the foramen buccinatorium, which also occurs among other multituberculates (Kielan-Jaworowska *et al.* 1986; Hurum 1998b; Wible and Rougier 2000). Posteromedially from the foramen buccinatorium, the alisphenoid occupies the floor of the sphenoidal recess. Laterally, it contacts the tall petrosal wall that guards the lateral extension of the sphenoidal recess. Sutures between the anterior lamina of the petrosal and the alisphenoid in this area are not apparent.

The orbitosphenoid portion of the sphenoid is a laminar process that forms the medial wall of the orbitotemporal fossa connecting the skull base with the elements forming the skull roof and the rear of the nasal cavity (Figs 7, 8, 18, 22). The orbitosphenoid contacts the frontal dorsally and anteriorly, the maxilla anteriorly, the anterior lamina posteriorly, and is continuous with the rest of the sphenoid posteromedially. The orbitosphenoid has extensive contact with the frontal, and together these bones form the ethmoidal foramen in the anterodorsal aspect of the temporal area. The dorsal suture with the frontal is shown in the right side of PSS-MAE 141. It is a smooth line running obliquely from the vicinity of the anterior opening of the orbitotemporal canal to the ethmoidal foramen (Fig. 22). The contact between frontal and orbitosphenoid under the ethmoidal foramen, as already mentioned, is less clear. With the exception of the left side of PSS-MAE 141, most of the orbitosphenoid spanning from the sphenoidal recess to the ethmoidal foramen is missing in both specimens. The left side of the skull PSS-MAE 141, however, is crushed and the suture pattern cannot be made out.

The orbitosphenoid abuts the medial aspect of the anterior lamina and forms the medial edge of the sphenorbital fissure. In PSS-MAE 142 the skull is deformed so that the fissure and its contents can be clearly seen, through the artificially enlarged fissure. The sphenorbital fissure is a large, oval-shaped foramen leading anteriorly and cannot be seen in lateral view, due to the lateral extension of the anterior lamina and alisphenoid, broken portions of these bones alow partial views of the fissure in PSS-MAE 141 and 142 (Figs 7, 8, 18) The sphenorbital fissure transmits the contents of the cavum epiptericum into the orbit including V_1, V_2 branches and the nerves to the eye muscles (II, IV, VI). Directly medial to the edge of the sphenorbital fissure, and slightly above its midpoint, there is a small foramen piercing the orbitosphenoid. This foramen is interpreted here as transmitting the oculomotor nerve (III). The multituberculates *Chulsanbaatar*, *Nemegtbaatar*, *Kryptobaatar*, and *Sloanbaatar* Kielan-Jaworowska, 1970 have been identified as having a separate foramen for cranial nerve III (Hurum 1998b; Rougier *et al.* 1997; Wible and Rougier 2000). Medial to the oculomotor foramen, slightly above its level, in the deepest part of the orbit, there is a circular foramen in both specimens PSS-MAE 141 and 142: the optic foramen. A broad, shallow sulcus extends anterodorsally from the optic foramen, grooving the external surface of the orbitosphenoid. The portion of the orbitosphenoid directly in front of and ventral to the optic foramen is the jugum sphenoidale (Wible and Rougier 2000), which, in multituberculates, is relatively narrow and proportionally tall. This is also the condition in *Mangasbaatar*. Anteroventral to the optic foramen, there is another foramen of relatively large size in both specimens that penetrates the substance of the sphenoid. This corresponds to the transverse canal identified in *Kryptobaatar* (Wible and Rougier 2000). The size of the transverse canal in *Mangasbaatar* is substantial and it grooves, slightly, the floor of the sphenorbital recess.

The orbitosphenoid appears to have been convex externally and would have essentially provided support (ventrolateral) for the frontal lobes of the brain. The orbitosphenoid contacts the anterior lamina immediately under the anterior opening of the orbitotemporal canal. The suture between these two elements is best shown

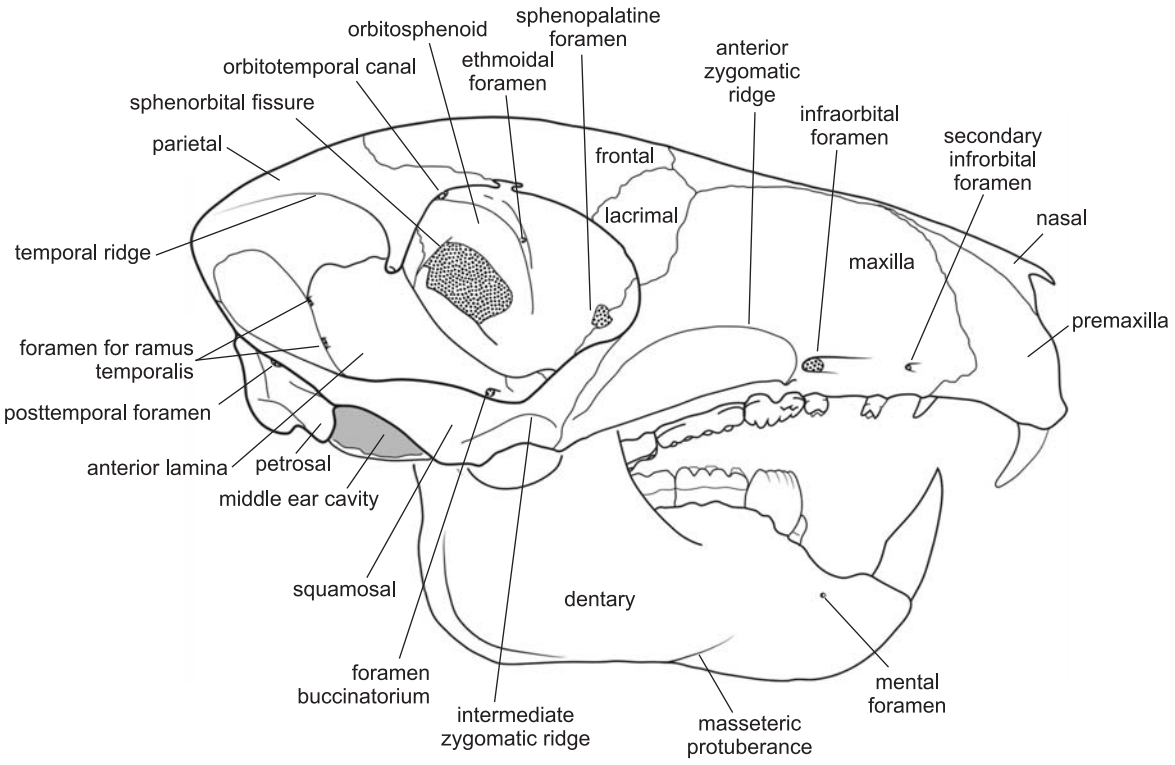

Fig. 22. Reconstruction of the skull and mandible of *Mangasbaatar* in lateral view. The mandible is in occlusion with the skull in expected life position.

on the right side of PSS-MAE 141. This suture is heavily interdigitated and runs almost vertically down towards the sphenorbital recess, but the ventral portion of the suture is not recognizable.

The presphenoid, if present in *Mangasbaatar*, is not recognizable in the specimens currently available. What remains of the sphenoid can be vaguely identified as part of the basisphenoid. It has a relatively small exposure in ventral view and a more substantial one in the area of the sphenorbital recess. The ventral exposure contacts the pterygoids, petrosals, and basioccipital. The orbital exposure is in contact with the alisphenoid and the anterior lamina, and possibly the maxilla.

The ventrally exposed basisphenoid is subtriangular with a smooth surface and lacks any evidence of carotid foramina (Figs 3, 16, 20). The basisphenoid, as part of the mosaic formed by the pterygoids, alisphenoid, and petrosal, is involved in the formation of the posteromedial wall of the lateral palatine trough. Concomitantly, these elements shape the enormously excavated posterior expansion of the lateral palatine trough, but their individual contributions are unclear.

Petrosal. — The petrosal, or parts thereof, are preserved in both specimens (Figs 3, 9, 10, 16, 24, 25). When viewed aneriorly, it is obvious that both skulls have been somewhat deformed from left to right. This makes observation of the left portion of the ear region, in particular, problematic but helps to expose the right sides very satisfactorily. In addition, the right squamosal and part of the petrosal are missing in PSS-MAE 141 and 142, helping observation (Figs 24, 25).

In therian mammals, the petrosal can be divided into two main portions: the pars cochlearis, housing the organs of hearing; and the pars canalicularis, housing the organs of equilibrium and balance. Breakage through the petrosal exposes some of these components of the inner ear in both skulls. A third element, the anterior lamina, is described here jointly with the petrosal. Among living mammals, monotremes are the only group presenting this structure (Kermack and Kielan-Jaworowska 1971; Griffiths 1978; Zeller 1989). In monotremes, the anterior lamina results from the ossification of the lamina obturans, which fuses at various stages of development with the endochondral petrosal (Presley and Steel 1976; Griffiths 1978; Presley 1981; Kemp 1983; Kuhn and Zeller 1987a, b; Zeller 1989; Hopson and Rougier 1993). Although the presence of an anterior lamina has been widely documented among basal mammaliaforms, thus far no sutural distinction between the anterior lamina and the petrosal proper has been identified. In multituberculates, these ossifications seem to be continuous. However, without developmental evidence, it cannot be excluded that the

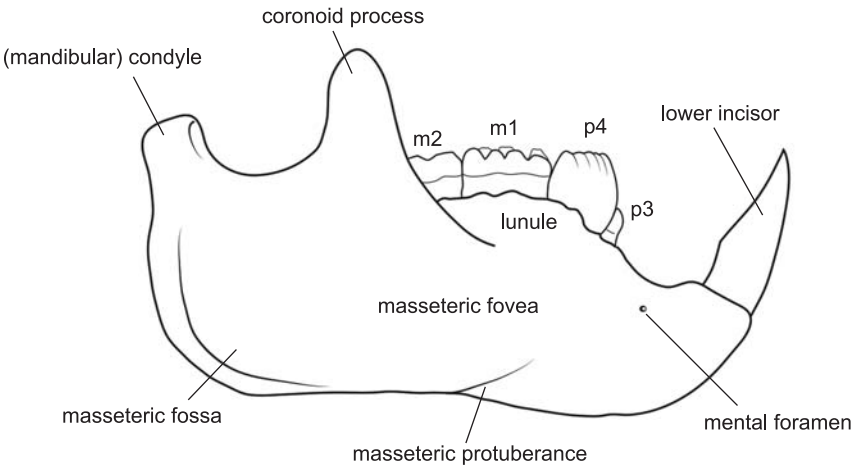

Fig. 23. Reconstruction of the jaw (lateral view) of *Mangasbaatar*.

anterior lamina and the petrosal were separate ossifications embryonically, but fused in adult. Nor is there evidence to reject a developmental fusion of the two. Nonetheless, considering the evidence afforded by monotremes, it is most parsimonious to assume a similar fundamental pattern in multituberculate mammals. As the petrosal proper and the anterior lamina cannot be strictly differentiated, and in order to be consistent with treatment of this area by other authors, the anterior lamina will be described as part of the petrosal (see Rougier and Wible 2006 for a review).

In lateral view (Figs 7, 18, 22), the petrosal contacts the basisphenoid anteriorly and medially, the frontal anteriorly, the parietal dorsally, and the squamosal posteriorly and laterally. In occipital view, the petrosal contacts the exoccipital and the supraoccipital medially, while contacting the squamosal dorsally. In ventral view (Figs 3, 9, 10, 16, 21), the petrosal contacts the exoccipital in the middle ear recess, basioccipital medially, basisphenoid, alisphenoid, and pterygoids anteriorly, and squamosal laterally.

None of the specimens show the endocranial surface of the petrosal and, therefore, its description will be limited to three views: lateral, ventral, and occipital. In ventral view, the most distinctive feature is the enormously excavated middle ear cavity. This cavity has an approximate volume of 4 mm^3 (average of four measurements of the left ear region of PSS-MAE 141, other ear regions are too damaged to provide reliable estimates). The middle ear cavity is formed mostly by the petrosal with sizeable contributions from the alisphenoid, basioccipital, and exoccipital. The limits of the middle ear cavity are defined by tall crests that approach each other ventrally and form a partial, but fairly extensive, floor for this cavity. Deeply recessed in this middle ear space, and occupying an approximate central position in it, is an elongated and ventrally bulging prominence, the promontorium. Several crests at the front and back of the promontorium connect it with other structures of the middle ear. Nevertheless, the main axis and bulging of the promontorium reflect the morphology of the finger-like cochlea, which is partially exposed on the right side of PSS-MAE 141. The three-dimensional arrangements of these crests connecting the promontorium to other structures are best preserved in PSS-MAE 142 (Figs 24, 25) because the specimen has sustained less damage to this area. The anterior pole of the promontorium forms a sharp crest that extends ventrally to form an extremely long and robust process, which, on its medial side, is continuous with the middle ear cavity and, on its lateral side, is grooved and is in communication with the epitympanic recess. This very peculiar process in *Mangasbaatar* is produced by elaboration of the rostral tympanic process of the petrosal (RTPP), which is present in other multituberculates such as *Kryptobaatar* (Wible and Rougier 2000). However, its extreme dorsoventral elongation results from a ventral projection of the basioccipital and anterior portions of the petrosal in order to accommodate a grossly enlarged middle ear cavity. The recess of the promontorium and medial margins of the epitympanic recess might also be factors in enlarging the middle ear space and in determining the unusual morphology of the middle ear of *Mangasbaatar*.

The groove on the RTPP opens ventrally at the likely junction of the pterygoids, basioccipital, and petrosal. This notch would accommodate the internal carotid artery (ICA). The ICA leaves no other traces of its presence on the skull base, but it was dorsoventrally oriented and tightly pressed to the lateral wall of the RTPP (Fig. 24). The broad ICA groove bifurcates at the level of the promontorium, sending a branch posteriorly and a larger one anteriorly. The larger branch excavates a recess in the bony floor of the epitympanic

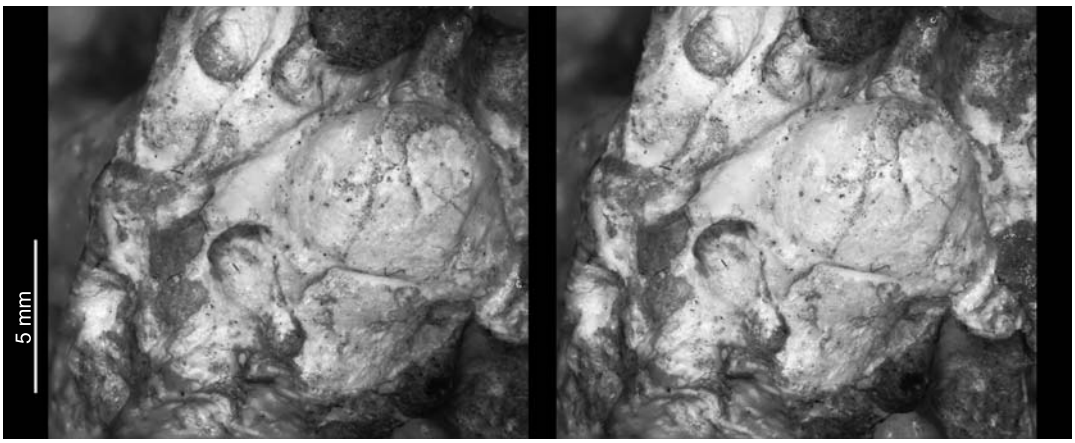

Fig. 24. *Mangasbaatar udanii* gen. et sp. n., PSS-MAE 142. Stereophotograph of the middle ear region of the right side in ventral view.

recess. This recess leads to a canal located between the medial edge of the epitympanic recess and the crest marking the dorsal-most extent of the RTPP (Figs 24, 25). The opening of this canal is the carotid foramen (internal carotid foramen), well shown in the right side of PSS-MAE 141 and 142. A small fragment of bone is in the ICA foramen in PSS-MAE 142, obstructing the view of the ICA canal further into the bone. The ICA foramen is formed solely by the petrosal, but a slender posterior process of the alisphenoid, already mentioned, reaches its proximity (this is best shown on the right side of PSS-MAE 141). The condition in *Mangasbaatar* is different than that presumed to be primitive for members of Djadochtatheriidae, such as *Kryptobaatar*, where the posterior opening of the carotid canal is jointly formed by the petrosal and the alisphenoid before reaching the deeper-lying basisphenoid (Wible and Rougier 2000). Kielan-Jaworowska *et al.* (2005, p. 499) illustrated the carotid foramen in *Catopsbaatar* as exposed ventrally and in a very different position than in *Kryptobaatar* and *Mangasbaatar*; however, in their description they mention that the "carotid foramina have not been preserved" (Kielan-Jaworowska *et al.* 2005, p. 500). The posterior extension of the deep lateral palatine trough extends posteriorly to the edge of the petrosal formed by the RTPP and the carotid foramen.

The posteriorly directed groove originating from the ICA corresponds to the stapedial artery (Figs 24, 25). This extremely rostral position for the stapedial artery is unusual for mammals in general (Wible 1987) but is actually the condition present in all LCMM for which this area is known. This is also probably the case in most other cimolodont multituberculates given that is also present in *Lambdopsalis* (Miao 1988), but basal paulchoffatiids appear to retain the generalized mammalian condition (Hahn 1998). The groove for the stapedial artery is proportionally small and runs along the lateral aspect of the promontorium and ventral to the level of the epitympanic recess. The stapedial groove is shallow in all of the specimens and runs along the ventral edge of the fenestra vestibuli. In the vicinity of the fenestra vestibuli the direction of the groove is ambiguous when considering whether the stapes was columelliform or bicrurated. After traversing the fenestra vestibuli, or running in its vicinity, the stapedial artery is directed toward the common canal for the ramus superior and the prootic sinus.

At the posterior end of the promontorium, there are two fenestrae, one of them laterally positioned (the already mentioned fenestra vestibuli) and the other one medially positioned (the perilymphatic foramen) (Figs 9, 10, 16, 21, 24, 25). The fenestra vestibuli can be observed only on PSS-MAE 142 because those of 141 are obscured. The fenestra vestibuli is subcircular and is hardly recessed, if at all, in a fossula fenestra vestibuli. The stapedial ratio (Segall 1970) is 1.3 (average of right and left side of PSS-MAE 142). The fenestra vestibuli is separated from the perilymphatic foramen by a narrow, posteriorly trending bony ridge, the crista interfenestralis (Wible *et al.* 1995; Rougier *et al.* 1996a, b). The crista projects ventral to the body of the promontorium and marks the ventral-most extension of the petrosal. The back of the promontorium and the crista interfenestralis are damaged on the right side of both specimens. The crista, well-preserved on the left side of PSS-MAE 142 (Fig. 25), remains very tall behind the promontorium and partially subdivides the middle ear cavity into two areas: the first area, lateral to the promontorium, is formed mostly by the epitympanic recess. The second, more medial area, is developed around the jugular foramen and the portion of the middle ear created by contributions of the exoccipital, basioccipital, and petrosal.

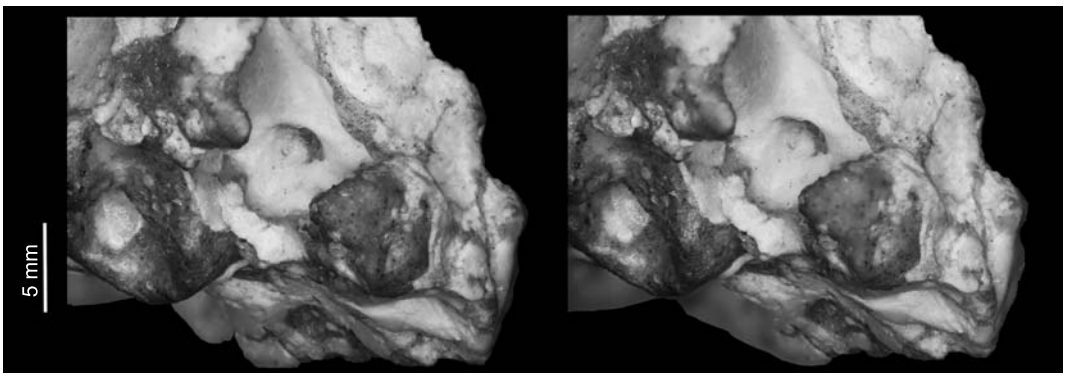

Fig. 25. *Mangasbaatar udanii* gen. et sp. n., PSS-MAE 142. Stereophotograph of the middle ear region of the left side in ventral view.

The medial portion of the middle ear cavity is further subdivided into two realms, an anterior and a posterior one, by a low crest that extends posteromedially from the edge of the perilymphatic foramen. The posterior portion includes the perilymphatic foramen, the jugular foramen, and the exoccipital contribution to the middle ear space. The perilymphatic foramen is lodged in a deeply-excavated recessus scalae tympani. The edges of the perilymphatic foramen are best seen on the right side of PSS-MAE 142 (Fig. 24) and appear to be sharp and particularly well developed on the medial aspect of the foramen. The perilymphatic foramen is oriented posteromedially in its direction with respect to the jugular foramen. The large recessus scalae tympani has its major axis oriented in the same direction. The recessus itself extends to the edge of the jugular foramen. On the right side of PSS-MAE 142, the anterodorsal border of the recessus scalae tympani is marked by a small crest that extends from the vicinity of the perilymphatic foramen to the jugular foramen.

A second crest, in conjunction to the before-mentioned crest, determines a deep groove identified here to have contained the perilymphatic duct. This groove, the perilymphatic sulcus, is almost transformed into a canal by the closely approaching crests mentioned above. It is unsettling, however, to notice that on the left side of the same specimen (PSS-MAE 142), there are no traces of the perilymphatic sulcus, and instead, a poorly developed bulge in the petrosal runs in a similar direction to the groove. The conspicuous absence of the groove on the left side suggests that the perilymphatic duct has been fully enclosed in bone and transformed into a cochlear aqueduct. It is possible that the open groove on the right side is an artifact; the edges of the crests show some breakage, though other portions seem natural. The left side of PSS-MAE 141 (the only side observable for this feature) agrees with the left side of PSS-MAE 142 in showing no traces of a perilymphatic groove. In monotremes the development of the aqueductus cochleae (or lack thereof) differs between *Ornithorhynchus* Blumenbach, 1800 and *Tachyglossus* Illiger, 1811, as shown by the collection of monotremes housed at the American Museum of Natural History (AMNH 252512, AMNH 200255, AMNH 157072). The platypus retains a perilymphatic duct mostly open to the middle ear space throughout life (Zeller 1989), but the echidna closes it later in development. *Zaglossus* Gill, 1877 has, in general, an even more complete enclosure of the perilymphatic duct than the echidna. It is possible that a similar situation happened in *Mangasbaatar*, but the fact that its development seems to be different on left and right sides of the same specimen is problematic. Technically, one side of *Mangasbaatar* should be labelled perilymphatic foramen and the other fenestra cochleae, but this would be confusing; we choose to label associated structures as via the primitive term reflecting the wider presence of this primitive morphology in other multituberculates and the possibility that part of the perylimphatic duct expanded into the middle ear cavity (see below).

The area of the middle ear cavity developed between the perilymphatic groove, the jugular foramen, the hypoglossal foramen, and the crests subdividing the medial portion of the middle ear cavity is slightly concave and essentially featureless. The petrosal forms at least half of the jugular foramen, which is equal in size to the fenestra vestibuli. The presence of a large jugular bulb in *Mangasbaatar* is evidenced by the large depression surrounding the jugular foramen and its endocranial enlargement. A portion of the middle ear, anterior to the crest that subdivides the medial portion of the middle ear cavity, forms the bulk of the middle ear volume and determines a concave median surface for the petrosal by excavating all the elements forming the middle ear roof. The RTPP forms the anterolateral limit of this space.

The petrosal extends laterally and posteriorly from the promontorium to form what can be roughly described as an L-shaped platform (Figs 20, 21, 24, 25). The long arm of the “L” is formed by the epitympanic

recess, and the short one is formed mostly by the caudal tympanic process of the petrosal (CTPP). The epitympanic recess extends from its contact with the alisphenoid anteriorly to the level of the fenestra vestibuli posteriorly. The posteriormost portion of the epitympanic recess is lost from the right side of both specimens and is distorted/incomplete on the left side of both of them. The epitympanic recess is a strongly concave surface that projects ventrally, especially at its anterior pole as it continues into the alisphenoid. Its lateral limits are marked by the ventral edge of the anterior lamina and its medial boundary is formed by a low crest that runs posteromedially and that approaches the promontorium quite closely, especially at the level of the fenestra vestibule (Fig. 24). This posterior portion of the epitympanic recess is formed by the medial folding of the free edge of the lateral flange that contacts the promontoriun, a feature present in all the LCMM and other multituberculate groups (Presley *et al.* 1996; Wible and Rougier 2000; Kielan-Jaworowska *et al*. 2005). Foramina are present in the petrosal contribution to the epitympanic recess (Figs 24, 25). The most anterior one, already mentioned in connection with the alisphenoid, is oval, anteroventrally directed, and placed approximately along the midline of the epitympanic recess. A second, much smaller foramen, seen only on the right side of PSS-MAE 142, is near the lateral edge of the epitympanic recess and is also anteroventrally directed; this foramen is omitted in the reconstruction of the ear region because it is considered an individual variation. A third foramen, of very large size, is centrally positioned in the epitympanic recess, roughly at the level of the internal carotid sulcus. Leading anteroventrally from this foramen, there is a broad, deep sulcus that nearly extends to the anteroventral limits of the epitympanic recess. The three aforementioned foramina of the epitympanic recess likely transmitted branches of the mandibular division of the trigeminal nerve (V_3). The first two foramina are in turn associated with a third foramen that perforates the anterior lamina of the petrosal in lateral view. The three of them can be considered the foramen masticatorium, with two branches directed ventrally and one ventrolaterally.

The big foramen occupying a central position in the epitympanic recess is the foramen ovale inferium (Figs 20, 21). In other multituberculates (Kielan-Jaworowska 1970, 1971; Kermack and Kielan-Jaworowska 1971; Kielan-Jaworowska *et al.* 1986; Hurum 1988b; Wible and Rougier 2000) and in some rodents (Hill 1935; Wahlert 1974, 1985) the mandibular division of the trigeminal nerve is also divided into numerous foramina. Variations in the number, pattern, and size of these foramina seem to be very frequent (Wible and Rougier 2000), but in PSS-MAE 141 and 142 the morphology in this area is consistent. Behind the foramen ovale inferior, the epitympanic recess is walled laterally by the ventral extension of the anterior lamina and at least partially by the squamosal. This region is best preserved in PSS-MAE 141. The medial limit of the epitympanic recess becomes confluent, in this area, with a low crest: the crista parotica, which increases in size posteriorly.

Lateral to the crista parotica, there is a small portion continuous with the epitympanic recess (the space dorsal to the incus and malleus articulation) that is deeper than the surrounding area and it is here identified as the fossa incudis (Fig. 21), for the short crus of the incus. On the left side of PSS-MAE 141, there is a fragment of a small bone, most likely a middle ear ossicle, lying in the fossa incudis. Unfortunately, it is not possible to exactly identify the element. The fossa incudis is fully continuous anteriorly with the epitympanic recess and its posterior limit is formed by the squamosal and the petrosal jointly.

The crest marking the medial limit of the epitympanic recess is connected in the anterior two-thirds of its length to the promontorium. The anterior-most portion of this connection is occupied by the groove for the internal carotid artery. The posterior portion of this connection is almost flat and is notched, only slightly, by the groove for the stapedial artery. The posterior one-third of the crest marking the medial edge of the epitympanic recess is free: the rostral continuation of the crista parotica. At the level of the posterior margin of the fenestra vestibuli there is a small process arising from the medial aspect of the crista parotica, which is ventromedially directed, the tympanohyal. Behind the tympanohyal, there is a shallow notch, the stylomastoid notch, or stylomastoid foramen, which corresponds to the exit of the hyomandibular branch of the facial nerve (CN VII) from the tympanic cavity.

A series of structures occupies the space between the epitympanic recess and the fenestra vestibuli. Posterior to the bony shelf, already described as connecting the epitympanic recess, the petrosal, and the promontorium, there is a deep recess that excavates the lateral surface of the promontorium. This recess marks the likely site of attachment of the *m. tensor tympani* and is identified here as the tensor tympani fossa. The tensor tympani fossa in *Mangasbaatar* seems to be proportionally small in relation to the size of the middle ear as compared with *Kryptobaatar* (Wible and Rougier 2000; Fig. 26).

In other LCMM, the facial nerve opening into the middle ear and the prootic canal opening into the middle ear are found behind the tensor tympani fossa. This area is preserved on the left side of PSS-MAE 141 and

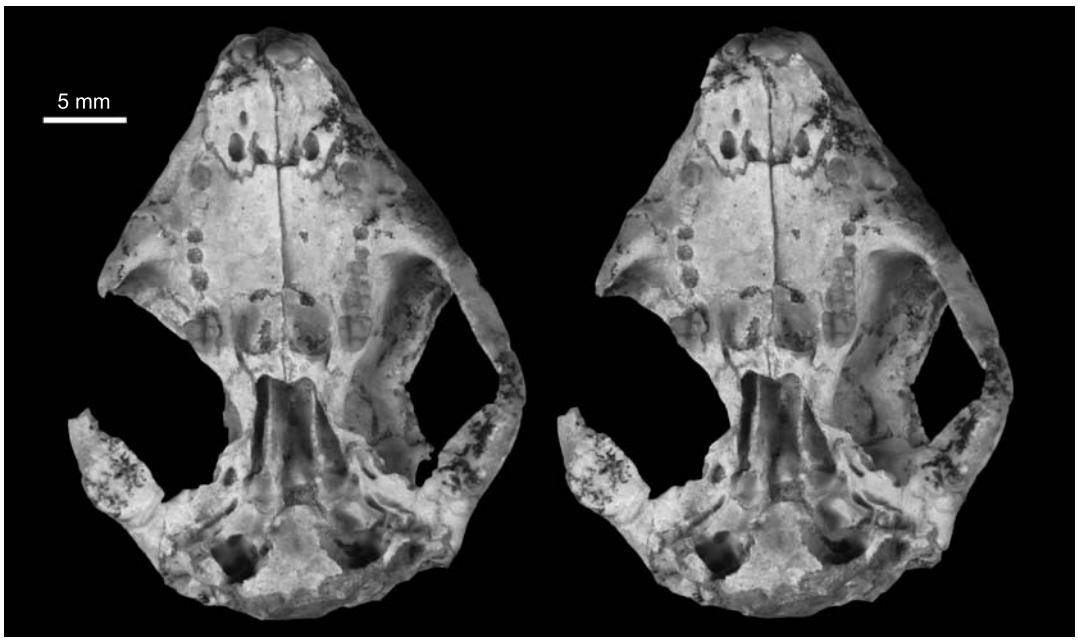

Fig. 26. Unpublished specimen of *Kryptobaatar*, field number PSS-MAE 631 from the Late Cretaceous of Mongolia. Stereophotograph of the skull in ventral view.

142. Unfortunately, preparation of this area is not possible due to the distortion of the skull and the deeply recessed position of these openings. Presence of these structures, namely the prootic canal and the tympanic opening of the facial nerve (Fig. 21), is evidenced on the broken right side of PSS-MAE 141. In this specimen, directly rostral to the vestibular structures and lateral to the promontorium, there are two canals shown in section through the lateral flange/anterior lamina. The most medial of these corresponds to the facial foramen, and the more lateral canal corresponds to the prootic canal. The prootic canal can be traced posterodorsally to the vicinity of the subarcuate fossa on the internal surface of the petrosal in PSS-MAE 141. A broad facial groove extends posterolaterally, parallel to the promontorium and directed towards the stylomastoid notch. This groove is jointly limited by the squamosal and petrosal (Fig. 21). The stylomastoid notch occupies a deeply recessed space between the root of the squamosal, the tympanohyal, and the tall paraoccipital process of the petrosal. Medial to the stylomastoid notch, at the base of the prominent crista interfenestralis, there is an oval depression: the stapedial fossa. This fossa, subequal in size to the fenestra vestibuli, served as an attachment point for the *m. stapedius* and is hidden in posteroventral view by the prominent paraoccipital process.

The paraoccipital process (Figs 9, 10, 21), in occipital view, is subtriangular with a broad, round apex. A sharp crest extends anteroventrally from the tip of the paraoccipital process and connects this process with the back of the promontorium. The crest on the paraoccipital process is continuous with the crista interfenestralis of the promontorium.This rather large, anteromedially trending crest, partially subdivides the rear of the middle ear cavity and results in the absence of a continuous post-promontorial tympanic sinus. The crista interfenestralis-paraoccipital process crest fully separates the structures of the lateral trough from those in the area of the perilymphatic foramen and jugular foramen.

The crista interfenestralis, the edge of the perilymphatic foramen, and the back of the middle ear cavity separate a small portion of the tympanic cavity around the jugular foramen. This is the jugular fossa of other multituberculates (Kielan-Jaworowska *et al.* 1986; Wible and Rougier 2000). The jugular fossa in *Mangasbaatar* represents another out-pocketing of the massive middle ear cavity, more specifically a portion of the post-promontorial tympanic sinus. The jugular fossa (Figs 16, 21) is dominated by the round ventral bulging of the common ampulla of the posterior and lateral semicircular canals. This structure is very similar to that of *Kryptobaatar* (Wible and Rougier 2000; Fig. 30). The ampullar prominence determines two deep pits in the roof of the middle ear cavity: a lateral and a medial pit. The lateral pit is walled off medially by the crista interfenestralis and posteriorly by the posterior wall of the middle ear cavity. The medial pit is closely associated with the perilymphatic foramen and shows a very well delimited oval depression immediately posterior to the perilymphatic foramen. This area is similar to the recessus scalae tympani described in monotremes (Zeller 1989). The excavation of this pocket is not as prominent in PSS-MAE 142 as it is in

PSS-MAE 141. Determining the occupant of this space is problematic. The resemblance of this area with the recessus scala tympani could suggest that an expansion of the perilymphatic duct would occupy this area, but it was previously noted that the perilymphatic duct is enclosed in an aqueductus cochleae throughout much of its length. The lateral opening of this aqueduct is on the medial edge of the perilymphatic foramen and continuous with rim of the foramen. It is possible that the perilymphatic duct expanded out of the perilymphatic foramen in a sac filled with perilymph occupying this recess, which is essentially the condition found in monotremes. Alternatively, in eutherians the secondary tympanic membrane closes the fenestra cochleae (the partial homologue of the perilymphatic foramen) and there is no expansion of the perilymphatic system into the middle ear cavity. Under this model the recess in *Mangasbaatar* would be empty and part of the middle ear cavity, a post-promontorial tympanic sinus. The rest of the jugular fossa is gently concave around the jugular foramen.

From the paraoccipital process there is another crest in the petrosal that extends medially; this is the CTPP, which extends to its contact with the exoccipital immediately lateral to the occipital condyles. The CTPP extends anteroventrally and contributes, along with other elements of the braincase, to the walls and partial floor of the middle ear cavity.

In lateral view (Figs 7, 22), the anterior lamina is the dominant component of the petrosal and, in an undistorted specimen, would probably completely hide the pars canalicularis and the pars cochlearis of the petrosal. The anterior lamina contacts the parietal dorsally through a fairly horizontal suture, which extends rostrally up to the anterior opening of the orbitotemporal canal under the root of the postorbital process. The anterior lamina forms the posteroventral edge of this foramen. Following approximately the direction of the anterior lamina-parietal suture, there is an endocranial groove interpreted here as a space for the orbitotemporal system. The major occupant would be the orbitotemporal artery (Kielan-Jaworowska *et al.* 1986; Rougier *et al.* 1992; Wible and Rougier 2000), likely accompanied by a vein. The orbitotemporal artery was fed posteriorly through a fairly vertical dorsal ascending canal. This canal runs between the anterior lamina and the squamosal and is shown by the right side of PSS-MAE 142 (Fig. 18). In the specimen, the overlying squamosal is missing, affording a direct view of the inside of the ascending canal. When complete, the canal would have been perforated by a few foramina that would distribute its contents to the temporal area. The foramina would be occupied by temporal rami feeding the temporal musculature (Rougier *et al.* 1992; Wible and Gaudin 2004).

The ascending canal contacts two other grooves: a larger posterodorsal one and a somewhat smaller anteroventral one. The posterodorsal canal opens on the occiput through the posttemporal canal and likely transmitted the arteria diploëtica magna and a companion vein (Kielan-Jaworowska *et al.* 1986; Rougier *et al.* 1992). The anteroventral canal is filled with matrix in PSS-MAE 142 and represents the ventral ascending canal, likely transmitting a fairly horizontal portion of the ramus superior of the stapedial artery. This canal, horizontally directed, runs through the thickened ventral edge of the anterior lamina: the lateral flange. The ventral extent of the lateral flange is mostly complete on the left side of PSS-MAE 141; it should be noted that this ventral extent is lateral to the edge of the lateral flange that, as in most multituberculates, contacts the promontorium medially. The ventral projection of the lateral flange extends anteriorly along the lateral edge of the epitympanic recess as a gently concave lamina. At its most anteroventral extent, near the suture with the alisphenoid, there is a foramen that faces ventrolaterally: the lateral opening of the foramen masticatorium, which has already been mentioned. On the left side of PSS-MAE 141, there is a small foramen on the lower third of the anterior lamina, corresponding to the supraglenoid foramen of *Kryptobaatar* (Wible and Rougier 2000) and other LCMM.

The anterior margin of the anterior lamina has a long anteroventrally trending ridge that forms the lateral wall of the sphenorbital fissure. The very long anteroventrally-extending portion of the anterior lamina is one of the most conspicuous features distinguishing *Mangasbaatar* from other LCMM. The extension of the anterior lamina is coupled with the general enlargement of the middle ear cavity through the ventral projection of the elements involved in its formation. The dorsal portion of the anterior edge of the anterior lamina is moderately concave and faces forward as in other LCMM. In *Mangasbaatar*, this surface is proportionally more dorsally located. The reorganization of this area is mostly due to the very large opening of the sphenorbital fissure, which occupies the floor of the orbitotemporal region. The size and proportions of this area are very well shown by PSS-MAE 142 and at least partially confirmed by the right side of PSS-MAE 141.

In occipital view, the petrosal is exposed between the squamosal, exoccipital, and supraoccipital. The mastoid exposure of the petrosal supports, dorsolaterally, the base of the lambdoidal crest. Along the dor-

solateral edge of the petrosal, there is a fairly prominent posttemporal foramen, partially obliterated by crushing in PSS-MAE 141. This anteroventrally directed foramen is formed solely by the petrosal. A broad groove extends ventrally from the posttemporal canal, continuing into the mastoid exposure of the paraoccipital process. The posttemporal foramen is also slightly notched dorsally, suggesting that a large occipital artery ran in close contact with the occiput and continued dorsally to supply the nuchal musculature. The area of the mastoid exposure of the petrosal medial to the posttemporal canal is slightly concave and forms a shallow depression on the side of the occipital condyles. This shallow depression probably accommodated the transverse processes of the atlas during skull movements.

Basioccipital. — The basioccipital is preserved in both specimens, although only the one in PSS-MAE 142 is incomplete. The basioccipital forms most of the basicranial axis (Figs 3, 9, 10); it is in contact anteriorly with the basisphenoid, laterally with the petrosals, and posteriorly with the exoccipital. It is also possible that a small portion of the pterygoids contacts the anterolateral corner of the basioccipital. In ventral view the basioccipital shows a deep odontoid notch, as described earlier, and a narrow median exposure that is flanked by the exoccipital. In front of the exoccipital, the basioccipital expands laterally, contributing to the floor of the middle ear cavity through a thin lamina (Figs 2, 9). Further rostrally, the basioccipital contribution to the floor is in contact with a similar lamina of the petrosal. At the rostral end of the basioccipital there is a transverse suture, mentioned earlier in the description of the pterygoid, that separates the basioccipital from the basisphenoid and probably the pterygoids. The contribution of the basioccipital to the floor of the middle ear is laminar and ventrally convex, similar to the processes of other bones delimiting the middle ear cavity.

In the middle ear cavity, the basioccipital is deeply excavated medially so that this bone forms not only a substantial part of the floor of the middle ear cavity, but also the medial wall and part of the roof. The medial excavation of the basioccipital results in a bone that is very thin, so much so that it can be transilluminated from the opposite middle ear space. This very close approximation of right and left middle ear cavities to the midline is ventral to the braincase proper because, as mentioned above, only a thin, tall crest of the basioccipital separates right and left cavities (see Fig. 27 for a comparative example). The suture with the petrosal runs deeply in the roof of the middle ear, obliquely from the jugular foramen towards the anteromedial pole of the middle ear recess. The basioccipital, the petrosal, and possibly the exoccipital, jointly form the jugular foramen. The aperture is of a relatively small size with respect to the overall size of the skull.

Exoccipital. — The exoccipital is incomplete in both specimens. The left side of PSS-MAE 141 is the best preserved (Figs 9, 10). The exoccipital contacts the basioccipital anteriorly, the supraoccipital dorsally, and the petrosal laterally and dorsally in the occiput. The exoccipital forms the occipital condyles, most of the foramen magnum, and the posteromedial wall of the middle ear cavity. The sutures on the occiput are clear and both specimens are very similar regarding position and extent.

Only part of the left condyle is preserved in PSS-MAE 141. What is preserved resembles the condyles present in other LCMM. The condyles are not very prominent, are moderately convex, and have a small lateral extension. The articular surface extends over the bony floor of the middle ear cavity. Right and left exoccipitals are separated ventrally along the midline by a wedge of the basioccipital bearing the odontoid notch. The exoccipital forms most of the lateral edge and floor of the foramen magnum and right and left are separated ventrally, as mentioned before, by the basiocciptal and dorsally by the supraoccipital. The contribution of the exoccipital to the occiput is limited to the area immediately surrounding the foramen magnum. This lamina is flat and slopes slightly forward, away from the foramen magnum. The suture with the petrosal runs obliquely, from slightly above the level of the foramen magnum downwards to the medial side of the paraoccipital process in the middle ear cavity.

Mangasbaatar has an extremely well-developed and expansive middle ear cavity formed jointly by the squamosal, petrosal, basioccipital, alisphenoid, and exoccipital. The exoccipital forms the posteromedial aspect of this cavity, providing a thin floor that extends anterolaterally. This floor is incomplete in both specimens. From what remains of the left side of PSS-MAE 141, it is clear that this floor almost completely enclosed the middle ear. The contribution of the exoccipital to the internal surface of the middle ear can be evaluated only on the right side of PSS-MAE 141. The exoccipital is deeply excavated medially forming a small infundibulum separated anteriorly from the main middle ear cavity by a sharp crest.

In the posteroventral corner of both sides of PSS-MAE 142, a single hypoglossal foramen can be recognized. The area surrounding this foramen is damaged on both sides, so it is unclear if *Mangasbaatar* had only one hypoglossal foramen or more. A second foramen, piercing the substance of the exoccipital, can be seen

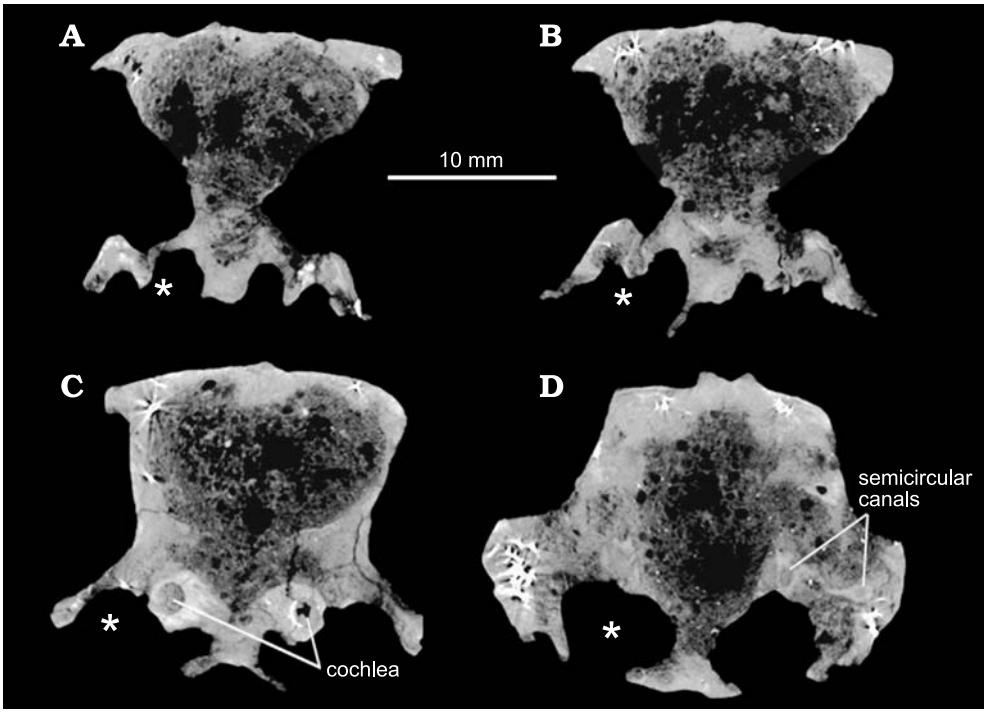

Fig. 27. CT cross sections through the mesocranium and ear region of a *Tombaatar* sp. skull from Ukhaa Tolgod, Mongolia, PSS-MAE 630. The * represents the middle ear cavity and its connection to the choanal passage.

on the right side of the exoccipital and part of the same foramen is preserved on the left side. The left exoccipital is more eroded than the right so that the above-mentioned foramen can be seen to be continuous with a cylindrical endocast of the left side. These foramina were inside a condylar area of the exoccipital and can be interpreted to be part of a condylar canal. The endocranial structure leading to the left condylar canal is congruent with similar endocasts described for *Kryptobaatar* (Wible and Rougier 2000). The relatively large size of these endocasts and the proportionally small size of the jugular foramen imply that most of the blood from the cranial venous system was drained in *Mangasbaatar* through the foramen magnum instead of the jugular foramen, a condition congruent with that reconstructed for other multituberculates (Kielan-Jaworowska *et al.* 1986; Rougier *et al.* 1992). The basioccipital-exoccipital suture in the middle ear region cannot be discerned in any of the specimens so the lateral extent of the bone cannot be ascertained with any certainty. However, it is likely that the relatively large hypoglossal foramen, present on the posteromedial corner of the middle ear cavity, is completely enclosed in the exoccipital (shown by the right side of PSS-MAE 141).

Supraoccipital. — The supraoccipital is a flat bone positioned sagittally on the occiput dorsal to the foramen magnum and is vertical, or inclined slightly forward. The supraoccipital is at least partially preserved in both of the specimens and its boundaries indicated by relatively clear sutures. This element contacts the parietals dorsally, the petrosals parasagittally and the exoccipitals ventrolaterally. A small portion of the supraoccipital forms the dorsal-most portion of the foramen magnum. In PSS-MAE 142 there are remnants of a small midline crest, which increases in size dorsally. The supraoccipital provides support to the lambdoidal crest but does not directly contribute to it and it is therefore limited to the occipital aspect of the skull.

Mandible (Figs 11–13, 23). — Fragments of both right and left lower jaws are preserved in both specimens. Those of PSS-MAE 142 were found dissociated among the numerous fragments that resulted from erosion of the skeleton. The jaws of PSS-MAE 141 were still articulated to the skull when found. The right jaw was almost completely eroded away, leaving only the tip of i1, p4–m2, and the apex of the coronoid process in articulation. An impression of the body of the jaw was present so that the shape and curvature of the area of the dentary surrounding i1 could be observed. Preparation of the specimen removed all of these remnants of the right jaw and destroyed the natural mold of the dentary. However, the specimen was molded before preparation and the relative positions of the elements are preserved in a rubber cast of the original. The left lower jaw is largely preserved (Figs 11, 12) but is missing the symphysis, most of the incisor, and the back of the jaw. This description is based on this jaw and is supplemented with details from PSS-MAE 142.

The jaw of *Mangasbaatar* is heavy and deep under the molars with a very steep diastema and i1 alveolus. The i1 is very high and almost reaches the level of the molars. The space between i1 and p3 is relatively short. The symphysis is very robust, as shown by the fragments of PSS-MAE 142. The bottom part of the body of the jaw is missing in both specimens, but can be observed in the cast of PSS-MAE 141. The external surface of the jaw is marked by a series of depressions. The first depression is ventral to the p4–m1 embrasure and has the masseteric fovea preserved as a gentle concavity. Between the masseteric fovea and p4, the alveolar ridge is slightly concave and continues along the chipped teeth to end directly medial to the coronoid process. The anterior portion of this depression under p4 is the lunule (Gambaryan and Kielan-Jaworowska 1995), which is not very well developed in *Mangasbaatar* (Fig. 23). The more substantial depression extending back is the temporal groove. As previously mentioned, the bottom of the jaw is not well preserved in the specimens and the masseteric crest cannot be fully recognized in any of them, but isolated fragments suggest the presence of the masseteric protuberance (Kielan-Jaworowska *et al.* 2005). The masseteric fossa, however, is slightly concave and not very large, restricted to the base of the coronoid process, and probably expanding towards the back of the jaw. The coronoid process in *Mangasbaatar* is high, narrow, and forms a sharp angle with the molariform occlusal plane (78º). The tall coronoid process resembles that described in *Catopsbaatar* (Kielan-Jaworowska 1974; Gambaryan and Kielan-Jaworowska 1995; Kielan-Jaworowska *et al.* 2005).

Only the dorsal-most portion of the condylar process is preserved in the left lower jaw of PSS-MAE 141. Fortunately, most of the condylar articular surface remains intact (Fig. 13). The condyle is perched in a broad neck and is separated from the coronoid process by a wide notch that places the condyle above the occlusal plane of the molars. An isolated left condyle is also preserved in PSS-MAE 142. The articular surface is tear-drop-shaped with the broad end directed anteriorly. The articular surface continues back along the posterior edge of the jaw for a short distance beyond the broader portions of the condyle, indicating the potential for a large range of jaw opening. The medial view of the jaw shows a deep pterygoid fossa that extends anteriorly up to the level of the m2. The pterygoid fossa is bordered anteriorly by the remnants of the pterygoid ridge, which is only partially preserved. At the anterior pole of the pterygoid fossa, there is a large foramen that is directed anteriorly into the substance of the dentary: this is the mandibular foramen or canal. All of the features of the medial view of the jaw described by Gambaryan and Kielan-Jaworowska (1995) cannot be described in these specimens.

Dentition (Figs 5, 6, 11–14). — *Mangasbaatar* is clearly a member of Djadochtatherioidea (Rougier *et al.* 1997; Kielan-Jaworowska and Hurum 1997, 2001) and, as seen in all members of this group, the lower dentition is reduced to one incisor, two premolars, and two molars. The upper dentition is reduced, like *Tombaatar* and *Catopsbaatar*, to two incisors, three premolars, and two molars. Therefore, the dental formula for *Mangasbaatar* is I2/1, C0/0, P3/2, M2/2 (Figs 6, 14)

PSS-MAE 141, the type, is a younger individual than PSS-MAE 142. The crown morphology of PSS-MAE 141 is very well preserved and most of the cusps are intact. PSS-MAE 142, on the other hand, shows extensive wear, which has reduced the cusps to their truncated bases. On the left side of PSS-MAE 141, there is a small element in the diastema between P1 and P3. This element is a tooth or parts thereof that might be incompletely preserved, but it seems more likely to be part of a deciduous tooth (likely a DP3) which is retained at this ontogenetic stage. The relevant area on the right side of PSS-MAE 141 is damaged, so the presence or absence of this element cannot be corroborated. There is, however, a fragment of a tooth in a position that approximately corresponds to the element mentioned above, but the damage to the area is so extensive that a positive identification is not warranted. PSS-MAE 141 is a young adult, but the older adult, PSS-MAE 142, shows no trace of this element between P1 and P3.

Upper dentition (Figs 5, 6, 16, 20). — The two incisors in LCMM are homologous to the I2 and I3 of the full complement of three incisors present among basal multituberculates such as of paulchoffatiids (Clemens 1963; Hahn 1969; Kielan-Jaworowska *et al.* 2004), we therefore refer to the teeth present in *Mangasbaatar* as I2–I3. The upper dentition is fairly well-preserved in PSS-MAE 141, although most of the I2s are missing, the left I3 and right P4 are damaged, and the right P1–P3 are missing. On the skull PSS-MAE 142, only part of the right and left I2 are preserved. Both of the I3, as well as the right P1 and P4, are damaged. The left P1–P4 and the right M1 are also missing.

Incisors: The upper I2 is a big, strong tooth that is sharply curved, and occupies most of the premaxilla. The tooth is strongly compressed mediolaterally with a thick layer of enamel covering its lateral aspect, wrapping around the dorsal aspect of the tooth to extend into the medial face (restricted enamel). The medial

extension of the enamel is limited to a small dorsal band that occupies less than a third of the medial height of the tooth. Right and left I2 were medially directed and probably contacted each other in the midline. This, however, cannot be seen in the specimens because of imperfect preservation.

The left I3s of both skulls seem to be complete and show heavy wear on their occlusal facets. The I3 in *Mangasbaatar* is a cylindrical tooth that is slightly curved posteriorly, occupying a position close to the midline on the palate (Figs 3, 16). The I3 projects ventrally as a long freestanding tooth that culminates into a flat subhorizontal wear facet. The wear of the I3 crowns is enough to obscure the original crown morphology of this element. It is, therefore, uncertain if the I3 had one or more cusps (a primitive condition). The wear on the I3 is so extensive that the boundary between the crown and the root is obliterated. The wear has also exposed, in the center of the cylinder, a small area showing the cementum surrounded by dentin. This condition is well developed in PSS-MAE 141, but in PSS-MAE 142 the wear on the I3 crown does not reach the cementum.

Premolars: PSS-MAE 141 bears a well-preserved left P1 which shows little wear. The P1 is biradiculated, short, and has a short crown that culminates in three conical cusps. The cusp formula is 1-2. The cusps are arranged in a closed triangle. The roots are unequal, the anterior root being larger and sloping backwards, a feature quite common among LCMM, likely associated with the palinal masticatory movements (Wall and Krause 1992; Gambaryan and Kielan-Jaworowska 1995).

The P2 seems to be absent in *Mangasbaatar*. No traces of it remain on both sides of PSS-MAE 142 (Fig. 16). The alveolar bone in this area is well preserved, showing a smooth, short diastema between P1 and P3. On PSS-MAE 141, however, the left side shows the remnant of a tooth between P1 and P3. As preserved, this remnant is little more than a rootlet. It is likely that this is a transitory remnant of a deciduous premolar, likely DP3. The right side of the same specimen is not preserved well enough to be certain of the presence or absence of a P2. Under this interpretation, *Mangasbaatar* shares the absence of a P2 in the adults with *Tombaatar* and *Catopsbaatar*. All these large LCMM represent a closely related group (Kielan-Jaworowska and Hurum 1997; Rougier *et al.* 1997). Kielan-Jaworowska *et al.* (2005) described that, in old *Catopsbaatar* specimens, P1 and P3 disappear without leaving traces of their respective alveoli. This does not seem to be the case in *Mangasbaatar* as attested by the relatively old PSS-MAE 142 that still preserves P1 and P3.

The P3 is a small subrectangular tooth in occlusal outline, with two roots that slant posteriorly. The crown is separated by a strong neck from the roots and bears four conical cusps. The cusp formula is 2-2. The four cusps of the P3 occupy the corners of a rectangle with a small posterior broadening of the crown behind the two posterior cusps. The posterobuccal and the two lingual cusps are subequal in height, but the anterobuccal is substantially shorter than the other three. The three larger cusps suggest a triangular pattern similar to that present in the P1.

The P4s are missing or badly broken in PSS-MAE 142 and the right side of PSS-MAE 141. The left side of the latter, though, has this element preserved almost completely (Fig. 5). The P4 is a large, strong premolar supported by two roots. The cusp formula on the P4 is 1-5-1?. The lingual row is damaged or worn down on both sides of PSS-MAE 141 and it is likely that only one cusp was present; however, it would be possible to have a very small cusp anteriorly positioned relative to the main one. The buccal cusp is small and conical, showing no wear on PSS-MAE 141. The middle row has five cusps that increase in size posteriorly from the first to the fourth, forming a continuous ridge. The fifth cusp is separated by a deep embrasure from the rear slope of the prominent fourth cusp. The buccal row, as in other multituberculates, is more dorsally placed than the middle and lingual rows in the P4. The lingual row is likely formed by a single cusp and forms a medially bulging projection that, in essence, represents the abraded base of that large cusp. The wear that obliterated the lingual cusp extends a flat surface to the lingual slopes of the cusps forming the middle row. The buccal bulge formed by the buccal row is offset by the medial bulge of the lingual row, resulting in a slightly oval crown view for the P4. In *Mangasbaatar*, as is common among multituberculates, the direction of the middle row is oblique, aligned anteriorly with the lingual row of the P3 but aligned posteriorly with the buccal line of the M1.

Molars: The M1 is well preserved in both sides of PSS-MAE 141 (Figs 4, 5), but is worn down or broken in PSS-MAE 142. There are three rows of cusps on this molar with a cusp formula of 5-5-3. As is common in other LCMM, the buccal and middle rows extend through the length of the tooth, but the lingual row is incomplete and has only posterior cusps (posterolingual cusps). In *Mangasbaatar*, the incomplete lingual row of the tooth reaches anteriorly to the level of the apex of the third cusp of the middle row, or to the embrasure between the second and third buccal cusps. The elongated M1 is supported by two roots. The anterior root is buccolingually compressed and the posterior root, which supports the back half of the tooth, is massive and cylindrical.

The cusps have subrectangular to hexagonal bases (Fig. 6) and probably culminated in conical apices when unworn. At present, the M1 in PSS-MAE 141 shows small crater-like depressions centrally positioned on each cusp of the middle row, reflecting wear through the enamel and exposing the softer dentin. PSS-MAE 142 shows that in older individuals the molars lose almost all relief in their crowns and that the "craters" seen in PSS-MAE 141 expand to occupy the whole crown. The only remnants of the original cusp pattern are in PSS-MAE 142, seen in the eroded bases of the cusps. The buccal row that is formed by five subequal cusps shows strong wear facets in all of the lingual slopes. The individual cusps of the buccal row are separated by valleys that become shallower posteriorly; therefore, the first buccal cusp, which is somewhat removed from the anterior margin of the molar, is also separated from the rest of the cusps by the deepest valley. The valley between the second and third cusps of the buccal row is relatively shallow and the bases of these two cusps are partially merged together, a condition that is also present in *Tombaatar* and other LCMM (Rougier *et al.* 1997). The fifth buccal cusp is small and poorly separated from the fourth. A blunt ridge extends posterolingually from its apex towards the last cusp in the middle row, thus closing the trough between the buccal row and other rows. The middle row has five cusps that increase in size progressively toward the back. The cusps in the middle row are positioned at the level of the valleys between the cusps in the buccal row. The imbrication between the cusp bases of the buccal and middle row results in a strongly angular trough between the buccal and middle row. The lingual row has three poorly differentiated posterior cusps, of which the middle is the highest. The bases of these cusps are not as well-developed as those of the first two rows and they develop a fairly uniform, straight slope that is continuous from the most mesial cusp to the most distal one. Wear facets are developed only on the buccal slope of these cusps.

Both M2s are preserved in both specimens, but those of PSS-MAE 142 are very heavily worn. The M2 is a pear-shaped tooth supported by two roots, a large anterior one and a smaller posterior one that slopes backwards. This position of the roots of the M2 make the occlusal surface of the last molar face anteroventrally, giving the dental arcade a slightly concave outline in lateral view, that is characteristic of multituberculates (Wall and Krause 1992). The cusp formula of the M2 is ridge-2-3. The two cusps in the middle row are larger than the rest in the molar and continue the posterior increase in size of the middle row of the M1. The bases of these cusps are not polygonal as in the M1. The lingual row is much more prominent in the M2 than the M1, forming a fairly sharp ridge that is separated from the middle row by a broad valley. The middle cusp of the three is the largest and has heavy wear as shown by the left molar of PSS-MAE 142. The cusps on the lingual row are very poorly differentiated from one another. The buccal row is very short and does not extend throughout the length of the tooth. It reaches, posteriorly, the middle of the cusp space of the posterior cusp of the middle row. The row lacks distinct cusps and forms a broad, low, shallow crest aligned with the buccal row of the M1.

Lower dentition (Figs 11–14, 23). — The best lower dentition is that of the specimen PSS-MAE 141, which is complete (with the exception of the i1). In PSS-MAE 142, only part of the right dentition is still in place in a small fragment of the dentary. The left is represented only by isolated broken crowns of the i1, m1, and m2.

The first lower incisor is a strong tooth, buccolingually compressed with a partial covering of enamel that, as in the I1, covers only the external and a small portion of the lingual surface of the tooth. As in all large LCMM, the i1 are very large teeth with an anterior-posterior length subequal to the m1 length, the largest cheek tooth.

As in all LCMM, *Mangasbaatar* shows only two premolars, conventionally called p3 and p4. The p3 is, in *Mangasbaatar* and other LCMM, a very small element, essentially "peg"-like in front of the towering p4. The p3 in *Mangasbaatar* has only one anteriorly curved root. This root follows the concave contour of the mandibular diastema between i1 and the p3. There is a clear distinction between the crown and root, indicated by a conspicuous neck. The crown is essentially a more bulbous, enamel-clad continuation of the root that culminates in a single blunt cusp. The apex of the p3 is at roughly the level of the neck between the roots and the crown of the p4. The anterior margin of the p4 overhangs the minute p3 so that the anterior edge of the p4 is continuous anteroventrally with the mesial edge of the p3. The p3 is well preserved in both the left jaw of PSS-MAE 141 and the right jaw of 142.

The p4 is well preserved in both jaws of PSS-MAE 141, but missing on the left of 142. The p4 in all cimolodont multituberculates is blade-like with a serrated margin. This is also the condition in *Mangasbaatar*. The p4 in *Mangasbaatar* is a peculiar trapezoidal shape with a nearly straight mesial edge and a fairly horizontal occlusal surface. A similar condition is seen in *Catopsbaatar* and in *Tombaatar* (unpublished

specimens). The premolar is supported by three roots, two large and stout located mesially and distally and a small one between the two, a condition also known in other LCMM including *Kryptobaatar* (Kielan-Jaworowska 1971). The cusp formula in the premolar is ridge-5. The labial ridge is substantial, forming a broad platform on the posterior one-third of the tooth, approximately the area supported by the back root. This ridge becomes broader and stronger posteriorly, reaching the occlusal plane of the buccal row of the m1 at its posterior extent. The cusps in the central row are very blunt and form a weakly-serrated edge that reaches the level of the occlusal plane of the lingual row of cusps of the m1.

The first molars (m1) are present bilaterally in both specimens. The best preserved are those in PSS-MAE 141. The m1 is the largest of the lower cheek teeth, has a cusp formula 4-3, and is supported by two massive cylindrical roots. The crown of the m1 is very low and the cusps of the buccal and lingual rows have different heights (the buccal cusps are lower than the lingual cusps). This difference in height may be exaggerated by differential wear. As is common in other LCMM, the cusps of the buccal and lingual rows occupy alternate positions, with the lingual cusps placed between two successive buccal cusps. The cusps on the buccal side have subhexagonal bases but those on the lingual side are less so. All the cusps in the m1 were, in the unworn state, conical.

The m2 is well preserved and lodged in the dentaries, or fragments thereof, with the exception of the left m2 of PSS-MAE 142 that was found isolated. The m2 is a relatively small tooth with only two cusps in the labial and lingual rows. Therefore, its cusp formula is 2-2. The crown outline is subrectangular and cusps in both rows are subequal in height. The two rows of cusps are further apart than in the m1 and, the cusps of different rows do not alternate with each other so that the first cusp of the lingual row is at the same level as the first cusp of the buccal row. The four cusps occupy the corners of the subrectangular m2, determining a broad basin between them. The left m2 of PSS-MAE 142 was found isolated and it had sustained substantial damage; however, the buccal row is almost complete and shows that the posterior buccal cusp is, in this tooth, subdivided into subequal cusps, a condition not clearly seen on the right m2 of the same specimen or those of PSS-MAE 141. The m2 is supported by one root. This root is approximately of the same diameter as the crown and is deeply constricted apically, but is not divided.

DISCUSSION

CLADISTIC ANALYSIS

Few published phylogenetic analyses include LCMM among a wider sample of multituberculates, most notably Simmons (1993), Rougier *et al.* (1997), and Kielan-Jaworowska and Hurum (1997, 2001). Following Rougier *et al.* (1997) and Kielan-Jaworowska and Hurum (1997), this study recognizes Djadochtatherioidea as a monophyletic group of Late Cretaceous multituberculates and based on shared diagnostic features (see diagnosis), the new taxon is included in a modified simple matrix compiled by Kielan-Jaworowska and Hurum (1997) for other LCMM, some of which are found in the same, or similarly-aged, sediments. The wider problem of the position of Djadochtatherioidea within Allotheria is not the main purpose of this study and Kielan-Jaworowska and Hurum (2001); Kielan-Jaworowska *et al.* (2004), Yuan *et al.* (2013), and Bi *et al.* (2014) provide a framework for the higher-level relationships of Djadochtatherioidea. The matrix scores 45 characters across 17 taxa. The resultant data were analyzed using implicit enumeration via Asado version 1.7, which uses TNT as its base searching algorithm. The analysis recovered one most parsimonious tree of 101 steps (CI: 0.64 and RI: 0.68) that concurs in its structure with that of Kielan-Jaworowska and Hurum (2001) and recovers Djadochtatherioidea as a distinctive taxonomic unit, among which the large-sized multituberculates including *Djadochtatherium*, *Catopsbaatar*, *Tombaatar*, and *Mangasbaatar*, are terminal taxa (Fig. 28). These very distinctive mulituberculates reduce the blade-like lower p4, have very robust jaws, and dorsoventrally shallow skulls with small temporal areas, but preserve, overall, the typical cimolodontan morphology for the upper and lower molars. *Kryptobaatar* is a more generalized LCMM and, as a point of comparison, can be interpreted as pleisomorphic within LCMM with regards to the more derived characters seen in *Mangasbaatar* (Figs 29, 30). Namely, among those, is the development of a very prominent jugular fossa and middle ear cavity, which develops to an unparalleled degree in *Mangasbaatar* and *Tombaatar*.

The topology of the tree does not identify any clear geographical or stratigraphic pattern. Udan Sayr, where the specimens of *Mangasbaatar* are from, has traditionally been considered of likely affinities with Barun Goyot from the western Gobi (Kurzanov 1992; Szalay and Trofimov 1996). It should be noted, however, that the closest relative of *Mangasbaatar* appears to be *Tombaatar* from Ukhaa Tolgod, a locality that is likely to be a Djadochta near-equivalent (Loope *et al.* 1998; Dingus *et al.* 2008). Obviously, the faunas from Ukhaa Tolgod, Barun Goyot, and Udan Sayr are all very similar, though, lacking any clearly datable horizons, the relative temporal resolution is somewhat poor (but see Makovicky 2008).

Four taxa can be considered as large LCMM: they are *Djadochtatherium*, *Tombaatar*, *Mangasbaatar*, and *Catopsbaatar* (Figs 29–31). The first two are poorly known, mostly based on palate and jaws, while *Catopsbaatar* and *Mangasbaatar* are represented by better-preserved specimens. A skull of *Djadochtatherium* has been utilized in discussing cranial evolution of the large-sized Late Cretaceous Mongolian multituberculates (Kielan-Jaworowska and Hurum 2001) based on photographs published in reports (sent by Mahito Watabe to Zofia Kielan-Jaworowska in 1996) and popular articles (Webster 1996). However, the specimen has never been thoroughly studied and it is uncertain if it actually is *Djadochtatherium*. As such, there are limited opportunities for comparisons with those bona fide *Djadochtatherium* specimens recovered by the American expeditions (Simpson 1925) and deposited in the AMNH (Rougier *et al.* 1997). It follows that most of what is known about the cranial morphology of these multituberculates is based on *Catopsbaatar* and now these two specimens of *Mangasbaatar*. *Catopsbaatar* has been the focus of a detailed revision by Kielan-Jaworowska *et al.* (2005), where a detailed description is provided of the known specimens. All of them, however, have a missing or poorly preserved basicranium. *Mangasbaatar*, on the other hand, has a relatively complete ear region preserved, with some deformation, in two specimens. It is presently uncertain if the extreme development of sinuses and cavities in the ear region of *Mangasbaatar* is characteristic of all four of these large LCMM. However, in unpublished specimens of *Tombaatar* (PSS-MAE 630; Fig. 27), the ear region is also greatly excavated but differs substantially in detail from that of *Mangasbaatar*. In conjunction with the fact that, in *Kryptobaatar* there is already a substantial excavation of the middle ear region (Fig. 30), and particularly of the area surrounding the jugular fossa (Wible and Rougier 2000, figs 13, 19, 20), it seems likely that at least some degree of middle ear expansion was present in all of these large-sized LCMM. The specimen of cf. *Tombaatar* published by Ladevèze *et al.* (2010) is not illustrated to determine if the middle ear cavity is similarly expanded, but their fig. 1 seems to suggest that this is indeed the case. The enlargement of the middle ear cavity would therefore be a synapomorphy of this group that is further elaborated and taken to an extreme among the large forms.

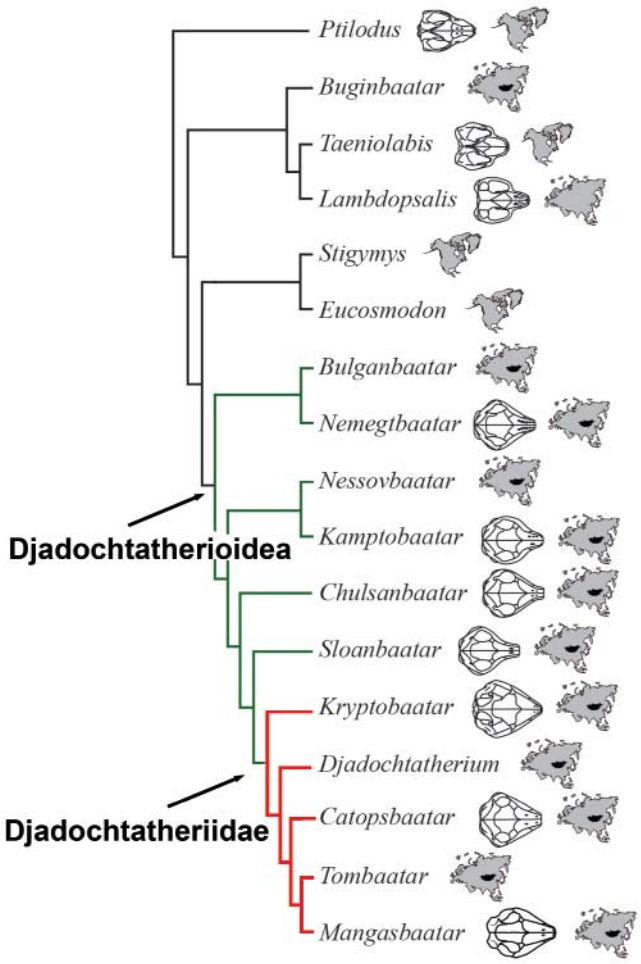

Fig. 28. Phylogenetic tree showing interrelationships between multituberculates. Green branches indicate Djadochtatherioidea. Red branches indicate Djadochtatheriidae.

Status of Djadochtatheriidae. — The results of our analysis are consistent with recent LCMM phylogenies and discusssions (Rougier *et al.* 1997; Kielan-Jaworowska and Hurum 1997, 2001; Kielan-Jaworowska *et al*. 2005) that assign *Kryptobaatar, Djadochtatherium*, *Catopsbaatar*, and *Tombaatar* to the monophyletic

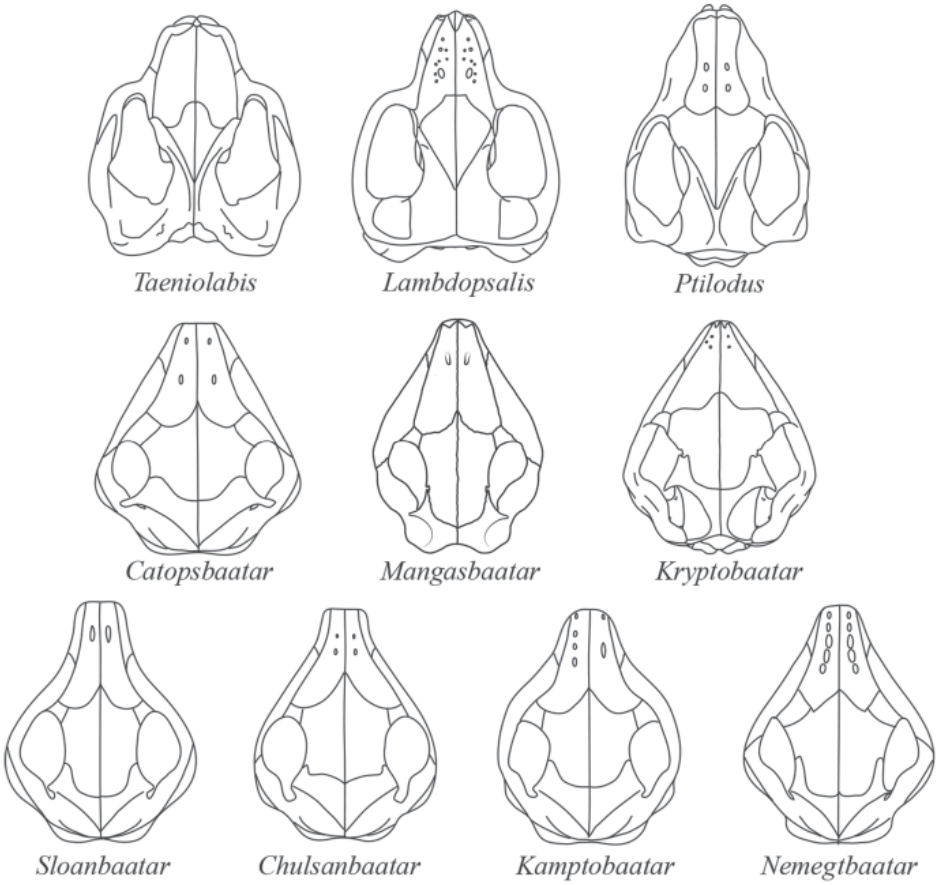

Fig. 29. Multituberculate skull reconstuctions in dorsal view, rendered to be approximately the same length. Drawing is modified from Kielan-Jaworowska *et al.* (2004) to include *Mangasbaatar*.

clade Djadochtatheriidae. This family of LCMM is recognized by cranial characters, differing from the remaining members of Djadochtatherioidea (Figs 29–31) in having a subtrapezoidal snout in dorsal view that is confluent with the zygomatic arches, an irregular, non-oval anterior part of the promontorium, in addition to the snout extending for more than 50% of the skull length (Kielan-Jaworowska *et al.* 1997). Given the anatomical evidence provided by the two skulls in this study and the resulting cladogram, *Mangasbaatar* is here referred to Djadochtatheriidae. Ultimately, this contribution adds yet another Mongolian taxon represented by well-preserved skull material, that provides details that can potentially serve as a reference for the derived multituberculate morphology characteristic of the large-sized LCMM.

Kryptobaatar is perhaps the best known LCMM (Kielan-Jaworowska 1971; Wible and Rougier 2000), with hundreds of skulls known from Ukhaa Tolgod, Mongolia (Dashzeveg *et al.* 1995; Wible and Rougier 2000). There are, however, discrepancies regarding its relationships within Djadochtatheriidae, mostly due to differences in the characters used in the phylogenetic analyses; Kielan-Jaworowska *et al.* (1997) placed *Kryptobaatar* within Djadochtatheriidae in contrast with a cladistic analysis by Rougier *et al.* (1997), which placed *Kryptobaatar* between *Chulsanbaatar* and *Bulganbaatar* Kielan-Jaworowska, 1974. Kielan-Jaworowska reasoned that the character for the subtrapezoidal snout, which is unique for Djadochtatheriidae within all of Mammalia, likely evolved only once, which places *Kryptobaatar* as a sister group to *Djadochtatherium, Tombaatar* and *Catopsbaatar*; however, *Kryptobaatar* is similar in size to the smaller and more generalized LCMM. Given the matrix employed, it is not surprising that *Kryptobaatar* is here recoverd as a related form to the LCMM multituberculates.

COMPARISONS WITH OTHER LCMM

Premaxilla. — In ventral view the premaxilla has thickenings between the alveoli for I2 and I3, a feature which is present in several other forms such as *Tombaatar*, *Nemegtbaatar*, *Kryptobaatar*, and

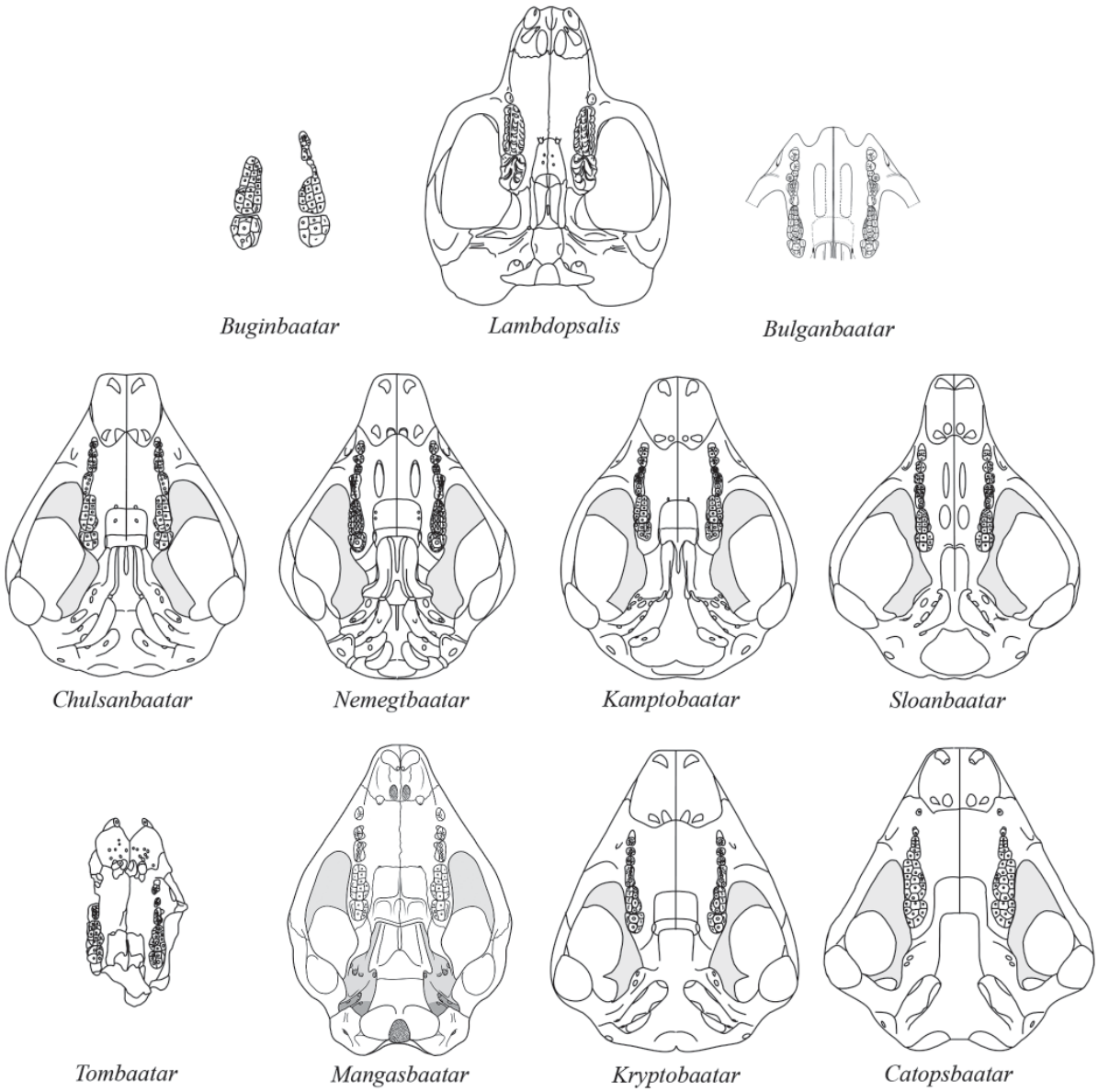

Fig. 30. Multituberculate skull reconstuctions in ventral view, rendered to be approximately the same length. Drawing is modified from Kielan-Jaworowska *et al.* (2004) to include *Mangasbaatar*.

Chulsanbaatar, but not present in *Kamptobaatar* Kielan-Jaworowska, 1970 (Kielan-Jaworowska *et al.* 1986; Wible and Rougier 2000; Rougier *et al.* 1997).

As is the condition for nearly all multituberculates described to date, there is no internarial bar or septomaxilla present in *Mangasbaatar.* The internarial bar was noted by Miao (1988) in two specimens of *Lambdopsalis*, though this finding is controversial as both of these bars were of differing size between specimens. Regardless, the feature has no taxonomic utility, as *Lambdopsalis* is the only known multituberculate to express this condition. The condition is currently unknown in *Haramiyavia* Jenkins *et al.*, 1997, *Arboroharamiyavia* Zheng *et al.*, 2013, and *Megaconus* Zhou *et al.*, 2013 and is absent in other primitive forms, only making an appearance within basal mammaliaformes such as *Morganucodon* Kühne, 1949 (Kermack *et al.* 1981), *Haldanodon* Kühne *et* Krusat, 1972 (Lillegraven and Krusat 1991), and possibly *Docodon* Marsh, 1881 (Rougier *et al.* 2015). *Vintana sertichi* Krause *et al.*, 2014 shows an elevated internarial process of the premaxilla that, however, does not reach the nasals.

Hahn and Hahn (1994) described and illustrated a septomaxilla in *Pseudobolodon krebsi* Hahn, 1977, a paulchoffatiid from the Jurassic of Portugal; this putative septomaxilla was wedge-like and located posterior to the premaxilla, between the nasal and the maxilla. Wible *et al.* (1990) argue that the septomaxilla in

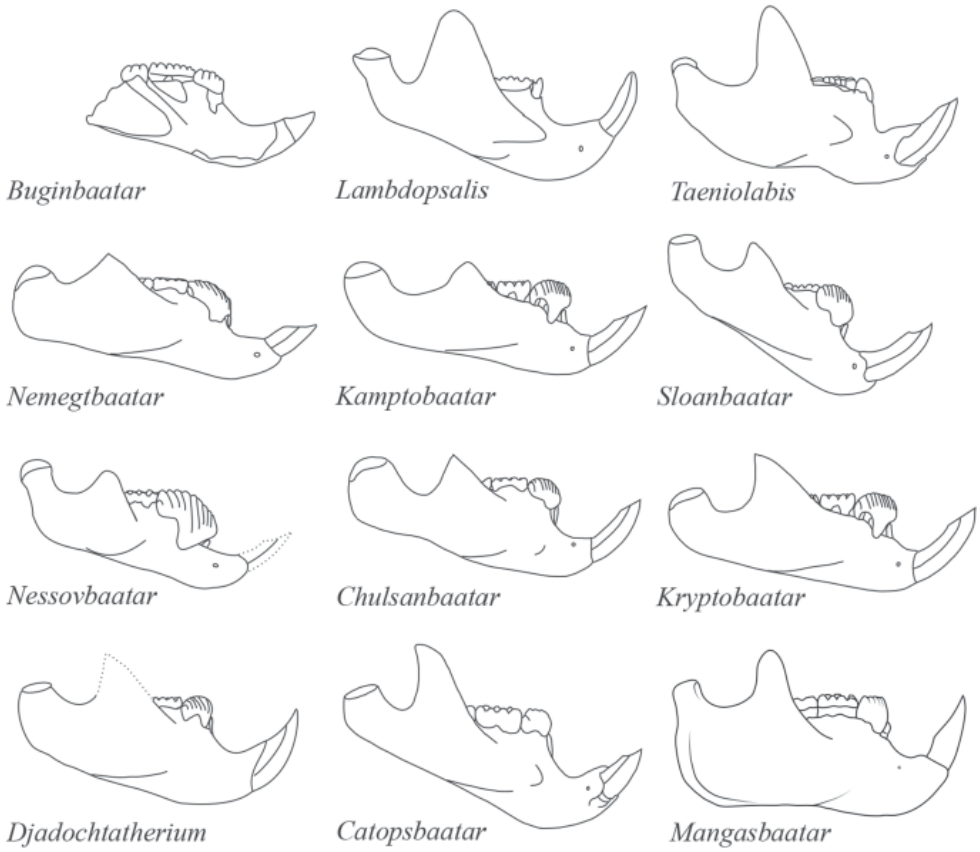

Fig. 31. Multituberculate mandible reconstructions in lateral view, rendered to be approximately the same length. Drawing is modified from Kielan-Jaworowska *et al.* (2004) to include *Mangasbaatar.*

Pseudobolodon was an artifact, an interpretation followed by Kielan-Jaworowska *et al.* (2004) in their revision of the morphological diversity of multituberculates. One of us had the opportunity to study the specimen and we agree with Wible's *et al.* (1990) interpretation; as far as we are aware there is no reliable record of a septomaxilla in any multituberculate including the LCMM. The premaxilla is hypertrophied in early multituberculates probably related to the large size of the incisors, a feature present with variable development in all multituberculates.

Maxilla. — The sub-trapezoidal shape of the skull is due, in part, to the lateral bulging of the maxilla. This bulging is, as indicated by CT scans (Kielan-Jaworowska and Hurum 1997, 2001; Rougier *et al.* 1997; Kik 2002; Kielan-Jaworowska *et al.* 2004, 2005), an accommodation for an enlarged maxillary sinus. Such a large development of the maxillary sinuses is found uniquely within some members of Djadochtatherioidea, namely *Kryptobaatar*, *Djadochtatherium*, *Catopsbaatar*, and *Tombaatar* (Kielan-Jaworowska and Hurum 1997; Rougier *et al.* 1997; Wible and Rougier 2000; Kielan-Jaworowska *et al.* 2005) and results in a distinctive trapezoidal snout. Other LCMM, ptilodontoids, and taeniolabidoids such as *Lambdopsalis* and *Taenolabis,* exhibit an arcuate snout which forms a sharp angle with the zygomatic arches at their point of contact (Miao 1988; Kielan-Jaworowska and Hurum 1997) and represents the generalized mammalian condition.

Like *Catopsbaatar* (Kielan-Jaworowska *et at.* 2002, 2005)*,* there appears to be a secondary infraorbital foramen present in *Mangasbaatar,* though the utility of this feature in cladistics has been questioned by Miao (1988) and others, as it may be variable within a species. Nevertheless, multiple rostral exits for the infraorbital canal is a basal mammaliaform feature present in morganucodontids (Kermack *et al.* 1981), basal multitubeculates (Hahn 1985), some dryolestoids, and *Vincelestes* Bonaparte, 1986 (Rougier *et al.* 1992; Rougier 1993) in addition to monotremes (Kuhn 1971; Zeller 1989).

Palatine. — The bones that contribute to the formation of the "orbital mosaic" are best known in *Kryptobaatar* and *Lambdopsalis*, in which the palatine has no contribution and the maxilla forms the anterior part of the orbital roof. Like these two taxa, *Mangasbaatar* also lacks an exposure of the palatine

within the orbital fossa. Miao (1988) speculated that the lack of the palatine within the orbit may be a synapomorphy for multituberculates, which is supported by *Lambdopsalis*, *Kryptobaatar*, and *Mangasbaatar.* Interpretations of the orbital fossa of *Nemegtbaatar* by Hurum (1994, 1998a) and illustrations of *Ectypodus* Matthew *et* Granger, 1921 (Sloan 1979, fig. 1) noted a palatine exposure within the orbital area that would, if interpreted correctly, suggest that the feature is polymorphic within LCMM. In contrast, Wible and Rougier (2000), though unable to examine some of the reported specimens of *Nemegtbaatar*, examined *Ectypodus* (YPM-PU 14724) and did not identify the sutures suggesting the presence of this exposure, confirming that the same area in *Kryptobaatar* is formed of maxilla. It appears likely that in LCMM the palatine is excluded from the orbital mosaic or it is at least very small.

Djadochtatheriid multituberculates routinely share a uniquely developed postpalatine torus, most strongly developed in *Mangasbaatar.* The presence, absence, and relative size of this feature has been scored for several multituberculates including *Kryptobaatar* (Wible and Rougier 2000)*, Tombaatar* (Rougier *et al.* 1997), *Catopsbaatar* (Kielan-Jaworowska *et al.* 2005), *Lambdopsalis* (Miao 1988), and a variety of therian such as *Zalambdalestes* Gregory *et* Simpson, 1926 and metatherians (Rougier *et al.* 1998). The postpalatine torus in *Tombaatar* is strongly developed; however, when compared with that in *Mangasbaatar,* the central ridge on the torus lacks the shallow recess that the torus of *Mangasbaatar* exhibits. The torus in *Kryptobaatar* is weaker than in either one of the large multitubeculates, *Tombaatar* and *Mangasbaatar*, and shares with *Tombaatar* the lacks of a central recess. In 2005, a specimen of *Catopsbaatar*, ZPAL MgM-I/80, was published in which the torus was completely preserved but weakly developed. Nevertheless, some degree of postpalatine torus development is consistently present among large Mongolian multituberculates.

Though the exact role of the postpalatine torus in extinct and extant mammals remains ambiguous, the degree of development within djadochtatheriids to the exclusion of other multituberculates suggests that it may represent, at least, a useful phylogenetic character. In extant mammals, such as the aardvark or the hedgehog, this bony feature is located at the attachment for the tensor veli palatini muscle (Barghusen 1986), which tenses the soft palate. It is unclear what benefit a more robust process of this sort confers, as modern taxa that share it do not establish a clear pattern among diet, body size, and the morphology of the torus.

Pterygoid. — The mesocranium, the portion of the skull between the hard palate and the anterior pole of the promontorium, is dramatically altered in early mammals from the primitive condition present in non-mammaliaform cynodonts like brasilodontids and probainognathians (Martinelli and Rougier 2007; Kielan-Jaworowska *et al.* 2004).

In multituberculates the pterygoids are rarely separated by sutures from the surrounding elements but they have been consistently identified as the main element forming the bulk of the lateral wall of the median or medial choanal passage, the number of choanal passages depending on the presence of a mid-line crest (Kielan-Jaworowska 1971; Kielan-Jaworowska *et al.* 1986; Miao 1988; Wible and Rougier 2000). In *Mangasbaatar* a strong median ridge is missing and therefore there are only three choanal passages: one in the midline interpreted as the nasopharyngeal passage and bounded laterally by the pterygoids, and two lateral ones developed between pterygoids and alisphenoid, interpreted as for the eustachian tube and the pharyngotympanic connection. Barghusen (1986) recognized the complex nature of the mesocranium in non-mammalian cynodonts and called the ridges medial to the transverse process of the pterygoid present in *Thrinaxodon* Seeley, 1894 and relatives pterygopalatine ridges. He also recognized these ridges in *Kamptobaatar* (Barghusen 1986, fig. 6) and by extension in other LCMM with similar palatal morphology. This nomenclature and identification has been followed since by most researchers working in multituberculates until quite recently (*i.e.*, Wible and Rougier 2000; Kielan-Jaworowska *et al.* 2005). Implicit in Barghusen identifications is the fact that the hamulus (or lateral pterygoid process) is not homologous with the pterygopalatine ridges and that both structures are separated. However, Kielan-Jaworowska (1971 and subsequent papers) and Wible and Rougier (2000) recognized a hamular process in the distal portions of the pterygopalatine ridges, but doubted its homology with the therian hamulus. In *Mangasbaatar* and other LCMM the hamulus develops in the pterygoid wall separating the lateral from the medial choanal passages (medial and lateral pterygopalatine troughs of Wible and Rougier 2000). The lateral passage is bounded laterally by the forward extension of the alisphenoid and it is presumably, at least in the degree of development, a derived feature of multituberculates. It would follow that the hamulus in multituberculates and the transverse process of the pterygoid of non-mammalian cynodonts can be homologized. Therefore, the pterygopalatine ridges of *Thrinaxodon* and similar forms would not be homologous with the "pterygopala-

tine ridges" of multituberculates. Despite concerns on the position and relationships of the multituberculate hamulus (Kielan-Jaworowska 1971; Wible and Rougier 2000), we believe its homology with the therian hamulus is the most likely assumption.

Nasal. — PSS-MAE 142 retains the posteriormost portion of the right nasal, which reveals that the frontals project as a wedge in between the suture between the nasals posteriorly, a primitive character present in nearly all Mesozoic mammals, save for perhaps *Catopsbaatar*, though it is likely that this is due to poor preservation of the sutural pattern in this form (Kielan-Jaworowska *et al.* 2005). Unlike some of the small LCMM, *Nemegtbaatar* for example (Kielan-Jaworowska *et al.* 1986), that show a multitude of nasal foramina, *Mangasbaatar* and relatives seem to have a few large-sized foramina.

Lacrimal. — The lacrimal of the LCMM is characteristic; it is present as a large, roughly rectangular bone visible on the dorsal surface of the skull, separating the frontal from the maxilla (Kielan-Jaworowska and Hurum 1997). Wible and Rougier (2000) were unable to identify with certainty the presence of a lacrimal in the specimens of *Sloanbaatar*, *Catopsbaatar*, or *Bulganbaatar* stored in Warsaw, though other specimens of *Catopsbaatar* show the character clearly. A sizable lacrimal is a primitive feature in multituberculates, present in paulchoffatiids and LCMM, though the extent of the orbital exposure of this bone was uncertain in other taxa. *Lambdopsalis* (Miao 1988) lacks the lacrimal completely and *Taeniolabis* must have lacked a facial exposure of the bone if it were present as claimed by Kielan-Jaworowska and and Hurum (1997). *Mangasbaatar* fits the condition described for other LCMM, displaying a large, subrectangular lacrimal that separates the frontal from the maxilla on the dorsal surface of the skull. In *Mangasbaatar*, the lacrimal contributes to the formation of an orbital pocket, as in *Kryptobaatar*, which has a small orbital process (Wible and Rougier 2000).

Frontal. — The ethmoidal foramen in *Mangasbaatar* is formed by both the frontal and orbitoshpenoid and likely distributed the ethmoidal nerve and artery. Though the presence of this foramen was questioned by Simmons (1993) in both *Ectypodus* and *Ptilodus* Cope, 1881, a more recent analysis by Wible and Rougier (2000) refuted this claim, holding that the foramen is present, not only in *Kryptobaatar* but in all multituberculates including *Ptilodus* and *Ectypodus*, as well as in most or all living mammals.

Parietal. — The postorbital process is common among mammalian skulls (Novacek 1986), and its morphology, whether long, short, or composed of frontal, parietal or both has been a point of interest in distinguishing relationships within multituberculates. Miao (1988) held that the postorbital process seen in multituberculates is not homologous to that seen in other mammals because the parietal position of the postorbital process does not delimit the back of the orbit. This claim has, however, been refuted numerous times (see Wible and Rougier 2000). Among multituberculates the postorbital process is positioned more posteriorly over the orbit than in other therians and among LCMM this feature is entirely formed by the parietal (Gambaryan and Kielan-Jaworowska 1995). In *Tombaatar*, *Catopsbaatar*, *Mangasbaatatar*, and *Djadochtatherium*, the postorbital process is comprised entirely by the parietal and, contrary to the condition in *Chulsanbaatar*, *Kamptobaatar*, and *Nemegtbaatar* (Kielan-Jaworowska and Hurum 1997), is very long (Kielan-Jaworowska and Hurum 1997; Wible and Rougier 2000; Kielan Jaworowska *et al.* 2005) and is best seen on the left side of PSS-MAE 141.

Squamosal. — The exposed region on the right side of PSS-MAW-141 reveals the contact between the squamosal and the petrosal, showing that the squamosal forms the lateral and dorsal walls of the ascending canal. This has been previously described in *Kryptobaatar* and *Vincelestes* (Rougier *et al.* 1992; Wible and Rougier 2000) and it is a primitive component of the basal mammaliaform circulatory pattern (Wible 1983, 1986, 1987; Rougier *et al.* 1992; Wible and Hopson 1993; Rougier and Wible 2006).

Petrosal. — The perilymphatic duct is primitively exposed in the middle ear cavity, and such is the condition regarded as primitive among monotremes, despite the partially enclosed perilymphatic duct of the echidnas (Rougier and Wible 1996). Most therians enclose the duct via a process, the processus recessus (Goodrich 1930; de Beer 1937), which is a derived feature present also among other mammals closely related to marsupials and placentals, like *Vincelestes* and dryolestoids (Rougier *et al.* 1992; Luo *et al.* 2012). It is notable that the perilymphatic grooves differ on the left and right of PSS-MAE 142, presenting a hurdle in the comparison of these specimens. The left side of PSS-MAE 141 has no evidence of a groove, agreeing with the condition on the right side of PSS-MAE 142, suggesting that, in *Mangasbaatar*, the groove is covered by

bone forming an enclosed duct. Despite some variability in this particular feature, the jugular fossa between the two is highly similar. Multituberculates, though, have shown some variability in the perilymphatic duct's enclosure by bone. Several isolated petrosals, likely belonging to taeniolabidoids collected from the Late Cretaceous of North America, displayed a condition wherein the perilymphatic duct was not fully bounded by bone, but rather by two bony lappets bordering the groove without making contact with one another (Rougier and Wible 2006).

Some multituberculates share certain features with monotremes such as a large anterior lamina of the petrosal, and, like adult monotremes, in *Mangasbaatar* no clear suture can be seen between the anterior lamina and the petrosal. Given the developmental origin of this feature within monotremes (Presley and Steel 1976; Kemp 1983), however, it is parsimonius to assume that a similar origin accounts for the feature within multituberculates. The anterior lamina of the petrosal is lacking in *Lambdopsalis* but present in *Mangasbaatar* and other LCMM, further distinguishing Djadochtatherioidea from *Lambdopsalis* (Miao 1988; Kielan-Jaworowska *et al.* 2004) and potentially other taeniolabidoids.

On the ventral view it becomes apparent that the region surrounding the braincase is significantly dorsally depressed posterior to the palatine, which produces several exaggerated features such as an enlarged rostral tympanic process of the petrosal. In *Mangasbaatar* the RTPP is significantly larger in proportion with the rest of the skull when compared with *Kryptobaatar,* likely owing to the deeply excavated ear region. Within this area, a concave space formed between the RTPP and the basioccipital is composed of both the petrosal and the basioccipital in *Mangasbaatar* as in *Kryptobaatar* (Wible and Rougier 2000). The two bones both contribute to this cavity; however, in *Mangasbaatar,* the bordering basioccipital bone which forms the cavity's medial wall has a greater height dorso-ventrally and the contribution of this bone to the aforementioned cavity is nearly vertical in its entirety. This space is further subdivided by crests expanding into the middle ear cavity from the petrosal and the basioccipital; these extensions do not fully divide the region in compartments, but determine specific areas within the cavernous middle ear.

Middle ear (petrosal, basioccipital and exoccipital). — Due to the acquisition of several derived features, particularly in the ear region, *Mangasbaatar* appears as a highly specialized member of Djadochtatherioidea, closely related to *Tombaatar* and *Catopsbaatar.* Observations of *Kryoptobaatar,* currently the most thoroughly-documented multituberculate, and related members establish a trend among derived members of this group to enlarge the middle ear space. This region in *Mangasbaatar* is unique among other LCMM in the depth created by a dorsal excavation of the basicranium, measured at approximately 4 mm^3. It is difficult to compare this specimen to related taxa due to lack of consistent preservation of the region; however, it is clear that this cavity is proportionally larger than that of *Kryptobaatar* or *Catopsbaatar,* and similar to *Tombaatar* (Fig. 27).

In *Mangasbaatar*, all of the surrounding elements of the ear region project ventrally and help to encompass a very large space. The membranous component of the middle ear cavity likely extended ventrally from the edges of those cavities, and it was certainly of sizable proportions. But if compared with other LCMM, the proportion of the cavity delimited by bone is much larger in *Mangasbaatar* than in any of the other previously described multituberculates from the region. In *Kryptobaatar*, the same elements — exoccipital, basioccipital, basisphenoid, squamosal, and petrosal — also project ventrally and form distinct pockets, but these are not as prominent. The circumscribing of the middle ear region by bony projections in *Mangasbaatar* results in a relatively extensive bony encasing of the middle ear region, analogous to the auditory bulla present in many lineages of therians (Klaauw 1931; MacPhee 1981; Novacek 1977, 1986). A similar "sinking" of the petrosal into the braincase can been seen in some borhyenoid marsupials (de Muizon *et al.* 1997), and the surrounding elements also provide a partial enclosure of the middle ear cavity; in these marsupials, as in multituberculates, most of the middle ear space was enclosed ventrally by a membrane in the absence of a fully developed bulla.

The functional significance of an expanded middle ear region is not straightforward to ascertain. The mammalian middle ear is an impedance transformer that matches the impedance between air-transmitted sound and the perilymphatic fluid in the inner ear (Webster and Webster 1984). Among most of living therian mammals, the middle ear cavity is surrounded by a rigid osseous bulla composed by a variety of bony elements that include the ectotympanic as the main support for the tympanic membrane. The ectotympanic can contribute to the enclosure of the middle ear by forming a substantial portion of the bulla, but depending on the group, a variety of neomorphic elements or other bones from the basicranium can participate in the formation of the bulla. The specific composition of the bulla has traditionally been a source of systematic and phylogenetic data (Novacek and Wyss 1986). The combination of elements, shapes, sizes, and presence

of internal division by septae, etc., of the ear region determine an optimal frequency for a given array of morphologies; this is the natural frequency of a middle ear (Fleischer 1978; Mason 2015, 2016a). This frequency increases with stiffness of both membrane-ear ossicles and tympanic cavity, but decreases with a greater mass of the membrane (functionally including the ossicular chain) and a larger air volume (Dallos 1973; Fleischer 1978; Mason 2006, 2013, 2015, 2016a, b). However, the primitive condition for mammals is the absence of a bulla, and most of the tympanic cavity is surrounded by a membrane that has, on its lateral aspect, a ring formed by the ectotympanic that supports the tympanic membrane. Such a middle ear is susceptible to deformation by chewing and jaw movements that deform the middle ear space and alter its auditory tuning; additionally, a membrane-encased middle ear region is more susceptible to interference of the low frequency sounds (Tonndorf *et al.* 1966; Mason 2015, 2016b). This primitive mammalian ear is present among monotremes and basal marsupials (Klaauw 1931; Simpson 1938; Griffiths 1978; Ashwell 2013). Similarly, in *Mangasbaatar* the middle ear cavity is surrounded only partially by bone and most of its ventral surface must have been enclosed by membrane; given the osteological morphology, most likely multituberculates lacked the stiffness of the middle ear enclosure as, for example, in desert dwelling rodents with large middle ear spaces enclosed by a bulla (Webster 1966; Fleischer 1973; Mason 2006, 2013, 2015, 2016a). Nevertheless, many of these recent mammals with large middle ear spaces (Mason 2004, 2013) live in arid environments or spend a substantial portion of their lives underground; the environmental conditions in Ukhaa Tolgod and most of the Late Cretaceous Mongolian sites seem to indicate that the environment was dominated by sands and some degree of periodical or seasonal aridity (Loope *et al.* 1998; Dingus *et al.* 2008). Dry air rapidly dissipates high frequency sound (Huang *et al.* 2002), therefore it would be expected some reliance on low frequency sound by the LCMM. In this context, an enlarged, more rigidly enclosed middle ear region would be consistent with an optimization for the perception of low frequency sound by increasing the non-pliable surfaces surrounding the middle ear.

Talpids (moles) and golden moles share a medially sunken middle ear cavity which forms an open connection between the two middle ears through an opening in the basicranium, which allows for pressure-difference localization in the low frequency range (Mason 2013). Though such an adaptation is common among non-mammalian tetrapods, it is rare among mammals, which typically have these two cavities separated by bone and soft tissue. Among the talpids and golden moles the expansion of the middle ear cavity is done by recession of the basicranium bordering the medial wall of the middle ear cavity, while other mammals typically expand their middle ear cavities via ventral expansion of the bulla (Mason 2013). If the volume of the middle ear spaces of *Kryptobaatar* and *Mangasbaatar* are compared, it is clear that the increase is due mostly to the "sinking" of the petrosal and promontorial area into the braincase. Though there is no known open connection between the middle ear spaces of any multituberculate studied thus far, the medial expansion of the middle ear cavity is similar to what must have occurred in the ancestors of golden or talpid moles.

Furthermore, the tensor tympani fossa, which is formed via attachment of the *m. tensor tympani*, is relatively small in *Mangasbaatar* in comparison with the rest of the middle ear space. It can be inferred, by extension, that the *m. tensor tympani* was also relatively small. A similar morphology is noted in the marsupial mole *Notoryctes* Stirling, 1891 (Ladevèze *et al.* 2008), while the muscle is completely lost in adult golden moles (Mason 2003) and a variety of mammals with a fossorial life-style (Mason 2013). Indeed, the tensor tympani muscle has been lost, convergently, in at least 4 distantly-related groups: marsupial moles, spalacid mole-rats, golden moles and talpid moles, all of which occupy a subterranean habitat (Mason 2013). The stapedius muscle is also often missing in forms with enlarged middle ear cavities (Hinchcliffe and Pye 1969; Webster and Webster 1975; Heffner *et al.* 2001), however, no mammal is known to be missing both muscles, the tensor tympani and the stapedius muscle. The stapedius muscle increases stiffness of the middle ear ossicles and this in turn dampens transmission of low frequency sound. The presence or absence of a stapedius muscle cannot be unequivocally ascertained in *Mangasbaatar*; however, a stapedius fossa has been identified in multituberculates (Kielan-Jaworowska *et al.* 1986; Rougier *et al.* 1992, 1996a; Wible and Rougier 2000) and it appears likely that the muscle was present among LCMM. Meng (1992) described the stapes of *Lambdopsalis*; the element is well preserved, columelliform, and without a distinct stapedius process. It is therefore possible that in at least some multituberculates the stapedius muscle was much reduced or absent. A partial stapes of *Kryptobaatar* was described by Rougier *et al.* (1996a) as bicrurate, but the specimen is incomplete and no evidence of a stapedius process is preserved. It is clear that some degree of diversity existed among multituberculates and that the LCMM and *Lambdopsalis* are both radically different regarding their adaptation related to the ear region. Reports of middle ear bones by Hurum *et al.* (1995,

1996) in some LCMM are hampered by misidentification of calcite concretions as fragmentary ear ossicles and cannot be discussed further until the specimens are restudied.

Regardless of the functional similarities that may exist between the middle ears of LCMM and therians it is clear that the expansion of the middle ear cavity was acquired independently in both linages. Basal members of the therian lineage, like symmetrodonts, dryolestoids and *Vincelestes*, lack any particularly enlarged ear regions (Hughes *et al.* 2015; Ji *et al.* 2009; Rougier *et al.* 1992, 2003; Ruf *et al.* 2009).

Dentition. — The dental formula of both *Mangasbaatar* specimens (I2/1, C0/0, P3/2, M2/2) and their molar and premolar morphology clearly refer these multituberculates to Djadochtatherioidea, and further analysis of their skull morphology and petrosal anatomy refers them as terminal members of Djadochtatheriidae. Unlike *Tombaatar,* and similar to all other LCMM, the I3 is placed entirely within the premaxilla, whereas in *Tombaatar,* the I3 is in direct contact with the maxilla and premaxilla, lying within the suture between the two bones. Like *Tombaatar*, the biradiculated P1 has three, conical cusps and the P3 in turn has four conical cusps; all that remains between P1 and P3 is a short diastema which likely housed the remnants of the DP3 (Rougier *et al.* 1997). The best preserved P4 among these two specimens is highly similar to that in *Tombaatar,* differing in the relative heights of the cusps within the middle row. In *Tombaatar,* the middle cusp row in P4 contains five cusps, with the third in the row being the tallest of them all (Rougier *et al.* 1997), in contrast to *Mangasbaatar,* in which the 5 cusps of the middle row of P4 increase in size posteriorly. Aside from this difference, the overall morphology of this cusp row is highly similar to *Tombaatar* and other LCMM, aligned posteriorly with the buccal cusp row of M1 and anteriorly with the lingual cusp row of P3 (Rougier *et al.* 1997).

The M1 cusp formula in *Mangasbaatar* (5:5:2) differs from *Tombaatar* (4:5:2)*, Catopsbaatar* (5-6:5-6:4) and *Kryptobaatar* (4-5:4:3-5), while the M1 is not preserved in the type specimen of *Djadochtatherium* (Rougier *et al.* 1997; Kielan-Jaworowska and Hurum 1997; Kielan-Jaworowska *et al.* 2004; Kielan-Jaworowska *et al.* 2005). *Mangasbaatar* most closely resembles *Tombaatar* in this regard, though the molars are slightly larger within *Mangasbaatar.* Additionally, in occlusal view, the outer edge of the lingual cusp row in the M1 of *Tombaatar*, *Mangasbaatar*, and *Kryptobaatar* forms a bulge from the remaining body of the tooth. In *Catopsbaatar*, the outer edge of the M1 lingual cusp row is confluent with the remaining rows in the M1.

Though the type specimen of *Tombaatar* is lacking the posterior half of the cranium, preliminary observations of another, more complete specimen of *Tombaatar* show a high degree of similarity with *Mangasbaatar* (Fig. 27). Despite their similarities, both specimens of *Mangasbaatar* are slightly larger in comparison with *Tombaatar.* The M2 on *Tombaatar* are slightly smaller with respect to *Mangasbaatar*, and the skull length of PSS-MAE 141 (6.30 cm) is greater than that of the unpublished specimen of *Tombaatar* (5.91 cm). Though PSS-MAE 141 and PSS-MAE 142 are somewhat deformed, the palatal region and the dental arch of *Mangasbaatar* can be accurately observed and exhibit less curvature than in *Tombaatar.* The dentition of the large members of Djadochtatherioidea retains the same overall morphology of more generalized multituberculates like *Kryptobaatar*, where the M/m1 is of moderate size and the M/m2 remains small but distinctive, while the P4 is relatively small and uncomplicated. The p4, on the other hand, loses the blade-like aspect characteristic of most multituberculates and it is supported mesially by a peg-like p3. The trapezoidal outline of the p4 and the absence of a P2 are distinctive dental feature of the large LCMM.

CONCLUSIONS

The skull of *Mangasbaatar* is highly similar to the closely related *Tombaatar*, *Catopsbaatar*, *Kryptobaatar*, and *Djadochtatherium*. The suite of features, including the subtrapezoidal shape of the skull, the dentition, petrosal anatomy and other features, clearly allies *Mangasbaatar* with these other taxa. The morphology of the postpalatine torus, though unknown in function, is a highly conspicuous character among more derived members of LCMM and is most strongly developed in *Mangasbaatar* and *Tombaatar.* Based on the phylogenetic analysis adapted from Kielan-Jaworowska and Hurum (1997), and amended here, this study recovers *Mangasbaatar* among the djadochtatherian LCMM. Specifically, *Mangasbaatar* is a terminal member of the monophyletic clade Djadochtatherioidea and sister-group to *Tombaatar.*

The degree of excavation of the middle ear cavity in *Mangasbaatar*, in addition to the relatively small tensor tympani fossa, may suggest a fossorial or semi-fossorial habit for *Mangasbaatar*, as this is a pattern

seen among modern, fossorial, desert-dwelling rodents (Mason 2013). The ventral expansion of the bones enclosing this space may have functioned similarly to the bulla in modern mammals, forming a rigid base for the soft structures encasing the middle ear, increasing the rigidity of the cavity, and thus aiding in low frequency audition (Fleischer 1978; Mason 2013), adding to the wide variety of habitats and niches occupied by multituberculates.

REFERENCES

Ashwell, K. (ed.). 2013. *Neurobiology of Monotremes*: *Brain Evolution in Our Distant Mammalian Cousins*. 536 pp. CSIRO PUBLISHING. Collingwood, Australia.

Barghusen, H.R. 1986. On the evolutionary origin of the therian tensor veli palatini and tensor tympani muscles. *In*: N. Hotton III, P.O. MacLean, J.J. Roth, and E.C. Roth (eds), *Ecology and Biology of Mammal-like Reptiles*, 253–262. Smithsonian Institution Press, Washington D.C.

Benton, M.J., Shishkin, M.A., Kurochkin, E.N., and Unwin, D.M. (eds) 2000. *The Age of Dinosaurs in Russia and Mongolia*. 696 pp. Cambridge University Press, Cambridge.

Beer, G.R. de. 1937. *The Development of the Vertebrate Skull*. 554 pp. Clarendon Press, Oxford.

Bi, S. Yuanqing, W., Jian, G., Xia, S., and Meng, J. 2014. Three new Jurassic euharamiyidan species reinforce early divergence of mammals. *Nature* **514**, 579–584.

Blumenbach, J.F. 1800. Ueber das Schnabeltier (*Ornithorinchus paradoxus*) ein neu entdecktes Geschlect von Säugetieren des fünften Weltthiels. *Voigt's Magazine* **2**, 205–214.

Bolortsetseg, M. 2008. *Descriptions of Three New Specimens of Cimilodontans and a Phylogenetic Study of the Postcranial Anatomy of Multituberculata (Mammalia, Synapsida)*. 256 pp. ProQuest, New York.

Bonaparte, J.F. 1986. Sobre *Mesungulatum houssayi* y nuevos mamíferos cretácicos de Patagonia. *Actas IV Congreso Argentino de Paleontología de Vertebrados* 2, 48–61.

Chow, M. and Qi, T. 1978. Paleocene mammalian fossils from Nomogen Formation of Inner Mongolia. *Vertebrata PalAsiatica* **16**, 77–85.

Clemens, W.A. 1963. Fossil mammals of the type Lance Formation, Wyoming. Part I. Introduction and Multituberculata. *University of California Publications in Geological Sciences* **48**, 1–105.

Clemens, W.A., Lillegraven, J.A., Lindsay, E.H., and Simpson, G.G. 1979. Where, when, and what — a survey of known Mesozoic mammal distribution. *In*: J.A. Lillegraven, Z. Kielan-Jaworowska, and W.A. Clemens (eds), *Mesozoic Mammals: The First Two-thirds of Mammalian History*, 7–58. University of California Press, Berkeley.

Cope, E.D. 1881. Eocene Plagiaulacidae. *American Naturalist* **15**, 921–922.

Cope, E.D. 1884. The Tertiary Marsupialia. *American Naturalist* **18**, 686–697.

Dashzeveg, D., Dingus, L., Loope, D.B., Swisher III, C.C., Dulam, T., and Sweeney, M.R. 2005. New stratigraphic subdivision, depositional environment and age estimate for the Upper Cretaceous Djadochta Formation, Southern Ulan Nur Basin, Mongolia. *American Museum Novitates* **3498**, 1–31.

Dashzeveg, D., Novacek, M.J., Norell, M.A., Clark, J.M., Chiappe, L.M., Davidson, A.R., McKenna, M.C., Dingus, L., Swisher III, C.C., and Altangerel, P. 1995. Extraordinary preservation in a new vertebrate assemblage from the Late Cretaceous of Mongolia. *Nature* **374**, 446–449.

Dallos, P. 1973.*The Auditory Periphery: Biophysics and Physiology*. 541 pp. Academic Press, New York.

Davis, B.M., Cifelli, R.L., and Kielan-Jaworowska, Z. 2008. Earliest evidence of Deltatheroida (Mammalia: Metatheria) from the Early Cretaceous of North America. *In*: E.J. Sargis and M. Dagosto (eds), *Mammalian Evolutionary Morphology: A Tribute to Frederick S. Szalay*, 3–24. Springer, Dordrecht.

de Muizon, C., Cifelli, R.L., and Paz, R.C. 1997. The origin of the dog-like borhyaenoid marsupials of South America. *Nature* **389**, 486–489.

Dingus, L., Loope, D.B., Dashzeveg, D., Swisher III, C.C., Minjin, C., Novacek, M.J., and Norell, M.A. 2008. The geology of Ukhaa Tolgod (Djadokhta Formation, Upper Cretaceous, Nemegt Basin, Mongolia). *American Museum Novitates* **3616**, 1–40.

Dong, Z-M. and Currie, P.J. 1993. Protoceratopsian embryos from Inner Mongolia, People's Republic of China. *Canadian Journal of Earth Sciences* **30**, 2248–2254.

Evans, H.E. and Christensen , G.C. 1979. *Anatomy of the Dog*. 1113 pp. W.B. Saunders, Philadelphia.

Fleischer, G. 1973. Studien am Skelett des Gehörorgans der Säugetiere, einschließlich des Menschen. *Säugetierkunde Mitteilungen* **21**, 131–239.

Fleischer, G. 1978. Evolutionary principles of the mammalian middle ear. *Advances in Anatomy, Embryology and Cell Biology* **55**, 1–70.

Freeman, E.F. 1976. Mammal teeth from the Forest Marble (Middle Jurassic) of Oxfordshire, England. *Science* **194**, 1053–1055.

Freeman, E.F. 1979. A Middle Jurassic mammal bed from Oxfordshire. *Palaeontology* **22**, 135–166.

Gambaryan, P.P. and Kielan-Jaworowska, Z. 1995. Masticatory musculature of Asian taeniolabidoid multituberculate mammals. *Acta Palaeontologica Polonica* **40**, 45–108.

Gidley, J.W. 1909. Notes on the fossil mammalian genus *Ptilodus* with descriptions of new species. *Proceedings U.S. National Museum* **36**, 611–627.
Gill, T. 1877. Vertebrate Zoology. *In*: *Annual Record of Science and Industry*, 166–175. Harper, New York.
Goodrich, E.S. 1930. *Studies on the Structure and Development of the Vertebrates*. 837 pp. Macmillian and Co., Ltd, London.
Gradziński, R., Kielan-Jaworowska, Z., and Maryańska, T. 1977. Upper Cretaceous Djadokhta, Barun Goyot and Nemegt formations of Mongolia, including remarks on previous subdivisions. *Acta Geologica Polonica* **27**, 281–318.
Gregory, W.K. and Simpson, G.G. 1926. Cretaceous mammal skulls from Mongolia. *American Museum Novitates* **225**, 1–20.
Griffiths, M. 1978. *The Biology of the Monotremes*. 367 pp. Academic Press, London.
Hahn, G. 1969. Beiträge zur Fauna der Grube Guimarota nr. 3. Die Multituberculata. *Palaeontographica Abteilung A* **133**, 1–100.
Hahn, G. 1977. Neue Schädel-Reste von Multituberculaten (Mammalia) aus dem Malm Portugals. *Geologica et Paleontologica* **11**, 161–186.
Hahn, G. 1985. Zum bau des infraorbital-foramens bei den Paulchoffatiidae (Multituberculata, Ober-Jura). *Berliner geowissenschaftliche Abhandlungen A* **60**, 5–27.
Hahn, G. 1987. Neue beobachtungen zum schadel-und gebiss-bau der Paulchoffatiidae (Multituberculata, Ober-Jura). *Palaeovertebrata* **17**, 155–196.
Hahn, G. 1998. Die ohr-region der Paulchoffatiidae (Multituberculata, Ober-Jura). *Palaeovertebrata* **18**, 155–185.
Hahn, G. and Hahn, R. 1994. Nachweis des Septomaxillare bei *Pseudobolodon krebsi* n. sp. (Multituberculata) aus dem Malm Portugals. *Berliner geowissenschaftliche Abhandlungen E* **13**, 9–29.
Handa, N., Watabe, M., and Tsogtbaatar, K. 2012. New specimens of *Protoceratops* (Dinosauria: Neoceratopsia) from the Upper Cretaceous in Udyn Sayr, Southern Gobi Area, Mongolia. *Palaeontological Research* **16** (3), 179–198.
Heffner, R.S., Koay, G., and Heffner, H.E. 2001. Audiograms of five species of rodents: implications for the evolution of hearing and the perception of pitch. *Hearing Research* **157**, 138–152.
Hill, J.E. 1935. The cranial foramina in rodents. *Journal of Mammology* **16**, 121–129.
Hinchcliffe, R. and Pye, A. 1969. Variations in the middle ear of the Mammalia. *Journal of Zoology* **157**, 277–288.
Hopson, J.A., Kielan-Jaworowska, Z., and Allin, E.F. 1989. The cryptic jugal of multituberculates. *Journal of Vertebrate Paleontology* **9**, 201–209.
Hopson, J.A. and Rougier, G.W. 1993. Braincase structure in the oldest known skull of a therian mammal: implications for mammalian systematics and cranial evolution. *American Journal of Science* **293**, 268–299.
Huang, G.T., Rosowski, J.J., Ravicz, M.E., and Peake, W.T. 2002. Mammalian ear specializations in arid habitats: structural and functional evidence from sand cat (*Felis margarita*). *Journal of Comparative Physiology A* **188**, 663–681
Hughes, E.M., Wible, J.R., Spaulding, M., and Luo, Z.-X. 2015. Mammalian petrosal from the upper Morrison Formation of Fruita, Colorado. *Annals of the Carnegie Museum* **83**, 1–17.
Hurum, J.H. 1994. Snout and orbit of Cretaceous Asian multituberculates studied by serial sections. *Acta Palaeontologica Polonica* **39**, 181–221.
Hurum, J.H. 1998a. The inner ear of two Late Cretaceous multituberculate mammals, and its implications for multituberculate hearing. *Journal of Mammalian Evolution* **5**, 65–93.
Hurum, J.H. 1998b. The braincase of two Late Cretaceous Asian multituberculates studied by serial directions. *Acta Palaeontologica Polonica* **43**, 21–52.
Hurum, J.H., Presley, R., and Kielan-Jaworowska, Z. 1995. Multituberculate ear ossicles. *In*: A.-L. Sun and Y. Wang (eds), *Sixth Symposium on Mesozoic Terrestrial Ecosystems and Biota, Short Papers*, 243–246. China Ocean Press, Beijing.
Hurum, J.H., Presley, R., and Kielan-Jaworowska, Z. 1996. The middle ear in multituberculate mammals. *Acta Palaeontologica Polonica* **41**, 253–275.
Illiger, C. 1811. *Prodromus Systematis Mammalium et Avium Additis Terminis Zoographicis Utriusque Classis*. 301 pp. C. Salfeld, Berlin.
Jenkins, F.A. Jr., Gatesy, S.M., Shubin, N.H., and Amaral, W.W. 1997. Haramyids and Triassic mammalian evolution. *Nature* **385**, 715–718.
Jerzykiewicz, T. 2000. Lithostratigraphy and sedimentary settings of the Cretaceous dinosaur beds of Mongolia. *In*: M.J. Benton, M.A. Shishkin, D.M. Unwin, and E.N. Kurochkin (eds), *The Age of Dinosaurs in Russia and Mongolia*, 279–296. Cambdridge University Press, Cambridge.
Jerzykiewicz, T. and Russell, D.A. 1991. Late Mesozoic stratigraphy and vertebrates of the Gobi Basin. *Cretaceous Research* **12**, 345–377.
Jerzykiewicz, T., Currie, P.J., Eberth, D.A., Johnston, P.A., Koster, E.H., and Zheng, J.-J. 1993. Djadokhta Formation correlative strata in Chinese Inner Mongolia: an overview of stratigraphy, sedimentary geology, and paleontology and comparison with type locality in pre-Altaian Gobi. *Canadian Journal of Earth Sciences* **30**, 2180–2195.
Ji, Q., Luo, Z.-X.; Zhang, X., Yuan, C.-X., and Xu, L. 2009. Evolutionary development of the middle ear in Mesozoic therian mammals. *Science* **326**, 278–281.
Kemp, T.S. 1983. The relationships of mammals. *Zoological Journal of the Linnean Society* **77**, 353–384.
Kermack, K.A. and Kielan-Jaworowska, Z. 1971. Therian and non-therian mammals. *Zoological Journal of the Linnean Society* **50** (Supplement 1), 103–115.
Kermack, K.A., Mussett, F., and Rigney, H.W. 1981. The skull of *Morganucodon*. *Zoological Journal of the Linnean* Society **71**, 1–158.
Kielan-Jaworowska, Z. 1969a. Discovery of a multituberculate marsupial bone. *Nature* **222**, 1091–1092.

Kielan-Jaworowska, Z. 1969b. Preliminary data on the Upper Cretaceous eutherian mammals from Bayn Dzak, Gobi Desert. Results of the Polish-Mongolian Palaeontological Expeditions. Part I. *Palaeontologia Polonica* **19**, 171–191.
Kielan-Jaworowska, Z. 1970. New Upper Cretaceous multituberculate genera from Bayn Dzak, Gobi Desert. Results of the Polish-Mongolian Palaeontological Expeditions. Part II. *Palaeontologia Polonica* **21**, 35–54.
Kielan-Jaworowska, Z. 1971. Results of the Polish-Mongolian Palaeontological Expeditions. Part III. Skull structure and affinities of the multituberculata. *Palaeontologia Polonica* **5**, 5–41.
Kielan-Jaworowska, Z. 1974. Multituberculate succession in the Late Cretaceous of the Gobi Desert (Mongolia). Results of the Polish-Mongolian Palaeontological Expeditions. Part V. *Palaeontologia Polonica* **30**, 23–44.
Kielan-Jaworowska, Z. 1975a. Evolution of the therian mammals in the Late Cretaceous of Asia. Part I. Deltatheridiidae. Results of the Polish-Mongolian Palaeontological Expeditions. Part VI. *Palaeontologia Polonica* **33**, 103–132.
Kielan-Jaworowska, Z.1975b. Possible occurrence of marsupial bones in Cretaceous eutherian mammals. *Nature* **255**, 598–599.
Kielan-Jaworowska, Z. 1975c. Preliminary description of two new eutherian genera from the Late Cretaceous of Mongolia. *Palaeontologia Polonica* **33**, 5–16.
Kielan-Jaworowska, Z.1977. Evolution of the therian mammals in the Late Cretaceous of Asia. Part II. Postcranial skeleton in *Kennalestes* and *Asioryctes*. Results of the Polish-Mongolian Palaeontological Expeditions. Part VII. *Palaeontologia Polonica* **37**, 65–83.
Kielan-Jaworowska, Z. 1978. Evolution of the therian mammals in the Late Cretaceous of Asia. Part III. Postcranial skeleton in Zalambdalestidae. *Palaeontologia Polonica* **38**, 5–41.
Kielan-Jaworowska, Z. 1979. Evolution of the therian mammals in the Late Cretaceous of Asia. Part III. Postcranial skeleton in Zalambdalestidae. Results of the Polish-Mongolian Expeditions. Part VIII. *Palaeontologia Polonica* **38**, 3–41.
Kielan-Jaworowska, Z. 1984a. Evolution of the therian mammals in the Late Cretaceous of Asia. Part V. Skull structure in Zalambdalestidae. Results of the Polish-Mongolian Expeditions. Part X. *Palaeontologia Polonica* **46**, 107–117.
Kielan-Jaworowska, Z. 1984b. Evolution of the therian mammals in the Late Cretaceous of Asia. Part VII. Synopsis. Results of the Polish-Mongolian Expeditions. Part XII. *Palaeontologia Polonica* **46**, 173–183.
Kielan-Jaworowska, Z. 1994. A new generic name for the multituberculate mammal "*Djadochtatherium*" *catopsaloides*. *Acta Palaeontologica Polonica* **39**, 134–136.
Kielan-Jaworowska, Z. 2013. *In Pursuit of Early Mammals*. 253 pp. Indiana University Press. Bloomington.
Kielan-Jaworowska, Z. and Dashzeveg, D. 1978. New Late Cretaceous mammal locality in Mongolia and a description of a new multituberculate. *Acta Palaeontologica Polonica* **23**, 115–130.
Kielan-Jaworowska, Z. and Gambaryan, P.P. 1994. Postcranial anatomy and habits of Asian multituberculate mammals. *Fossils & Strata* 36, 1–92.
Kielan-Jaworowska, Z. and Hurum, J.H. 1997. Djadochtatheria — a new suborder of multituberculate mammals. *Acta Palaeontologica Polonica* **42**, 201–242.
Kielan-Jaworowska, Z. and Hurum, J.H. 2001. Phylogeny and Systematics of Multituberculate Mammals. *Palaeontology* **44**, 389–429.
Kielan-Jaworowska, Z. and Hurum, J.H. 2005. Postcranial skeleton of a Cretaceous multituberculate mammal *Catopsbaatar*. *Acta Palaeontologica Polonica* **53**, 545–566.
Kielan-Jaworowska, Z. and Sochava, A.V. 1969. The first multituberculate from the Uppermost Cretaceous of the Gobi Desert (Mongolia). *Acta Palaeontologica Polonica* **14**, 355–367.
Kielan-Jaworowska, Z. and Trofimov, B.A. 1980. Cranial morphology of the Cretaceous eutherians mammal *Barunlestes*. *Acta Palaeontologica Polonica* **25**, 167–185.
Kielan-Jaworowska, Z., Cifelli, R. and Luo, Z.-X. 2004. *Mammals from the Age of Dinosaurs: Origins, Evolution, and Structure*. 630 pp. Columbia University Press, New York.
Kielan-Jaworowska, Z., Hurum, J.H., and Badamgarav, D. 2003. Multituberculate mammal *Kryptobaatar* and the distribution of mammals in the Upper Cretaceous rocks of the Gobi Desert. *Acta Palaeontologica Polonica* **48**, 161–166.
Kielan-Jaworowska, Z., Hurum, J.H., and Lopatin, A.V. 2005. Skull structure in *Catopsbaatar* and the zygomatic ridges in multituberculate mammals. *Acta Palaeontologica Polonica* **50**, 487–512.
Kielan-Jaworowska, Z., Hurum, J.H., Currie, P. M., and Barsbold, R. 2002. New data on anatomy of the Late Cretaceous multituberculate mammal *Catopsbaatar*. *Acta Palaeontologica Polonica* **47**, 557–560.
Kielan-Jaworowska, Z., Presley, R., and Poplin, C. 1986. The cranial vascular system in taeniolabidoid multituberculate mammals. *Philosophical Transactions of the Royal Society of London* **313**, 525–602.
Kik, P. 2002. *Computed Tomographic (CT) Examination of the Craniomandibular Morphology of* Kryptobaatar dashzevegi *(Mammalia Multituberculata)*. 92 pp. Masters dissertation, University of Louisville.
Klaauw, C.J. van der. 1931. The auditory bulla in some fossil mammals. *Bulletin of the American Museum of Natural History* **62**, 1–352.
Krause, D.W., Wible, J.R. Hoffman, S., Groenke, J.R., O'Connor, P.M., Holloway, W.L., and Rossie, J.B. 2014. Craniofacial morphology of *Vintana sertichi* (Mammalia, Gondwanatheria) from the Late Cretaceous of Madagascar. *Journal of Vertebrate Paleontology* **34**, 14–109.
Kuhn, H.-J. 1971. Die Entwicklung und Morphologie des Schädels von *Tachyglossus aculeatus*. *Abhandlungen der Senckenbergischen Naturforschenden Gesellschaft* **528**, 1–192.
Kuhn, H.-J. and Zeller, U. 1987a. The cavum epiptericum in monotremes and therian mammals. *In*: H.-J. Kuhn and U. Zeller (eds), *Mammalia Depicta, Heft 13, Beihefte zur Zeitschrift für Säugetierekunde*, 51–70. Paul Parey, Hamburg.
Kuhn, H.-J. and Zeller, U. (eds) 1987b. *Morphogenesis of the Mammalian Skull. Mammalia Depicta, Heft 13, Beihefte zur Zeitschrift für Säugetierekunde*. 114 pp. Paul Parey, Hamburg.

Kurzanov, S.M. 1992. A gigantic protoceratopsid from the Upper Cretaceous of Mongolia. *Paleontological Journal* **24**, 85–91.
Kühne, W.G. 1949. On a triconodont tooth of a new pattern from a fissure-filling in South Glamorgan. *Procedings of the Zoological Society of London* **119**, 345–350.
Kühne, W.G. and Krusat, G. 1972. Legalisierung des taxon *Haldanodon* (Mammalia, Docodonta). *Neues Jahrbuch für Geologie, Paläontologie und Mineralogie* **5**, 300–302.
Ladevèze S., Asher, R.J., and Sánchez-Villagra, M.R. 2008. Petrosal anatomy in the fossil mammal *Necrolestes*: evidence for metatherian affinities and comparisons with the extant marsupial mole. *Journal of Anatomy* **213**, 686–697.
Ladevèze, S., Muizon, C. de, Colbert, M., and Smith, T. 2010. 3D computational imaging of the petrosal of a new multituberculate mammal from the Late Cretaceous of China and its paleobiologic inferences. *Comptes Rendus Palevol* **9**, 319–330.
Lillegraven, J.A. and Krusat, G. 1991. Cranio-mandibular anatomy of *Haldanodon exspectatus* (Docodonta; Mammalia) from the Late Jurassic of Portugal and its implications to the evolution of mammalian characters. *Contributions to Geology*, *University of Wyoming* **28**, 39–138.
Lillegraven, J.A., Kielan-Jaworowska, Z., and Clemens W.A. (eds) 1979. *Mesozoic Mammals, the First Two-thirds of Mammalian History*. 311 pp. University of California Press, Berkeley.
Loope, D.B., Dingus, L., Swisher, C.C., and Minjin, C. 1998. Life and death in a Late Cretaceous dune field. *Geology* **26**, 27–30.
Luo, Z.-X., Meng, Q.-J., Ji, Q., Liu, D., Zhang, Y.-G., Neander, A.I. 2015. Mammalian evolution. Evolutionary development in basal mammaliaforms as revealed by a docodontan. *Science* **347**,760–764.
Luo, Z.-X., Ruf, I., and Martin, T. 2012. The petrosal and inner ear of the Late Jurassic cladotherian mammal *Dryolestes leiriensis* and implications for ear evolution in therian mammals. *Zoological Journal of the Linnean Society* **166**, 433–463.
MacPhee, R.D.E. 1981. Auditory region of primates and eutharian insectivores: morphology, ontogeny and character analyss. *Contributions to Primatology* **18**, 1–282.
Macrini, T.E. 2006. *The Evolution of Endocranial Space in Mammals and Non-mammalian Cynodonts*. 278 pp. Ph.D. Dissertation, University of Texas, Austin.
Makovicky, P.J. 2008. Telling time from fossils: a phylogeny-based approach to chronological ordering of paleobiotas. *Cladistics* **24**, 350–371.
Marsh, O.C. 1880. Notice on Jurassic mammals representing two new orders. *American Journal of Science* **20**, 235–239.
Marsh, O.C 1881. Notice on new Jurassic mammals. *American Journal of Science* **21**, 326–348.
Martinelli, A.G. and Rougier, G.W. 2007. On *Chaliminia musteloides* (Eucynodontia: Tritheledontidae) from the Late Triassic of Argentina, and phylogeny of Ictidosauria. *Journal of Vertebrate Paleontology* **27**, 442–460.
Mason, M.J. 2003. Morphology of the middle ear of golden moles (Chrysochloridae). *Journal of Zoology* **260**, 391–403.
Mason, M.J. 2004. The middle ear apparatus of the tuco-tuco *Ctenomys sociabilis* (Rodentia, Ctenomyidae). *Journal of Mammology* **85**, 797–805.
Mason, M.J. 2006. Evolution of the middle ear apparatus in talpid moles. *Journal of Morphology* **267**, 678–695.
Mason, M.J. 2013. Of mice, moles and guinea pigs: Functional morphology of the middle ear in living mammals. *Hearing Research* **301**, 4–18.
Mason, M.J. 2015. Functional Morphology of rodent middle ears. *In*: P.G. Cox and L. Hautier (eds), *Evolution of the Rodents: Advances in Phylogeny, Functional Morphology and Development*, 373–404. Cambridge University Press, Cambridge.
Mason, M.J. 2016a. Structure and function of the mammalian middle ear. I: Large middle ears in small desert mammals. *Journal of Anatomy* **228**, 284–299.
Mason, M.J. 2016b. Structure and function of the mammalian middle ear. II inferring function from structure. *Journal of Anatomy* **228**, 300–312.
Matthew, W.D. and Granger, W. 1921. New genera of Paleocene mammalas. *American Museum Novitates* **13**, 1–7.
Matthew, W.D., Granger, W., and Simpson, G.G. 1928. Paleocene multituberculates from Mongolia. *American Museum Novitates* **331**, 1–4.
Matthew, W.D., Granger, W., and Simpson, G.G. 1929. Additions to the fauna of the Gashato Formation of Mongolia. *American Museum Novitates* **376**, 1–12.
Meng, J. 1992. The stapes of *Lambdopsalis bulla* (Multituberculata) and transformational analyses on some stapedial features in Mammaliaformes. *Journal of Vertebrate Paleontology* **12**, 459–471.
Meng, Q.J., Ji, Q., Zhang, Y.G., Liu, D., Grossnickle, D.M., and Luo, Z.X. 2015. Mammalian evolution. An arboreal docodont from the Jurassic and mammaliaform ecological diversification. *Science* **347**, 764–768.
Miao, D. 1988. Skull morphology of *Lambdopsalis bulla* (Mammalia, Multituberculata) and its implications to mammalian evolution. *Contributions to Geology*, *University of Wyoming* (Special Paper 4), 1–104.
Miao, D. 1993. Cranial morphology and multituberculate relationships. *In*: F.S. Szalay, M.J. Novacek, and M.C. McKenna (eds), *Mammal Phylogeny: Mesozoic Differentiation, Multituberculates, Monotremes, Early Therians, and Marsupials*, 63–74. Springer Verlag, New York.
Moore, K.L. and. Agur, A.M.R. 2002. *Essentials of Clinical Anatomy*, *Second Edition*. 691 pp. Lippincott, Williams and Wilkins. New York.
Norell, M.A., Clark, J.M., Dashzeveg, D., Rhinchen, B., Chiappe, L.M., Davidson, A.R., McKenna, M.C., Altangerel, P., and Novacek, M.J. 1994. A therapod dinosaur embryo and the affinities of the Flaming Cliffs dinosaur eggs. *Science* **266**, 779–782.
Novacek, M.J. 1977. Aspects of the problem of variation, origin and evolution of the eutherian auditory bulla. *Mammal Review* **7** (3–4): 131–150.
Novacek, M.J. 1986. The Primitive Eutharian Dental Formula. *Journal of Vertebrate Paleontology* **6**, 191–196.

Novacek, M.J. and Wyss, A.R. 1986. Origin and transformation of the mammalian stapes. *Contributions to Geology, University of Wyoming* **3**, 35–53.
Novacek, M.J., Norell, M.A., McKenna, M.C., and Clark, J.M. 1994. Fossils of the Flaming Cliffs. *Scientific American* **271**, 60–69.
Novacek, M.J., Rougier, G. W., Wible, J. R., McKenna, M. C., Dashzeveg, D., and Horovitz, I. 1997. Epipubic bones in eutherian mammals from the Late Cretaceous of Mongolia. *Nature* **389**, 483–486.
Presley, R. 1981. Alisphenoid equivalents in placentals, marsupials, monotremes and fossils. *Nature* **294**, 668–670.
Presley, R. and Steel, F.L.D. 1976. On the homology of the alisphenoid. *Journal of Anatomy, London* **121**, 441–459.
Prothero, D.R. and Swisher III, C.C. 1992. Magnetostratigraphy and geochronology of the terrestrial eocene–oligocene transition in North America. *In*: D.R. Prothero and W.A. Berggren (eds), *Eocene–Oligocene Climatic and Biotic Evolution*, 46–73. Princeton University Press, Princeton.
Rougier, G.W. 1993. Vincelestes neuquenianus *Bonaparte (Mammalia, Theria) un primitivo mamífero del Cretácico Inferior de la Cuenca Neuquina*. 720 pp. Ph.D. Dissertation, Universidad Nacional de Buenos Aires, Buenos Aires.
Rougier, G.W. and Novacek, M.J. 1997. Nasal and endocranial morphology of Late Cretaceous multituberculates from Ukhaa Tolgod, Mongolia. *Journal of Vertebrate Paleontology* **17** (3), 72A.
Rougier, G.W. and Wible, J.R. 2006. Major changes in the mammalian ear region and basicranium. *In*: M.T. Carrano, T.J. Gaudin, R.W. Blob, and J.R. Wible (eds), *Amniote Paleobiology: Perspectives on the Evolution of Mammals, Birds, and Reptiles*, 269–311. University of Chicago Press, Chicago, Illinois.
Rougier, G.W., Davis, B.M. and Novacek, M.J. 2015 . A deltatheroidan mammal from the Upper Cretaceous Baynshiree Formation, eastern Mongolia. *Cretaceous Research* **52**, 167–177
Rougier, G.W., Ji, Q., and Novacek, M.J. 2003. A new symmetrodont with fur impressions from the Mesozoic of China. *Acta Geologica Sinica* **77**, 7–14.
Rougier, G.W., Novacek, M.J., and Dashzeveg, D. 1997. A new multituberculate from the Late Cretaceous locality Ukhaa Tolgod, Mongolia. Considerations on multituberculate interrelationships. *American Museum Novitates* **3191**, 1–26.
Rougier, G.W., Sheth, A.S., Carpenter, K., Appella-Guiscafre, L., and Davis, B.M. 2015. A new species of *Docodon* (Mammaliaformes: Docodonta) from the Upper Jurassic Morrison Formation and a reassessment of selected craniodental characters in basal mammaliaforms. *Journal of Mammalian Evolution* **22**, 1–16.
Rougier, G.W., Wible, J.R., and Hopson, J.A. 1992. Reconstruction of the cranial vessels in the Early Cretaceous mammal *Vincelestes neuquenianus*: implications for the evolution of the mammalian cranial vascular system. *Journal of Vertebrate Paleontology* **12**, 188–216.
Rougier, G.W., Wible, J.R., and Novacek, M.J. 1996a. Middle-ear ossicles of the multituberculate *Kryptobaatar* from the Mongolian Late Cretaceous: implications for mammaliamorph relationships and the evolution of the auditory apparatus. *American Museum Novitates* **3187**, 1–43.
Rougier, G.W., Wible, J.R., and Novacek, M.J. 1996b. Multituberculate phylogeny. *Nature* **379**, 406.
Rougier, G.W., Wible, J.R., and Novacek, M.J. 1998. Implications of *Deltatheridium* specimens for early marsupial history. *Nature* **396**, 459–463.
Ruf, I., Luo, Z.-X., Wible, J.R., and Martin, T. 2009. Petrosal anatomy and inner ear structures of the Late Jurassic *Henkelotherium* (Mammalia, Cladotheria, Dryolestoidea): insight into the early evolution of the ear region in cladotherian mammals. *Journal of Anatomy* **214**, 679–693.
Saneyoshi, M., Watabe, M., and Tsogtbaatar, K. 2008. Eolian environments, paleo-wind-direction and dinosaur habitats of the Upper Cretaceous Djadochta Formation, central Gobi Desert, Mongolia. *Geological Society of America Abstracts with Programs* **40**, 48.
Seeley, H.G. 1894. Research on the structure, organization, and classification of the Fossil Reptilia. Part IX, Section 3. On *Diademodon*. *Philosophical Transactions of the Royal Society of London* **185**, 1029–1041.
Segall, W. 1970. Morphological parallelisms of bulla and auditory ossicles in some insectivores and marsupials. *Fieldiana Zoology* **51**, 169–205.
Shuvalov, V.F. 2000. The Cretaceous stratigraphy and palaeobiography in Mongolia. *In*: M.J. Benton, M.A. Shishkin, D.M. Unwin, and E.N. Kurochkin (eds), *The Age of Dinosaurs in Russia and Mongolia*, 256–278. Cambridge University Press, Cambridge.
Simmons, N.B. 1993. Phylogeny of Multituberculata. *In*: F.S. Szalay, M.J. Novacek, and M.C. McKenna (eds), *Mammal Phylogeny: Placentals*, 146–164. Springer Verlag Publishers, New York.
Simpson, G.G. 1925. A Mesozoic mammal skull from Mongolia. *American Museum Novitates* **201**, 1–12.
Simpson, G.G. 1928a. *A Catalogue of the Mesozoic Mammalia*. 215 pp. The British Museum, London.
Simpson, G.G. 1928b. Affinities of the Mongolian Cretaceous insectivores. *American Museum Novitates* **330**, 1–11.
Simpson, G.G. 1937. Skull structure of the multituberculata. *Bulletin of the American Museum of Natural History* **73**, 727–763.
Simpson, G.G. 1938. Osteography of the ear region in monotremes. *American Museum Novitates* **978**, 1–15.
Sisson, S. and J. D. Grossman. 1955. *The Anatomy of the Domestic Animals*. 972 pp. Saunders, Philadelphia.
Sloan, R.E. 1979. Multituberculata. *In*: R.W. Fairbridge and D. Jablonski (eds), *Encyclopedia of Earth Sciences*, 492–498. Dowden, Hutchinson and Ross, Inc., Stroudsburg, PA.
Smith, T. and Codrea, V. 2015. Red iron-pigmented tooth enamel in a multituberculate mammal from the Late Cretaceous of Transilvanian "Hateg Island". *PLoS ONE* **10** (7), e0132550.
Stirling, E.C. 1891. Description of a new genus and species of Marsupialia, *Notoryctes typhlops*. *Transactions of the Royal Society of South Australia* **14**, 154–187.

Szalay, F.S. and Trofimov, B.A. 1996. The Mongolian Late Cretaceous *Asiatherium*, and the early phylogeny and paleobiogeography of Metatheria. *Journal of Vertebrate Paleontology* **16**, 474–509.

Tonndorf, J., Olesen, M.,King, A.F., Cottle, R.D., and Baker, D.C. 1966. Bone conducting studies in experimental animals VII. The effect of osseous discontinuities in upon the transmission of vibratory energy across the skull in rats. *Acta Oto-Laringologica Supplementum* **213**, 124–132.

Trofimov, B.A. and Szalay, F.S. 1994. New Cretaceous marsupial from Mongolia and the early radiation of Metatheria. *Proceedings of the National Academy of Science* **91**, 12569–12573.

Wahlert, J.H. 1974. The cranial foramina of protogomorphous rodents; an anatomical and phylogenetic study. *Bulletin of Museum of Comparative Zoology* **146**, 363–410.

Wahlert, J.H. 1985. Cranial foramina of rodents. *In*: W.P. Luckett and J.L. Hartenberger (eds), *Evolutionary Relationships Among Rodents: A Multidisciplinary Approach*, 311–332. Plenum Press. New York.

Wall, C. and Krause, D.W. 1992. A biomechanical analysis of the masticatory apparatus of *Ptilodus* (Multituberculata). *Journal of Vertebrate Paleontology* **12**, 172–187.

Watabe, M., Tsogtbaatar, K., Suzuki, S., and Saneyoshi, M. 2010. Geology of dinosaur-fossil-bearing-localities (Jurassic and Cretaceous: Cenozoic) in the Gobi Desert: Results of the HMNS-PMC Joint Paleontological Expedition. *Hayashibara Museum of Natural Sciences Research Bulletin* **3**, 41–118.

Webster, D.B. 1966. Ear structure and function in modern mammals. *American Zoologist* **6**, 451–466.

Webster, D. 1996. Dinosaurs of the Gobi. Unearthing a fossil trove. *National Geographic* **190** (1): 70–89.

Webster, D.B. and Webster, M. 1975. Auditory systems of *Heteromyidae*: functional morphology and evolution of the middle ear. *Journal of Morphology* **146**, 343–376.

Webster, D.B. and Webster, M. 1984. The specialized auditory system of Kangaroo Rats. *Contributions to Sensory Physiology* **8**, 161–196.

Wible, J.R. 1983. The internal carotid artery in early Eutharians. *Acta Palaeontologica Polonica* **28**, 281–293.

Wible, J.R. 1986. Transformations in the extracranial course of the internal carotid artery in mammalian phylogeny. *Journal of Vertebrate Paleontology* **6**, 313–325.

Wible, J.R. 1987. The eutherian stapedial artery: character analysis and implications for superordinal relationships. *Zoological Journal of the Linnean Society* **91**, 107–135.

Wible, J.R. and Gaudin, T.J. 2004. The cranial osteology of the yellow armadillo *Euphractus sexcinctus* (Dasypodidae, Xenartrha, Placentalia). *Annals of the Carnegie Museum* **73**, 117–196.

Wible, J.R. and Hopson, J.A. 1993. Basicranial evidence for early mammal phylogeny. *In*: F.S. Szalay, M.J. Novacek, and M.C. McKenna (eds), *Mammal Phylogeny: Mesozoic Differentiation, Multituberculates, Monotremes, Early Therians, and Marsupials*, 45–62. Springer-Verlag, New York.

Wible, J.R. and Rougier, G.W. 2000. Cranial anatomy of *Kryptobaatar dashzevegi* (Mammalia, Multituberculata), and its bearing on the evolution of mammalian characters. *Bulletin of the American Museum of Natural History* **247**, 1–124.

Wible, J.R., Miao, D., and Hopson, J.A. 1990. The septomaxilla of fossil and recent synapsids and the problem of the septomaxilla of monotremes and armadillos. *Zoological Journal of the Linnean Society* **98**, 203–228.

Wible, J.R., Rougier, G.W., Novacek, M.J., McKenna, M.C., and Dashzeveg, D. 1995. A mammalian petrosal from the Early Cretaceous of Mongolia: implications for the evolution aof the ear region and mammaliamorph interrelationships. *American Museum Novitates* **3149**, 1–19.

Wilson, G., Alistair, E., Corfe, I., Smits, P., Fortelius, M., and Jernvall, J. 2012. Adaptive radiation of multituberculate mammals before the extinction of dinosaurs. *Nature* **483**, 457–460.

Yuan, C.-X., Ji, Q., Meng, Q.-J. and Z.-X. Luo. 2013. Earliest evolution of multituberculate mammals revealed by a new Jurassic fossil. *Science* **341**, 779–783.

Zeller, U. 1989. Die entwicklung und morphologie des schadels von *Ornithorhynchus anatinus* (Mammalia: Prototheria: Monotremata). *Abhandlungen der Senckenbergischen Naturforscheiden Gesellschaft* **545**, 1–188.

Zheng, X., Bi, S., Wang, X., and Meng, J. 2013. A new arboreal haramyid shows the diversity of crown mammals in the Jurassic period. *Nature* **500**, 199–202.

Zhou, C.-F., Wu, S., Martin, T., and Luo, Z.-X. 2013. A Jurassic mammaliaform and the earliest mammalian evolutionary adaptations. *Nature* **500**, 163–167.

APPENDIX 1

Character list adapted from Kielan-Jaworowska and Hurum (1997), with the addition of character 44 for the postpalatine torus and the addition of *Mangasbaatar udanii* as a new taxon.

1. Enamel covering of lower incisor of uniform thickness (0), thicker on labial surface than on lingual surface (1), completely restricted to labial surface of tooth (2). ***Mangasbaatar* (2)**
2. p3 present (0), absent (1). ***Mangasbaatar* (0)**
3. p4 serration count 5 or less (0), 6–10 (1), more than 10 (2). ***Mangasbaatar* (0)**
4. p4 in lateral view rectangular (0), arcuate (1), trapezoidal (2), triangular (3). ***Mangasbaatar* (2)**
5. m1 cusp formula 4:3 (0), 4:4 (1), 5:4–5 (2), 7:4 or higher (3). ***Mangasbaatar* (0)**
6. Ratio of p4:m1 length less than 0.6 (0), 0.6–1.7 (1) above 1.7 (2). ***Mangasbaatar* (1)**
7. m2 cusp formula 2–2 (0), more (1). ***Mangasbaatar* (0)**
8. I2 bicuspid (0), single-cusped (1). ***Mangasbaatar* (?)**
9. I3 located on margin of palate (0), slightly shifted from the labial margin (1), in about the middle of the palatal part of the premaxilla (2). ***Mangasbaatar* (2)**
10. Upper premolars five (0), four (1), three (2) one (3). ***Mangasbaatar* (2)**
11. P3 double-rooted (0), single-rooted (1). ***Mangasbaatar* (0)**
12. P4 double-rooted (0), single-rooted (1). ***Mangasbaatar* (0)**
13. Length of upper premolar tooth row: molar tooth row more than 1.5 (0), 1.54.5 (1), 0.5–0.1 (2). ***Mangasbaatar* (1)**
14. P4 cusp formula 0–5:1–4:0–5 (0), 0–5:5–10:0–5 (1), 5–7:5–8:2–5 (2). ***Mangasbaatar* (1)**
15. M1 cusp formula 4–5:4–5:0–5 (0), 5–7:5–8:2–5 (1), 5–11:7–10:611 (2). ***Mangasbaatar* (0+1)**
16. M1 inner ridge length: length of M1 0.5 or less (0), more than 0.5 (1). ***Mangasbaatar* (0)**
17. Width of P4:M1 ratio more than 0.9 (0), 0.9–0.6 (1), 0.6–0.45 (2), 0.45–0.2 (3). ***Mangasbaatar* (2)**
18. M2 cusp formula 1:2:2 (0). 1:2:3 (1), more (2). ***Mangasbaatar* (0+1)**
19. Ridge between the palate and the lateral walls of the premaxilla absent (0), present (1). ***Mangasbaatar* (1)**
20. Shape of the snout in dorsal view: incurved in front of the zygomatic arches with anterior part directed posterolaterally (0), incurved with anterior part of zygomatic arches directed transversely (1), trapezoidal, not incurved in front of zygomatic arches (2). ***Mangasbaatar* (2)**
21. Number of pairs of vascular foramina on nasal: 1 (0), 2 (1), more (2). ***Mangasbaatar* (?)**
22. lnfraorbital foramen positioned dorsal to P1 (0), dorsal to P2 (1), dorsal to P3 or P3 (2). ***Mangasbaatar* (1)**
23. Base of zygomatic arch as marked by posterior edge directly dorsal to P4 (0), dorsal or posterior to P4/M1 embrasure (1). ***Mangasbaatar* (0)**
24. Postorbital process short (0), long (1). ***Mangasbaatar* (1)**
25. Snout length 49% or less of total skull length (0), 50% or more of skull length (1). ***Mangasbaatar* (0)**
26. Frontals pointed anteriorly and not deeply inserted between the nasals (0), pointed anteriorly and deeply inserted between the nasals (1), with subtransversal anterior margins (2). ***Mangasbaatar* (1)**
27. Frontal-parietal suture V-shaped (0), U-shaped (1). ***Mangasbaatar* (1)**
28. Contacts between nasal and parietal absent (0), present (1). ***Mangasbaatar* (0)**
29. Facial surface of lacrimal very small and arcuate (0), large, roughly rectangular (1). ***Mangasbaatar* (1)**
30. Thickening in palatal process of premaxilla absent (0), present (1). ***Mangasbaatar* (1)**
31. Incisive foramen situated within premaxilla (0), limited posteriorly by maxilla (1). ***Mangasbaatar* (1)**
32. Palatal vacuities absent (0), single (1), double (2). ***Mangasbaatar* (0)**
33. Foramen ovale inferium placed medial to foramen masticatorium (0), posterior to foramen masticatorium (1). ***Mangasbaatar* (0)**
34. Jugular fossa small and shallow (0), large and deep (1). ***Mangasbaatar* (1)**
35. Anterior part of the promontorium oval (0), irregular with incurvatures on both sides (1). ***Mangasbaatar* (1)**
36. Glenoid fossa (anterolateral to posteromedial) length: width ratio more than 1.7 (0), below 1.69 (1). ***Mangasbaatar* (1)**
37. Angle of coronoid process relative to tooth row steep, 45º or > 45º (0), low < 45º (1). ***Mangasbaatar* (0)**
38. Coronoid process parallel to the rest of the outer wall of the dentary (0), flared laterally (1). ***Mangasbaatar* (0)**
39. Posttemporal fossa large (0), reduced to a small foramen (1). ***Mangasbaatar* (0)**
40. Angle between the lower margin of the dentary and the occlusal level of the molars between 11–20º (0), above 20º (1). ***Mangasbaatar* (0)**
41. Mandibular condyle opposite or below the level of the molars (0), above the level of the molars (1). ***Mangasbaatar* (1)**
42. Width of the snout:skull length ratio below 0.3 (0), 0.3–0.39 (1), above 0.4 (2). ***Mangasbaatar* (2)**
43. Skull width:skull length ratio 0.79 and below (0), above 0.8 (1). ***Mangasbaatar* (1)**
44. Postpalatine torus absent or very faint (0), developed laterally and with a ventral projection from the palate, forming a distinctive bulge (1), strongly developed, forming a raised, ornate and sharply angled plate (2). ***Mangasbaatar* (2)**

APPENDIX 2

Scored character matrix, adapted from Kielan-Jaworowska and Hurum (1997) for 44 characters across 17 taxa including *Ptilodus*, *Stigymys*, *Taeniolabis, Eucosmodon*, *Lambdopsalis*, *Sloanbaatar*, *Buginbaatar*, *Kamptobaatar*, *Nemegtbaatar*, *Chulsanbaatar*, *Kryptobaatar*, *Djadochtatherium*, *Catopsbaatar*, *Tombaatar*, and *Mangasbaatar.* "A" denotes a multi-state (0+1).

Ptilodus	00212211010002210200120?0000001100010000100
Stigymys	21213210211011102??0?00??????111????10?0????
Taeniolabis	21033111032120213201?2??020100?0????001?1110
Eucosmodon	21213210??10??10?????????????????????1??00???
Lambdopsalis	21032011132120213201221?02010010?11?0?101110
Sloanbaatar	10110101210011002110010001101102O?0001011010
Buginbaatar	0101301????0?12132?????????????????????0?0????
Nessovbaatar	?011021?????????????????????????????????1?01??1
Bulganbaatar	???????12100110110?10?????11?1????????????
Kamptobaatar	101101?12100110121102000011011107?10011001101
Nemegtbaatar	20112111210011111210210001101111010010000101
Chulsanbaatar	20110101210011002010100001101110110110000001
Kryptobaatar	201101112100110021121100111011101111000021?
Djadochtatherium	20?101?121???0????12?10111101117????00001???
Catopsbaatar	20021101220011112212121111101100?11100011211
Tombaatar	2??????122001100211211O??1?01110???????????2
Mangasbaatar	2002010?220011A02A12?10101101110011100001212